

TECHNISCHE UNIVERSITÄT MÜNCHEN
Institut für Medizinische Mikrobiologie, Immunologie und
Hygiene

**Phosphoproteome Analysis of the Macrophage Response
to Toll-like Receptor (TRL)-Activation**

Gabriele Maria Weintz

Vollständiger Abdruck der von der Fakultät für Chemie der Technischen
Universität München zur Erlangung des akademischen Grades eines

Doktors der Naturwissenschaften (Dr. rer. nat.)

genehmigten Dissertation.

Vorsitzende: Univ.-Prof. Dr. Sevil Weinkauf
Prüfer der Dissertation: 1. Univ.-Prof. Dr. Johannes Buchner
2. Univ.-Prof. Dr. Roland Lang, Friedrich-
Alexander-Universität Erlangen Nürnberg
3. Univ.-Prof. Dr. Bernhard Küster

Die Dissertation wurde am 31.08.2009 bei der Technischen Universität München
eingereicht und durch die Fakultät für Chemie am 09.02.2010 angenommen.

To my parents

Table of contents

INDEX OF FIGURES	4
INDEX OF TABLES	5
ABBREVIATIONS	6
SUMMARY	12
1 INTRODUCTION	13
1.1 <i>Innate and adaptive immunity</i>	13
1.2 <i>Biology of macrophages</i>	14
1.2.1 Macrophage differentiation	15
1.2.2 Phagocytosis	16
1.2.3 Microbial danger signals and cytokines – regulators of macrophage activity	16
1.3 <i>Toll-like receptors (TLRs)</i>	18
1.3.1 Ligand specificities and expression	19
1.3.2 Structure and function	20
1.3.3 TLR signalling pathways	21
1.3.4 Transcriptional activation of gene expression	25
1.3.5 Negative regulation of TLR signalling	27
1.3.6 Requirement of a phosphoproteome study	28
1.4 <i>Quantitative phosphoproteomics</i>	29
1.4.1 Protein phosphorylation	29
1.4.2 Fractionation and phosphopeptide enrichment strategies	30
1.4.3 Phosphopeptide analysis by mass spectrometry	33
1.4.4 Quantitative measurements using Stable isotope labelling with amino acids in cell culture (SILAC)	36
2 AIM OF THE STUDY	38
3 MATERIAL	39
3.1 <i>Chemicals and reagents</i>	39
3.2 <i>Kits</i>	42
3.3 <i>Primers</i>	42
3.4 <i>Antibodies</i>	43
3.5 <i>DNA- and protein standards</i>	43
3.6 <i>Enzymes</i>	43
3.7 <i>Consumable items</i>	44
3.8 <i>Laboratory equipment</i>	44
3.9 <i>Databases and software</i>	46

4 METHODS	47
4.1 Mice	47
4.2 Cell culture	47
4.2.1 L-cell-conditioned medium (LCCM)	47
4.2.2 Standard protocol for differentiation of bone marrow-derived macrophages (BMDMs)	48
4.2.3 SILAC of BMDMs	48
4.2.4 Stimulation	50
4.3 Immunoassays	50
4.3.1 Enzyme-linked immunosorbent assay (ELISA)	50
4.3.2 Flow cytometry	51
4.4 Molecular biology	52
4.4.1 Isolation of genomic DNA	52
4.4.2 Polymerase chain reaction (PCR)	52
4.4.3 Agarose gel electrophoresis	53
4.4.4 Metabolic labelling and purification of total and nascent RNA	53
4.4.5 Microarray analysis of gene expression	54
4.5 Biochemistry – basic tools	55
4.5.1 Preparation of protein lysates	55
4.5.2 SDS-polyacrylamide gel electrophoresis (SDS-PAGE)	55
4.5.3 Coomassie staining of protein gels	56
4.5.4 Westernblot analysis	56
4.6 Phosphoproteome analysis	57
4.6.1 Stimulation and cell lysis	57
4.6.2 Reduction and alkylation of protein lysates	58
4.6.3 In-gel digest of chromatin pellet fraction	58
4.6.4 In-solution digest of proteins	58
4.6.5 Strong cation exchange (SCX) chromatography	59
4.6.6 Titansphere (TiO ₂) enrichment of phosphopeptides	59
4.6.7 Mass spectrometric analyses	60
4.7 Bioinformatic analyses	63
4.7.1 Definition of genes expressed in macrophages	63
4.7.2 Contribution of gene expression changes to regulation of the phosphoproteome	63
4.7.3 Gene Ontology (GO) analysis	63
4.7.4 Kinase motifs	64
4.7.5 Signalling pathways	64
4.7.6 Transcription factor (TF) phosphorylation and DNA binding sites	65
5 RESULTS	67
5.1 Quantitative phosphoproteome analysis of primary macrophages	67
5.1.1 Optimised protocol for SILAC of primary BMDMs	67
5.1.2 Experimental setup	71
5.1.3 Macrophage phosphorylation sites and proteins	72
5.2 Dynamics of the phosphoproteome after TLR4 activation	75

5.2.1	Minor effect of DUSP1-deficiency on global phosphorylation	75
5.2.2	Strong and dynamic regulation by LPS stimulation	76
5.2.3	Limited contribution of gene expression changes to the regulation of the phosphoproteome	78
5.3	<i>Kinase activity induced by LPS</i>	79
5.4	<i>Association of LPS-regulated phosphoproteins with signalling pathways and functional annotation</i>	81
5.4.1	Signalling pathways	81
5.4.2	GO analysis	85
5.5	<i>Connecting TF phosphorylation with LPS-induced transcriptional activation</i>	86
5.5.1	Identification of transcriptionally regulated genes in metabolically labelled nascent RNA	87
5.5.2	Integration of phosphoproteome and nascent transcriptome data by in-silico promoter analysis	88
5.5.3	Evolutionary conservation of TF phosphorylation sites and DNA binding sites	89
6	DISCUSSION	93
6.1	<i>TLR-induced phosphorylation – the global picture</i>	93
6.1.1	First global and quantitative study reveals extent of regulation comparable to transcriptional reprogramming	93
6.1.2	Dynamic regulation of phosphorylation	94
6.1.3	Variability in the effect of DUSP1-deficiency	96
6.1.4	Signalling pathways	97
6.1.5	The cell cycle	100
6.1.6	The cytoskeleton	101
6.2	<i>Integration of TF phosphorylation and transcriptional activation</i>	103
6.2.1	First study combining promoter motif scanning with regulated phosphorylation on TFs	103
6.2.2	Transcriptional target identification by biosynthetic mRNA labelling	103
6.2.3	Identification of known and novel candidate regulators of the transcriptional response to TLR ligation	104
7	OUTLOOK	109
	REFERENCES	111
	APPENDIX	125
	ACKNOWLEDGEMENTS	126

Index of figures

Fig. 1. Macrophage development and tissue distribution.	15
Fig. 2. Macrophage activation states and effector functions.	18
Fig. 3. Toll-like receptors (TRLs) and their ligand specificities.	20
Fig. 4. Recognition of Lipopolysaccharide (LPS) by LPS binding protein (LBP), CD14 and the TLR4-MD2 complex.	21
Fig. 5. Canonical signalling pathways triggered by TLR4.	22
Fig. 6. Overview of the Phosphatidylinositol-3 kinase (PI3K) signalling pathway.	24
Fig. 7. Comparison of binding capacities of peptides, 2,5-dihydroxy benzoic acid (DHB) and phosphopeptides to Titansphere (TiO₂).	31
Fig. 8. Peptide fractionation and phosphopeptide enrichment by Strong cation exchange (SCX) chromatography.	32
Fig. 9. Workflow of mass spectrometry-based phosphoproteomics.	35
Fig. 10. Quantitative phosphoproteomics using Stable isotope labelling with amino acids in cell culture (SILAC).	37
Fig. 11. Optimised protocol for SILAC of bone marrow-derived macrophages (BMDMs).	68
Fig. 12. Labelling efficiency and arginine to proline conversion.	69
Fig. 13. Quality control of macrophages obtained by the SILAC-adapted protocol.	70
Fig. 14. Strategy for global and quantitative analysis of LPS-regulated phosphorylation.	72
Fig. 15. Overlap of phosphorylation sites identified in two independent experiments.	73
Fig. 16. Distribution of phosphorylated amino acids.	73
Fig. 17. Distribution of phosphorylated proteins in cellular compartments.	74
Fig. 18. Influence of DUSP1 on phosphorylation of p38 MAPK.	75
Fig. 19. Extent of regulation by LPS.	76
Fig. 20. Kinetics of regulation.	77
Fig. 21. Contribution of gene expression changes to the regulation of the phosphoproteome.	78
Fig. 22. Protein interaction networks of over-represented signalling pathways.	85
Fig. 23. Transcription factor (TF) phosphorylation - strategy for detection of over- represented binding sites in promoters of LPS-induced genes.	86
Fig. 24. Nascent transcriptome analysis for detection of transcriptionally LPS-induced genes.	87
Fig. 25. Evolutionary conservation of TF binding sites in promoters of LPS-induced genes.	92
Fig. 26. Functions of serine/threonine phosphorylation.	95
Fig. 27. The phosphoproteome of LPS-activated macrophages - overview.	100

Index of tables

Tab. 1. Primers.....	43
Tab. 2. Antibodies for Westernblot.....	43
Tab. 3. Antibodies for flow cytometry.....	43
Tab. 4. PCR reaction mix.....	52
Tab. 5. PCR program.....	52
Tab. 6. SDS-PAGE gel recipes.....	56
Tab. 7. Kinase activation during TLR4 signalling.....	80
Tab. 8. Signalling pathways targeted by LPS-regulated phosphorylation.....	82
Tab. 9. Molecular functions and biological processes targeted by LPS-regulated phosphorylation.....	85
Tab. 10. TF families with over-represented binding sites in the promoters of transcriptionally LPS-regulated genes.....	89
Tab. S1. Reproducibly identified macrophage phosphorylation sites.....	125
Tab. S2. Phosphorylation sites on known TLR signalling molecules.....	125
Tab. S3. LPS-regulated phosphoproteins associated with enriched GO terms.....	125
Tab. S4. Microarray analysis of gene expression in nascent and total cellular RNA – regulated and non-regulated genes.....	125
Tab. S5. Phosphorylation sites on TFs with binding site enrichment in LPS-regulated promoters.....	125

Abbreviations

°C	Degrees Celsius
µL	Microliter
1D/2D-gel	One/two-dimensional gel
AP-1	Activating protein 1
ATF	Activating transcription factor
ATM	Ataxia-teleangiectasia mutated
ATP	Adenosin triphosphate
ATR	Rad 3-related
BMDMs	Bone marrow-derived macrophages
Ca ²⁺	Calcium
CAMK2	Ca ²⁺ /Calmodulin-dependent protein kinase 2
cAMP	Cyclic adenosine monophosphate
CCL3	Chemokine (C-C) motif ligand 3
CDK	Cyclin-dependent kinase
cDMEM	Complete DMEM medium
cDNA	Complementary DNA
C/EBP	CCAAT enhancer binding protein
CHK1/2	Checkpoint kinase 1/2
CID	Collisonally induced dissociation
CK1	Casein kinase 1
CLR	C-type lectin receptor
cm	Centimetre
cm ²	Square centimetre
CNS	Central nervous system
CpG	Cytosin-phosphatidyl-Guanosin
CRE	cAMP-responsive element
CREB	cAMP-responsive element binding protein
cRNA	Complementary RNA
cRPMI	Complete RPMI medium
Da	Dalton

DAI	DNA-dependent activator of Interferon regulatory factors
DC	Dendritic cell
DHB	2,5-dihydroxy benzoic acid
DMEM	Dulbecco's modified eagle medium
DNA	Deoxyribonucleic acid
dNTP	Deoxyribonucleoside triphosphate
dsRNA	Double-stranded RNA
DUSP1	Dual specificity phosphatase 1
EGFR	Epidermal growth factor receptor
ELISA	Enzyme-linked immunosorbent assay
ERK	Extracellular signal-regulated kinase
ESI	Electrospray ionisation
Fc receptor	Fragment, crystallisable, receptor
FCS	Fetal calf serum
FDR	False discovery rate
FHA domain	Forkhead-associated domain
FITC	Fluoresceineisothiocyanate
FOS	FBJ osteosarcoma oncogene
g	Acceleration of gravity (in centrifuge context), gram (other context)
G	Gauge
GEO	Gene Expression Omnibus
GM-CFU	Granulocyte/macrophage colony forming unit
GO	Gene Ontology
GR1	Granulocyte receptor 1
GSK3	Glycogen synthase kinase 3
h	Hour(s)
HDAC	Histone deacetylase
HILIC	Hydrophilic interaction chromatography
hnRNP	Heterogeneous ribonucleoprotein particle
HOX	Homeodomain
HRP	Horseradish peroxidase
HSC	Haematopoietic stem cell

HSF1	Heat shock factor 1
IFN- α/β	Interferon- α/β
IFN- γ	Interferon- γ
IKK	I κ B kinase
IL-1	Interleukin-1
IMAC	Immobilised metal affinity chromatography
iNOS	Inducible nitric-oxide synthase
IPI	International protein index
IRAK	IL-1 receptor associated kinase
IRF	Interferon regulatory factor
IRFF	IRF family
ISRE	IFN-stimulated response element
I κ B	Inhibitor of NF- κ B
JNK	c-jun N-terminal kinase
JUN	Jun oncogene
kb	Kilobases
kDa	Kilodalton
KO	Knockout
kV	Kilovolt
L	Litre
LBP	LPS binding protein
LC	Liquid chromatography
LCCM	L-cell-conditioned medium
LC-MS/MS	Liquid chromatography/tandem mass spectrometry
LIF	Leukemia inhibitory factor
LPS	Lipopolysaccharide
LRR	Leucine-rich repeat
LTA	Lipoteichoic acid
M	Mol/Litre
m/z	Mass-to-charge ratio
mA	Milliampere
MAF	Avian musculoaponeurotic fibrosarcoma oncogene
MAL	MyD88-adaptor-like protein

MALDI	Matrix-assisted laser desorption
MAPK	Mitogen-activated protein kinase
M-CFU	Macrophage colony forming unit
M-CSF	Macrophage colony stimulating factor
MEF	Myocyte enhancing factor
mg	Milligram
MHC	Major histocompatibility complex
min	Minute(s)
MIP-1a	Macrophage inflammatory protein 1a
mL	Millilitre
mM	Millimol/Litre
MMR	Macrophage mannose receptor
ms	Millisecond(s)
MS ¹ , MS	Survey scan in mass spectrometry
MS ² , MS/MS	Tandem mass spectrum
MSA	Multistage activation
mTOR	Mammalian target of Rapamycin
MyD88	Myeloid differentiation primary-response protein 88
NEK6	NIMA-related kinase 6
NFAT	Nuclear factor of activated T cells
NF- κ B	Nuclear factor 'kappa-light-chain-enhancer' of activated B cells
ng	Nanogram
NK cell	Natural killer cell
nL	Nanoliter
NLR	NOD-like receptor
OCT1	Octamer binding protein 1
PAMP	Pathogen associated molecular pattern
PBS	Phosphate buffered saline
PCR	Polymerase chain reaction
PDK1	Phosphoinositide-dependent kinase 1
PGE ₂	Prostaglandin E ₂
PGN	Peptidoglycan
PI3K	Phosphatidylinositol-3 kinase

PKB	Protein kinase B
PKD	Protein kinase D
PLK	Polo-like kinase
POU family	Pituitary-specific, Octamer TF, Unc-86 comprising family of TFs
ppm	Parts per million
PRR	Pattern recognition receptor
pS	Phosphorylated serine
pT	Phosphorylated threonine
PTB domain	Phospho-tyrosine-binding domain
PTEN	Phosphatase and tensin homologue deleted on chromosome 10
PTM score	Posttranslational modification score
pY	Phosphorylated tyrosine
RHD	Rel homology domain
RIP1	Receptor-interacting protein 1
RLH	RIG-like helicases
RMA	Robust multi-array average
RNA	Ribonucleic acid
RNAi	RNA interference
RNS	Reactive nitrogen species
ROS	Reactive oxygen species
rpm	Revolutions per minute
RPMI	Roswell Park Memorial Institute medium
RSV	Respiratory-syncytical-virus
RT	Room temperature
s	Second(s)
SCF	Stem cell factor
SCX	Strong cation exchange
SDS-PAGE	SDS-polyacrylamide gel electrophoresis
SH2 domain	Src-homology 2 domain
SILAC	Stable isotope labelling with amino acids in cell culture
SRF	Serum response factor
ssRNA	Single-stranded RNA
STAGE tip	Stop-and-go extraction tip

TAB	TAK1-binding protein
TAD	Transcriptional activation domain
TAK1	TGF- β -activated kinase
TANK	TRAF family member-associated NF- κ B activator
TBK1	TANK binding kinase 1
Tc	Cytotoxic T cell
TdT	Terminal deoxynucleotidyltransferase
TF	Transcription factor
TGF- β	Transforming growth factor-beta
Th1	T helper 1 cell
Th2	T helper 2 cell
TICAM1	TIR domain-containing adapter molecule 1
TiO ₂	Titansphere
TIR domain	Toll/IL-1 receptor homology domain
TIRAP	TIR-associated protein
TLR	Toll-like receptor
TNF	Tumour necrosis factor
TNFR	TNF receptor
TRAF6	TNFR-associated factor 6
TRAM	TRIF-related adaptor molecule
TRIF	TIR domain-containing adaptor protein
Ub	Ubiquitin
UBC13	Ubiquitin-conjugating enzyme 13
UEV1A	Ubiquitin-conjugating enzyme E2 variant 1
V	Volt
WT	Wild type
z	Charge

Amino acids and nucleotides are depicted according to IUPAC (<http://www.iupac.org>)

Summary

Recognition of microbial danger signals by Toll-like receptors (TLRs) causes substantial gene expression changes in macrophages. Chemokines, cytokines and anti-microbial effector molecules are produced and convey immediate innate host-defence as well as induction of a long-term protective adaptive response. While gene expression in response to TLR ligation has been analysed in several genome-wide studies, knowledge about the involved signalling pathways has been obtained by extensive analyses of single signalling components. A global study of phosphorylation in macrophages, the most common post-translational modification, has been hampered severely by lack of suitable technique. It was therefore unknown whether the described pathways comprised the main phosphorylation events, kinases and transcription factors (TFs), and which other molecular functions and biological processes could be regulated by phosphorylation in TLR-activated macrophages. The phosphoproteome study described here provides a novel, global perspective on TLR-induced innate immune signalling. To quantitatively investigate phosphorylation in response to the TLR4 ligand Lipopolysaccharide (LPS), Stable isotope labelling with amino acids in cell culture (SILAC) was established in primary bone marrow-derived macrophages and combined with phosphopeptide enrichment by Titansphere (TiO₂) and Strong cation exchange (SCX) chromatography, and high-resolution mass spectrometry. 1,850 phosphoproteins with 6,956 phosphorylation sites were reproducibly identified, two thirds of which were novel. LPS caused major dynamic changes in the phosphoproteome (24 % up- and 9 % down-regulation), demonstrating a massive activation of kinases that precedes transcriptional activation. By combining different bioinformatic data mining approaches, such as analyses for kinase motifs, Gene Ontology (GO) and signalling pathway annotation, canonical and novel TLR-activated signalling modules were consistently identified. In particular, the PI3K/AKT and related mTOR and GSK3 pathways, the cell cycle and Ca²⁺-dependent signalling were highlighted; furthermore, the cytoskeleton emerged as a novel and unexpected hotspot for phosphorylation. Finally, weaving together corresponding phosphoproteome and nascent transcriptome datasets through *in-silico* promoter analysis for binding sites for phosphorylated TFs, novel TFs were identified, which act at the intersection of TLR-induced kinase activation and gene expression.

1 Introduction

1.1 Innate and adaptive immunity

We are constantly exposed to infectious agents, and infectious diseases are a leading cause of morbidity and mortality world-wide. Hence, the detrimental effects of microbial infections led to the evolution of a variety of defence mechanisms. In mammals protection is accomplished by the interplay of two closely linked systems: While innate immunity is the first line of defence against invading pathogens, adaptive immunity comprises an antigen-specific, inducible response in the late phase of infection and immunological memory, protecting from re-infection with the same pathogen (Janeway, 2005).

Adaptive immunity relies on clonal selection of lymphocytes bearing highly diverse receptors, which are generated by somatic recombination of variable receptor gene segments. After encounter with specific antigen, B cells differentiate into memory cells and antibody-secreting plasma cells, while T cells differentiate into memory cells and effector cells with a variety of functions, such as killing of infected cells (cytotoxic T cells) and activation of phagocytes and B cells (T helper (Th) cells). While this response is capable of recognising any foreign antigen *specifically*, clonal selection takes time and requires professional antigen presentation. Innate immunity is therefore essential to control the potentially overwhelming growth of invading pathogens during the early phase of infection, and to prime adaptive immune responses (Janeway, 2005).

The innate system of defence is made up of several distinct components. First, the body's epithelia, low pH and antimicrobial peptides provide a physico-chemical barrier. Upon infection, soluble factors, for example the complement system and defensins, and cellular components, such as macrophages, dendritic cells (DCs), natural killer (NK) cells, polymorphonuclear leukocytes and mast cells, control and eventually eliminate the pathogen and can initiate an adaptive immune response (Medzhitov, 2007). Innate immune cells sense infectious danger through pattern recognition receptors (PRRs), a limited set of germ line-encoded receptors expressed mainly by macrophages and DCs (Akira et al., 2006). They recognise

highly conserved microbial structures common to many pathogens, so called pathogen associated molecular patterns (PAMPs). Signalling through these receptors rapidly induces an inflammatory response, mediated by substantial reprogramming of gene expression, which is pivotal for control of pathogen replication. This includes production of anti-microbial effector molecules, chemokines, which recruit leukocytes to the site of infection, and cytokines that initiate and control the adaptive immune response. Furthermore, cellular effector functions are important in innate immunity: Whereas NK cells can kill infected cells, phagocytes are crucial for killing of pathogens (macrophages and neutrophils), for presentation of foreign antigen to cells of the adaptive immune response (macrophages and DCs), and for clearing of apoptotic cells, once the immune response ceases (macrophages) (Medzhitov, 2007).

Recognising infectious danger, mediating inflammation and killing pathogens, macrophages are important players of the first line of defence. In this thesis, the phosphoproteome of macrophages triggered by ligation of the PRR Toll-like receptor 4 (TLR4) with the bacterial endotoxin Lipopolysaccharide (LPS), a cell wall component of Gram-negative bacteria, has been studied. The biology of macrophages and signalling pathways triggered by TLRs are therefore outlined in more detail below.

1.2 Biology of macrophages

Metchnikoff (1893) was the first person to use the term “macrophage” to describe a large cell able to take up microorganisms (Greek: big eaters, from *makros* “large” and *phagein* “eat”) (Sasmono and Hume, 2004). As mentioned above, recognising, engulfing and destroying pathogens as well as apoptotic cells and cellular debris is the main function of macrophages (Mosser and Edwards, 2008). Apart from pathogen killing, macrophages elicit an inflammatory response, which attracts and activates other cells of the innate and adaptive immune systems. Furthermore they play roles in wound healing, tissue remodelling and in regulation of haemo- and lymphopoiesis and homeostasis in adults as well as during development (Henson and Hume, 2006; Leibovich and Wiseman, 1988; Mosser and Edwards, 2008).

1.2.1 Macrophage differentiation

Macrophages are present in virtually all tissues. They originate from a common myeloid progenitor in the bone marrow, which sequentially gives rise to monoblasts, pro-monocytes, and monocytes circulating in the bloodstream. Upon migration into tissue, in steady state or during infection, monocytes differentiate into specific tissue macrophages, such as Kupffer cells in the liver or alveolar macrophages in the lung (Mosser and Edwards, 2008) (Fig. 1).

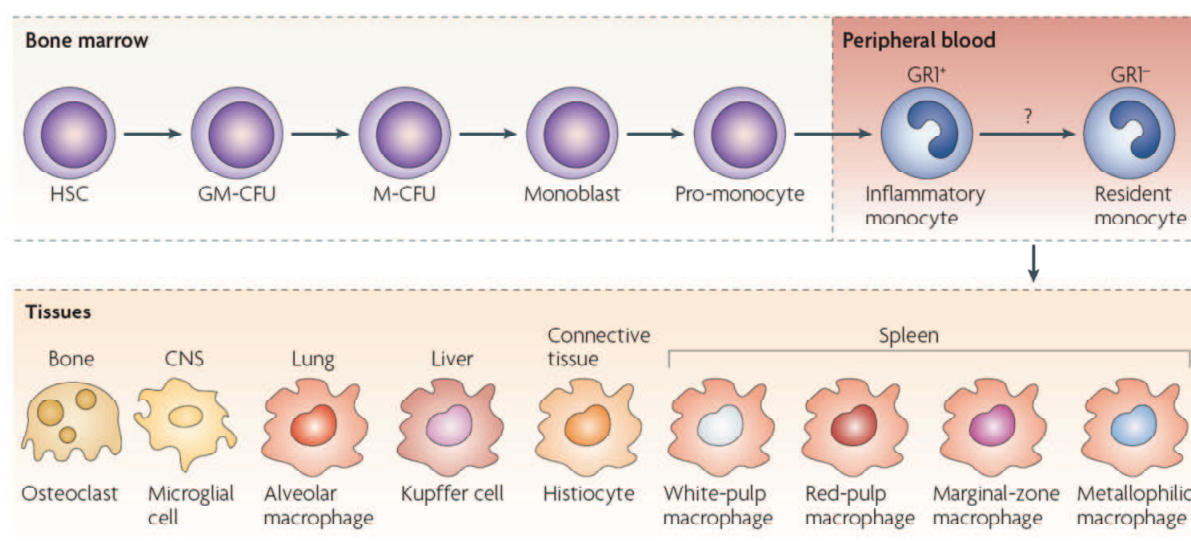


Fig. 1. Macrophage development and tissue distribution.

Monocytes originate in the bone marrow from a common haematopoietic stem cell (HSC). They undergo differentiation steps during which they commit to the myeloid and then to a monocyte lineage. In response to macrophage colony-stimulating factor, they divide and differentiate into monoblasts and then pro-monocytes before becoming monocytes, which exit the bone marrow and enter the bloodstream. Monocytes migrate to different tissues, where they replenish tissue-specific macrophages. (GM-CFU) granulocyte/macrophage colony forming unit, (M-CFU) macrophage colony forming unit, (GR1) granulocyte receptor 1, (CNS) central nervous system (Mosser and Edwards, 2008).

Growth and differentiation of macrophages depends on lineage-determining cytokines, such as Macrophage colony-stimulating factor (M-CSF) and Granulocyte-macrophage colony-stimulating factor (GM-CSF), Interleukin-6 (IL-6), Interleukin-3 (IL-3), Stem cell factor (SCF), Interleukin-1 (IL-1), Leukaemia inhibitory factor (LIF) and Interferon- γ (IFN- γ) (Lee, 1992; Metcalf, 1989, 1997), and on interactions with stroma in haematopoietic organs (Gordon, 2003). Amongst the above factors, M-CSF is the only one that is clearly absolutely required for macrophage differentiation and proliferation *in vivo*. As the sole added factor, M-CSF can also direct macrophage differentiation from bone marrow progenitors *in vitro* (Hume and

Gordon, 1983; Stanley et al., 1997; Tushinski et al., 1982). Surface antigens defining macrophages are F4/80 in the mouse, and CD68 in human as well as the mouse (Gordon et al., 1992). CD11b, another widely-employed macrophage marker, is also expressed on NK cells, granulocytes and subsets of B and T lymphocytes (Lai et al., 1998).

1.2.2 Phagocytosis

Several macrophage receptors induce phagocytosis of opsonised or non-opsonised pathogens and dying cells. Examples are Fragment, crystallisable (Fc), receptors, complement receptors, scavenger receptors and the Macrophage mannose receptor (MMR) (Gordon, 2003). Phagosome formation and fusion with lysosomes are accompanied by cytoskeletal rearrangements mediated by Rho family GTPases (Greenberg and Grinstein, 2002). Rho GTPases also play a role in adhesion and migration (Ridley, 2008), another key feature of macrophages. In phagolysosomes, killing of pathogens is accomplished by acidification and production of reactive oxygen (ROS) and nitrogen species (RNS), antimicrobial peptides (e.g. defensins) and proteins (e.g. the iron scavenger Lactoferrin) or lysosomal proteases (e.g. Cathepsin H and S). Besides killing pathogens and degrading apoptotic cells, phagocytosis is important for presentation of degraded antigen for adaptive immune responses. Certain bacterial species have developed strategies to evade phagosomal degradation (Flannagan et al., 2009).

1.2.3 Microbial danger signals and cytokines – regulators of macrophage activity

Forming the first line of defence, macrophages possess a number of pattern recognition receptors (PRRs) that sense microbial danger signals common to many different pathogens (section 1.1). PRRs include C-type lectin receptors (CLRs), NOD-like receptors (NLRs), cytosolic sensors of RNA and DNA (RIG-like helicases (RLH) and DNA-dependent activator of Interferon regulatory factors (DAI)), and the Toll-like receptors (TLRs) (Latz, 2008), which are the best characterised group of PRRs (Takeda and Akira, 2004). Signalling through these receptors causes, within hours, substantial reprogramming of gene expression, which is pivotal for host defence and includes production of inflammatory cytokines and chemokines

(section 1.1). As signalling through TLR4, the best characterised member of the TLR family, is the topic of this thesis, TLRs and the induced signalling pathways are described in more detail in chapter 1.3.

Furthermore, different activation states of macrophages are induced by cytokine receptors, which transmit signals from other immune cells (Fig. 2). Classical activation is mediated by Interferon- γ (IFN- γ), produced by activated CD4⁺ T helper 1 cells (Th1) and CD8⁺ cytotoxic T cells (Tc) during an adaptive immune response, or during an innate response by NK cells. This cytokine converts resting macrophages into potent effectors for killing of bacteria, especially of intracellular pathogens, and perhaps tumours: Characteristic are increased secretion of pro-inflammatory cytokines, such as Interferon- α/β (IFN- α/β), Interleukin-1 (IL-1), Tumour-necrosis factor (TNF), Interleukin-6 (IL-6), chemokines like Macrophage inflammatory protein-1a (MIP-1a or CCL3), production of ROS and RNS, and expression of co-stimulatory molecules like MHC class II and CD86 favouring antigen presentation (Gordon and Taylor, 2005; Mosser and Edwards, 2008). Inflammatory cytokine production and production of ROS and RNS are also triggered by stimulation of PRRs alone, which is then termed “innate activation”, or in synergism of PRR stimulation with IFN- γ (Gordon and Taylor, 2005) (Fig. 2). In contrast to the classical and innate activation states, macrophages alternatively activated by Interleukin-4 (IL-4) and Interleukin-13 (IL-13) from CD4⁺ T helper 2 cells (Th2) develop a phenotype is that promotes multi-cellular parasite killing, tissue repair and suppresses inflammation (Martinez et al., 2009). To limit potentially harmful inflammatory reactions, macrophage activation is followed by a regulated anti-inflammatory response, involving the immunosuppressive cytokines Interleukin-10 (IL-10) and Transforming growth factor-beta (TGF- β), steroids and intrinsic negative regulators of signalling cascades (Liew et al., 2005), as described in section 1.3.5.

Much of the evidence that macrophages acquire distinct phenotypes and physiological activities has been observed *in vitro*. If these phenotypes are distinct *in vivo* or whether they indicate a continuum of physiological responsiveness is still not completely understood, but now being facilitated by recent advances in following the fate of the monocytes lineage *in vivo* through identification and adoptive transfer

of monocytes subsets, in conjunction with single-cell analysis (Gordon and Taylor, 2005).

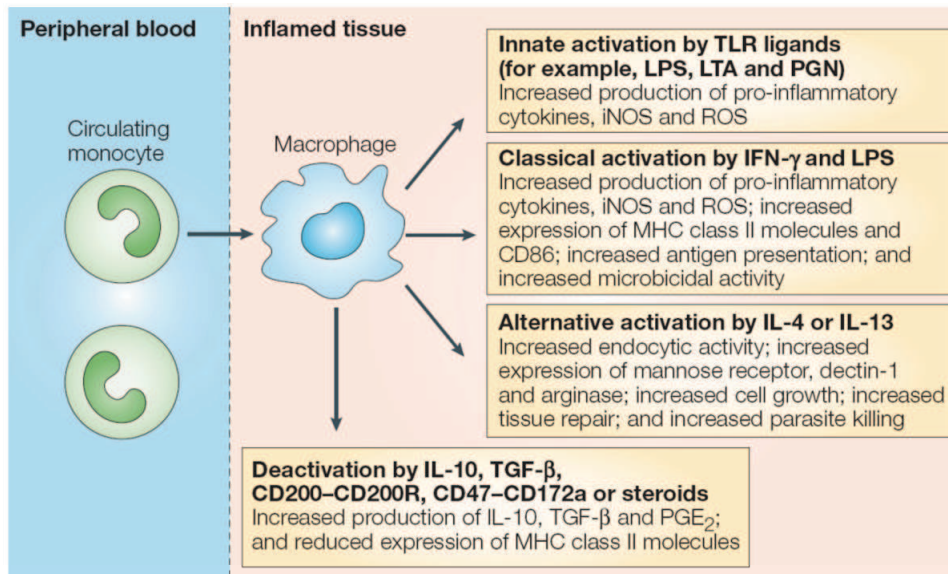


Fig. 2. Macrophage activation states and effector functions.

Macrophages can be activated by TLR ligands, or by cytokines secreted through other immune cells. When stimulated with Interferon- γ (IFN- γ) (classical activation) or TLR ligands (innate activation), macrophages show high microbicidal activity and produce pro-inflammatory cytokines, reactive oxygen and nitrogen species. In contrast, when cultured with Interleukin-4 (IL-4), IL-13 (alternative activation), IL-10 or Transforming growth factor-beta (TGF- β) (de-activation), a phenotype is generated that promotes tissue repair and suppresses inflammation. (iNOS) Inducible nitric-oxide synthase, (LPS) Lipopolysaccharide, (LTA) Lipoteichoic acid, (PGE₂) Prostaglandin E₂, (PGN) Peptidoglycan, (TLR) Toll-like receptor, (TNF) Tumour-necrosis factor. (Gordon and Taylor, 2005).

1.3 Toll-like receptors (TLRs)

Toll, the founding member of the TLR family, was originally identified in *Drosophila melanogaster* as an essential receptor for the establishment of the dorso-ventral pattern in developing embryos (Hashimoto et al., 1988). Only later, it was also shown to play a critical role in the antifungal response of adult flies (Lemaitre et al., 1996). The year after, a mammalian homologue of *Drosophila* Toll, now termed TLR4, was found to induce the expression of genes involved in inflammatory responses (Medzhitov et al., 1997). Subsequently, in mice hypo-responsive to LPS, a mutation in the *Tlr4* gene was discovered, proving that LPS is the natural ligand of TLR4 and definitely linking the receptor to innate immune responses (Poltorak et al., 1998). To date, 13 members of the TLR family have been identified in mammals, ten in humans and twelve in mice (Beutler, 2004). TLRs 1 to 9 are conserved between mice and

humans, TLR10 can be found exclusively in humans (Chuang and Ulevitch, 2001) and TLR11 is only functionally active in mice and not expressed in humans (Zhang et al., 2004).

1.3.1 Ligand specificities and expression

While the biological roles of TLR10, 12 and 13 still need to be identified, the molecular specificity of most TLRs is clear: they are capable of detecting PAMPs, conserved molecular motifs found in a wide range of organisms ranging from bacteria to viruses, fungi and protozoa (West et al., 2006). Fig. 3 gives an overview of the known ligand specificities of TLRs, which can be sub-divided into several families: TLR1, TLR2 and TLR6 recognise lipids, TLR3, TLR7, TLR8 and TLR9 are specific for nucleic acid-like structures, TLR5 was described as the receptor activated by flagellin, and TLR4 recognises LPS (Akira and Takeda, 2004). LPS, a glycolipid located in the outer membrane of Gram-negative bacteria, is composed of an amphipathic lipid A component and hydrophilic polysaccharides of the core and O-antigen (Raetz, 1990; Raetz and Whitfield, 2002). It is extracted from the bacterial membrane and transferred to a complex of TLR4 and MD-2 by the circulating LPS binding protein (LBP) and the membrane protein CD14 (Miyake, 2006) (see below and Fig. 4).

TLRs are expressed by various immune cells including macrophages, DCs, B cells, specific types of T cells, and even by non-immune cells such as fibroblasts, endothelial and epithelial cells in various combinations (Akira et al., 2006). Macrophages and DCs, as the main sentinels of the innate immune system, express most of them constitutively (Hopkins and Sriskandan, 2005). Expression is modulated rapidly in response to pathogens, a variety of cytokines and environmental stresses (Akira et al., 2006). Certain TLRs (TLR1, 2, 4, 5 and 6) are located on the cell surface, while others (TLR3, 7, 8 and 9) are restricted intracellularly within endosomal compartments and require internalisation of their ligands to be detected (Akira et al., 2006). For TLR4, sequential signalling from the plasma membrane and the endosomal compartment has been proposed (Kagan et al., 2008).

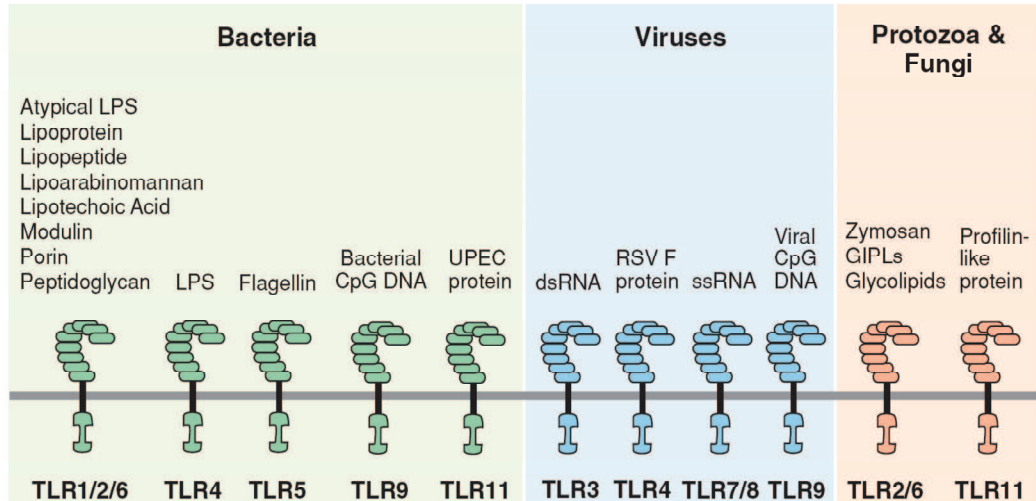


Fig. 3. Toll-like receptors (TRLs) and their ligand specificities.

TLRs recognise a diverse array of pattern associated molecular patterns (PAMPs) from bacteria, viruses, protozoa and fungi. For detection of bacteria, heterodimeric TLR2/1 binds triacyl lipopeptides, whereas TLR2/6 dimers bind diacyl lipopeptides and Lipoteichoic acid. Homodimeric TLR2 binds Peptidoglycan, atypical LPS, Phenol-soluble modulin from *Staphylococcus epidermidis*, and porin proteins from *Neisseria*. TLR4 binds LPS, TLR5 flagellin and TLR9 bacterial CpG DNA. TLR11 detects an unidentified protein(s) from uropathogenic *Escherichia coli*. Viral dsRNA, Respiratory-syncytial-virus (RSV) F protein, ssRNA, and un-methylated CpG motifs are recognised by TLR3, 4, 7/8, and 9, respectively. For antifungal responses, a TLR2/6 dimer senses zymosan, as well as glycolipids and glycoproteins from *Trypanosoma cruzi*. Finally, TLR11 can also recognise Profilin-like protein from *Toxoplasma gondii*. Adapted from West et al., 2006.

1.3.2 Structure and function

TLRs are type I integral membrane glycoproteins characterised by the extracellular/endosomal domains containing varying numbers of leucine-rich repeat (LRR) motifs and a cytoplasmic signalling domain homologous to that of the Interleukin 1 receptor (IL-1R), termed the Toll/IL-1R homology (TIR) domain, which also occurs in IL-1 and IL-18 receptors (Akira and Takeda, 2004). The TIR domain comprises three conserved regions termed boxes 1, 2 and 3, which are crucial for signalling. Amino acid sequence conservation among the TIR domains is generally 20 to 30 %, and the domains vary in size (~ 200 amino acids). This diversity might be crucial for the specificity of signal transduction among the different TLRs by ensuring specific complex formation with the proper adapter molecules. The extracellular/endosomal LRRs differ markedly between TLRs and are responsible for direct recognition of various pathogens. They are composed of 19 to 25 tandem LRR motifs, each of which is 24 to 29 amino acids in length, containing the motif XLXXLX₂LXX and another conserved sequence XØXXØX₄FXXLX (Ø = hydrophobic

residue) (Akira and Takeda, 2004). Three crystal structures of TLR-ligand complexes have been reported (Jin et al., 2007; Kim et al., 2007; Liu et al., 2008a; Ohto et al., 2007), including that of the TLR4-MD-2-LPS complex (Park et al., 2009a). They show that TLRs differ in the way of ligand recognition: hydrophobic ligands of TLR1, 2 and 4 interact with internal protein pockets, while dsRNA, a hydrophilic ligand, interacts with the solvent-exposed surface of TLR3 (Jin and Lee, 2008). Binding induces dimerisation of the ectodomains of the various TLRs, forming “m”-shaped complexes (Jin and Lee, 2008), in the case of LPS a multimer composed of two copies of the TLR4-MD-2-LPS complex (Park et al., 2009a) (Fig. 4). Ligand-induced dimerisation is believed to trigger recruitment of adaptor proteins to the intracellular TIR domains and to initiate signalling (O'Neill and Bowie, 2007).

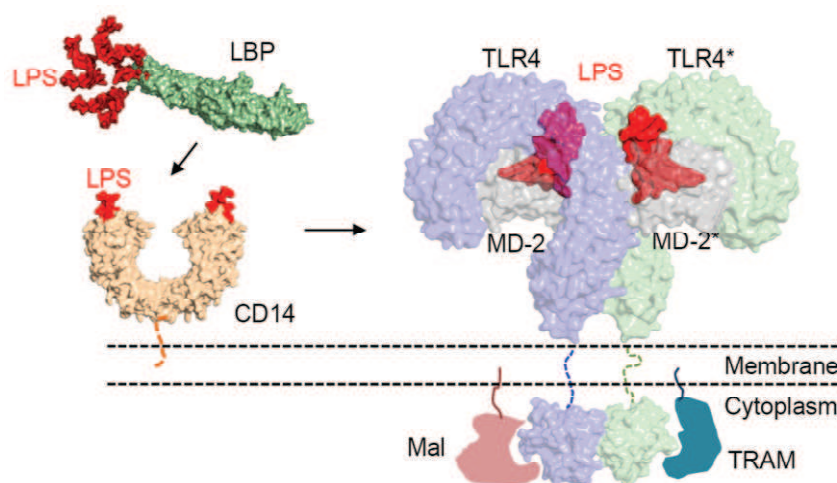


Fig. 4. Recognition of Lipopolysaccharide (LPS) by LPS binding protein (LBP), CD14 and the TLR4-MD-2 complex.

Circulating LBP binds LPS, which is transferred via CD14 to the TLR4-MD-2 receptor complex. LPS binding induces the formation of an “m”-shaped multimer composed of two copies of the TLR4-MD-2-LPS complex arranged symmetrically. LPS interacts with a large hydrophobic pocket in MD-2 and directly bridges the two components of the complex. Ligand induced dimerisation triggers recruitment of adaptor proteins like MyD88-adaptor-like protein (Mal, also known as TIRAP) and TRIF-related adaptor molecule (TRAM), which initiate signalling. Adapted from Park et al., 2009a.

1.3.3 TLR signalling pathways

Unique among the TLR family, TLR4 engages two distinct pairs of adaptor proteins (Takeda and Akira, 2005): (i) Myeloid differentiation primary-response protein 88 (MyD88), which is recruited by TIR-associated protein/MyD88-adaptor-like (TIRAP)/(MAL), signals via Mitogen-activated protein kinase (MAPK) and Nuclear factor 'kappa-light-chain-enhancer' of activated B cells (NF-κB) pathways and elicits

the production of pro-inflammatory cytokines; (ii) and TIR domain-containing adaptor protein-inducing IFN- β /TIR domain-containing adapter molecule 1 (TRIF)/(TICAM1), which is recruited by TRIF-related adaptor molecule (TRAM) and activates the production of type I Interferons (IFNs) and of pro-inflammatory cytokines (O'Neill and Bowie, 2007) (Fig. 5). These core pathways have been analysed in detail and proceed as follows (sections 1.3.3.1 and 1.3.3.2):

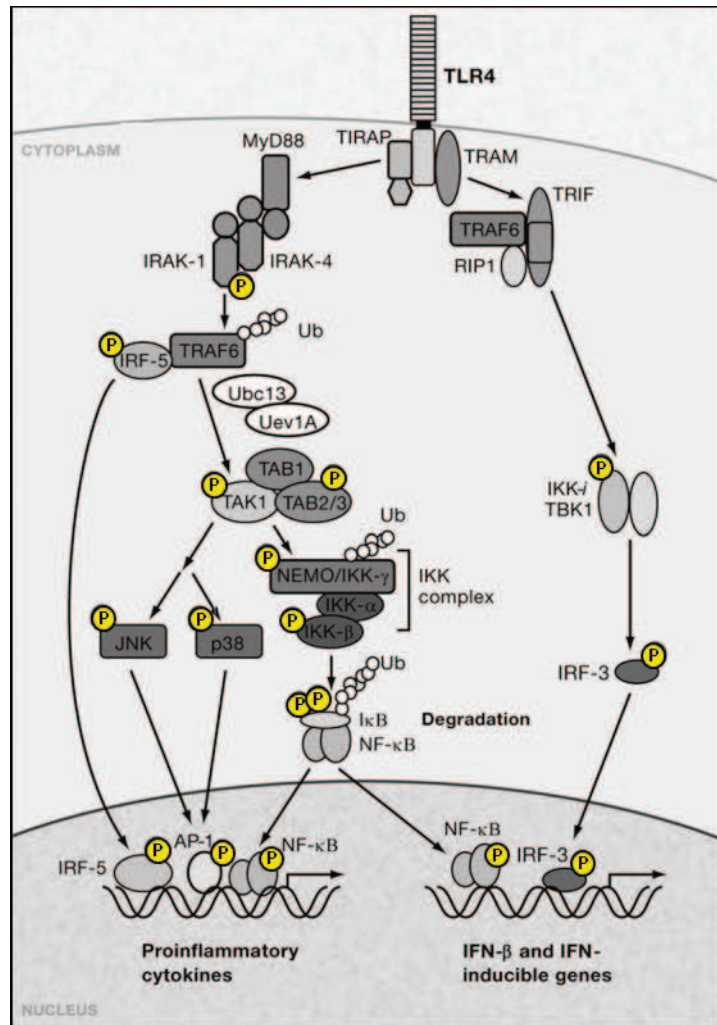


Fig. 5. Canonical signalling pathways triggered by TLR4.

LPS stimulation of TLR4 induces, via the adaptor proteins MyD88 and TRIF, activation of the MAPK, NF- κ B and Interferon regulatory factor (IRF) signalling pathways, resulting in production of pro-inflammatory cytokines, IFN- β and IFN-inducible genes. Details are given in the text (sections 1.3.3.1 and 1.3.3.2). (P) Phosphorylation. (Ub) Ubiquitin (indicated by white circles attached to a protein). Adapted from Akira et al., 2006.

1.3.3.1 Inflammatory cytokine production via MAPKs and NF- κ B

MyD88 is critical for the signalling from all TLRs except TLR3. Upon stimulation, MyD88 associates with the cytoplasmic portion of TLRs and then recruits IL-1R-associated kinase 4 (IRAK-4) and IRAK-1 through a homophilic interaction of the

death domains. In TLR2 and TLR4 signalling, TIRAP/Mal is required for recruiting MyD88 to the receptor. IRAK-1 is phosphorylated by the activated IRAK-4 and subsequently associates with TNF receptor (TNFR)-associated factor 6 (TRAF6), which acts as an ubiquitin protein ligase (E3). Phosphorylated IRAK1 and TRAF6 then dissociate from the receptor and form a complex with TGF- β -activated kinase (TAK1) and TAK1-binding proteins (TAB1, TAB2/3), which induces the phosphorylation of TAB2 and TAK1. IRAK1 is degraded and the remaining complex associates with the ubiquitin ligases Ubiquitin-conjugating enzyme 13 (UBC13) and Ubiquitin-conjugating enzyme E2 variant 1 (UEV1A). This leads to the ubiquitination of TRAF6, which induces the activation of TAK1. TAK1, in turn, phosphorylates both MAPKs and the Inhibitor of NF- κ B (I κ B)-kinase (IKK) complex, which consists of IKK- α , IKK- β , and NF- κ B essential modulator NEMO (also known as IKK- γ), and after degradation releases the transcription factor (TF) NF- κ B for translocation to the nucleus. MAPKs phosphorylate and activate TFs of the Activating protein 1 (AP-1) and cAMP-response element binding protein (CREB) families, and other molecular effectors in the nucleus and cytosol, such as proteins involved in mRNA stability (Hao and Baltimore, 2009). In addition, Interferon regulatory factor 5 (IRF5) is activated downstream of TRAF6. All three - NF κ B, CREB/AP-1 and IRF - pathways result in induction of genes involved in inflammatory responses (section 1.3.4) (Akira and Takeda, 2004; Akira et al., 2006; Latz, 2008; Lu et al., 2008; Palsson-McDermott and O'Neill, 2004; Takeda and Akira, 2004, 2005).

1.3.3.2 Type I Interferon production via Interferon regulatory factors

Stimulation with TLR3, TLR4, TLR7 and TLR9 ligands, but not the TLR2 ligand, induces type I IFN production in addition to pro-inflammatory signals (Honda and Taniguchi, 2006). TLR3 and TLR4 have the ability to induce IFN- β and IFN-inducible genes in MyD88-deficient cells. This MyD88-independent pathway is initiated by the adaptor TRIF, and in TLR4 signalling additionally involves TRAM. TRIF interacts with Receptor-interacting protein 1 (RIP1), which is responsible for the activation of NF- κ B. On the other hand, TRIF activates TRAF-family-member-associated NF- κ B activator (TANK) binding kinase 1 (TBK1) via TRAF3. TBK1 comprises a family with inducible I κ B kinase (IKK-i, also known as IKK- ϵ) and these kinases directly phosphorylate IRF-3 and IRF-7, which enter the nucleus and induce transcription of

type I IFNs and IFN-inducible genes. Signalling through TLR4 results in induction of the *Ifnb* but not the *Ifna* genes and IRF3, rather than IRF7, is essential for this pathway (Honda and Taniguchi, 2006).

1.3.3.3 Emerging role of additional signalling pathways

In addition to the core pathways described above, the Phosphatidylinositol-3 kinase (PI3K) and Protein kinase B (PKB or AKT) signalling module has been shown to be activated by TLR stimulation. Activated PI3K generates 3-phosphorylated inositol lipid products, which serve as membrane targeting signals for proteins containing pleckstrin homology domains, including AKT and its activating kinase Phosphoinositide-dependent kinase 1 (PDK1). The effects of PI3K/AKT are further relayed by divergent signalling via Glycogen synthase kinase 3 (GSK3) or the Mammalian target of Rapamycin (mTOR). PI3K signalling pathways are counteracted by Phosphatase and tensin homologue deleted on chromosome 10 (PTEN), a 3-phosphoinositide-specific lipid phosphatase (Koyasu, 2003).

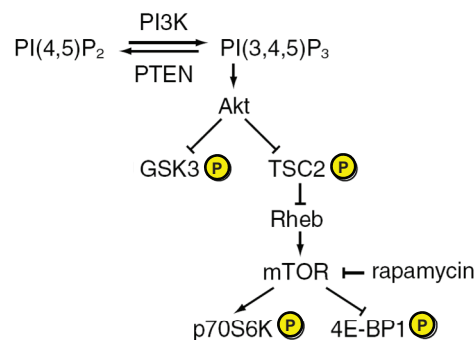


Fig. 6. Overview of the PI3K signalling pathway.

Phosphatidylinositol-(3,4,5) trisphosphate (PI(3,4,5)P₃) generated by PI3K triggers AKT, which regulates the diverging GSK3 and mTOR pathways. Adapted from Othani et al., 2008.

PI3K is mainly known to regulate diverse aspects of T and B lymphocyte behaviour (Fruman and Bismuth, 2009), but also plays a role in innate immunity, for example in neutrophil migration, Fc receptor signalling, and development of the oxidative burst (Deane and Fruman, 2004; Koyasu, 2003). In response to TLR ligation, PI3K has been assigned a negative regulatory role as feedback inhibitor for IL-12 production (Fukao and Koyasu, 2003).

Thus, phosphorylation is an important post-translational modification in the signalling cascades triggered by TLR ligation.

1.3.4 Transcriptional activation of gene expression

The consequences of TLR signalling have been studied extensively in several genome-wide studies (Foster et al., 2007; Huang et al., 2001; Lang et al., 2002; Mages et al., 2007; Nau et al., 2002): Stimulation of macrophages *in vitro* with the TLR4 ligand LPS causes within a few hours substantial reprogramming of gene expression. This rapid response is pivotal for control of pathogen replication, and includes production of chemokines, which recruit leukocytes to the site of infection, anti-microbial effector molecules and cytokines that initiate and control the adaptive immune response (section 1.2.3), anti-viral type I IFNs (in the case of TLR4 only IFN- β), but also negative feedback regulators (section 1.3.5). Major families of TFs activated in response to TLR activation are the NF- κ B, AP-1, CREB and IRF families mentioned above (sections 1.3.3.1 and 1.3.3.2). Besides a function in signal transduction cascades, phosphorylation plays an essential role in TF activation:

1.3.4.1 Nuclear factor 'kappa-light-chain-enhancer' of activated B-cells (NF- κ B) family

In the case of NF- κ B, phosphorylation of the I κ B-kinase complex is the first step in the process leading to I κ B degradation and release of active NF- κ B for translocation to the nucleus (Vallabhapurapu and Karin, 2009). The NF- κ B family consists of NF- κ B1 (p50 and its precursor p105) and NF- κ B2 (p52 and its precursor p100), and Rel proteins (RelA, also called p65, c-Rel and RelB), all of which are characterised by an N-terminal Rel homology domain (RHD) responsible for homo- and heterodimerisation as well as for sequence-specific DNA binding. The Rel proteins also contain a C-terminal transcriptional activation domain (TAD), whereas the p52 and p50 subunits do not and therefore rely on interactions with other factors to positively regulate transcription. A number of post-translational modifications at different parts of these molecules, including phosphorylation and acetylation, further modulate DNA binding and transcriptional activation activities (Vallabhapurapu and Karin, 2009). In response to TLR activation, NF- κ B activates transcription of pro-inflammatory cytokines as well as type I IFNs (Akira and Takeda, 2004; Akira et al., 2006; Latz, 2008).

1.3.4.2 Activating protein-1 (AP-1) family

Activated MAPKs translocate to the nucleus and phosphorylate TFs of the AP1-family, the activity of which is highly regulated by these post-translational modifications (Eferl and Wagner, 2003; Shaulian and Karin, 2002). AP-1 is a dimeric TF complex that contains members from the Jun oncogene (JUN), FBJ osteosarcoma gene (FOS), Activating transcription factor (ATF) and Avian musculoaponeurotic fibrosarcoma oncogene (MAF) protein families in various combinations. AP-1 regulates a wide range of cellular processes, including cell proliferation, death, survival and differentiation. In response to TLR ligation, AP-1 activates expression of inflammatory cytokines such as TNF- α , IL-6, IL-8 and IL-1 β (Akira et al., 2006; West et al., 2006).

1.3.4.3 cAMP-responsive element binding protein (CREB) family

CREB family TFs are also phosphorylated by MAPKs, in response to TLR4 ligation with LPS in macrophages particularly by p38 (Bradley et al., 2003; Park et al., 2005). They bind as dimers to a conserved cAMP-responsive element (CRE) (TGACGTCA) similar to the closely related AP-1 site (TGACTCA), or to a less active half site motif (CGTCA). Phosphorylation of CREB at S133 promotes recruitment of the transcriptional co-activators CREB-binding protein (CBP) and its paralogue p300 (Mayr and Montminy, 2001) and is required for example for CCAAT enhancer binding protein (C/EBP) (Bradley et al., 2003) and IL-10 (Hu et al., 2006) expression. ATF proteins have been assigned to both, the AP-1 and the CREB families in the literature (see also section 1.3.4.2), but will here be dealt with as CREB family members, since they are assigned so in the Genomatix description of the DNA binding site used in this thesis (<http://www.genomatix.de>). Phosphorylation of ATF2 induces LPS-target genes, among them *Socs3* (Hirose et al., 2009). ATF3 binds closely to NF- κ B and negatively regulates transcription of important cytokines such as IL-6 and IL-12b (Gilchrist et al., 2006).

1.3.4.4 Interferon regulatory factor (IRF) family

IRF family TFs form dimers after phosphorylation, enabling them to enter the nucleus and transactivate promoters with IFN-stimulated response elements (ISREs) of genes with various roles in development and function of immune cells (Honda and Taniguchi, 2006). In response to TLR activation, these are genes for type I IFNs and

IFN-inducible genes as well as pro-inflammatory cytokines (Akira et al., 2006; Honda and Taniguchi, 2006; Latz, 2008). *Ifnb* gene induction in response to TLR4 ligation is usually mediated by an IRF3 homodimer that has been activated by phosphorylation through TBK1. In addition, induction of the *Nitric-oxide synthase 2* (*iNOS* or *Nos2*) gene depends on IRF1 in LPS-stimulated macrophages (Kamijo et al., 1994), and IRF5 regulates the expression of cytokine genes (Takaoka et al., 2005).

1.3.5 Negative regulation of TLR signalling

Although essential for provoking the innate response and enhancing adaptive immunity against pathogens, inflammation is potentially harmful to the host and needs to be tightly controlled to prevent immunopathology. Inappropriate control can lead to autoimmunity and hyper-inflammation, and members of the TLR family have been implicated in the pathogenesis of various diseases, including sepsis (Cook et al., 2004; Gao et al., 2008). Down-regulation of macrophage activity is mediated by multiple mechanisms, which are reviewed in Liew et al., 2005. Many of them are induced as negative-feedback regulators by TLR signalling itself. Apart from the PI3K pathway described in section 1.3.3.3, they involve soluble mediators such as the immunosuppressive cytokine IL-10 (Lang, 2005; Lang et al., 2002). On the level of signal transduction, down-regulation is reflected by the transient activation of key signalling modules: NF- κ B signalling is down-regulated by re-synthesis of I κ B protein and export of NF- κ B from the nucleus (Vallabhapurapu and Karin, 2009). De-phosphorylation and in-activation of MAPKs is brought about by members of the MAPK phosphatase family (reviewed in Lang et al., 2006; Liu et al., 2007), for example by Dual specificity phosphatase 1 (DUSP1), which can de-phosphorylate p38 MAPK at both, threonine and tyrosine residues. DUSP1 expression is induced by LPS in macrophages and prevents excessive cytokine production and death in the LPS-shock model in mice, by deactivating p38 (Chi et al., 2006; Hammer et al., 2006; Lang et al., 2006; Salojin et al., 2006; Zhao et al., 2006).

1.3.6 Requirement of a phosphoproteome study

Thus, many aspects of TLR signalling have been studied extensively. A recent review of TLR signalling compiled a network of 340 proteins and 444 reactions involved (Oda and Kitano, 2006). However, although phosphorylation plays important roles in signal transduction as well as TF activation, a comprehensive analysis of phosphorylation events in macrophages in response to TLR stimulation is missing. A former study restricted to tyrosine phosphorylation was further limited by its non-quantitative nature and did not use primary cells (Aki et al., 2005). Furthermore, studies to discover new TFs in the response to TLR ligation so far only rely on the inference of transcriptional networks from microarray gene expression analyses combined with promoter motif scanning (Nilsson et al., 2006; Ramsey et al., 2008). They do not account for the fact that many TFs are regulated not on the level of expression but post-translationally.

Therefore, it is unknown (i) whether the pathways described above comprise the main phosphorylation events, kinases and TFs for gene expression reprogramming, and (ii) which other molecular functions and biological processes are regulated by phosphorylation in LPS-activated macrophages. In addition to contributing to the mechanistic understanding of the molecular aspects of cellular physiology, information on protein phosphorylation permits – as it has been shown for diseases such as cancer and diabetes (Blume-Jensen and Hunter, 2001; De Meyts and Whittaker, 2002; Zanivan et al., 2008) – pinpointing of drug targets, thus rationalising the development of kinase-specific, therapeutic strategies. And there is great interest in inhibitory agents that may prevent the excessive inflammatory response in sepsis (Gao et al., 2008).

Recent progress in mass-spectrometry based proteomics driven by leaps in instrument performance and advances in computational proteomics have opened the possibility to quantitatively investigate changes in protein abundance and post-translational modifications, including phosphorylation, on a global level (Cox and Mann, 2007). This thesis comprises a phosphoproteome analysis in macrophages activated with the TLR ligand LPS, making use of these newly developed strategies. Thus, the following chapter (section 1.4) gives an overview of the current methods in quantitative phosphoproteomics.

1.4 Quantitative phosphoproteomics

1.4.1 Protein phosphorylation

Protein phosphorylation is a key posttranslational modification, which regulates various molecular aspects such as the structure, activity, localisation, binding properties or stability of about one third of all proteins in a eukaryotic cell (Schreiber et al., 2008). Thereby, it has a major influence on various essential functions, including signal transduction, regulation of TF activity, cell cycle control, differentiation and metabolism. Importantly, phosphorylation is reversible and occurs rapidly: Protein kinases and phosphatases recognising specific target sequences continuously control phosphorylation (usually with adenosine triphosphate (ATP) as a donor) and de-phosphorylation, respectively (Macek et al., 2009). Autophosphorylation of the Epidermal growth factor receptor (EGFR), for example, has been shown to occur within 1 s after ligand stimulation (Dengjel et al., 2007). In signal transduction, protein phosphorylation often presents an activating or de-activating switch of protein activity (Macek et al., 2009).

In cells, phosphate groups are predominantly attached to the hydroxyl groups in serine, threonine and tyrosine residues, which is termed O-phosphorylation (Reinders and Sickmann, 2005). N-, S- and acyl-phosphorylation are far less spread and occur mostly on histidine and lysine (N-), cysteine (S-) and aspartic and glutamic acid residues (acyl-phosphorylation). Due to bioinformatic limitations when performing database searches, analysis of phosphorylation in this thesis is restricted to the most common forms: serine, threonine and tyrosine phosphorylation. While ubiquitously distributed, phosphoproteins are typically of low abundance. Furthermore, their levels of phosphorylation vary widely, and specific sites may be phosphorylated from less than 1 % to greater than 90 % (Macek et al., 2009).

Although phosphorylation is easily detected and visualised in 1D- and 2D-gels by radioactive phosphor-32 (^{32}P)-labelling or by Westernblotting with phosphorylation site-specific antibodies, it is far more challenging to identify *novel* phosphoproteins and, in particular, to *localise* their phosphorylation sites: Classical techniques such as phosphopeptide mapping and peptide sequencing by Edman degradation, often combined with mutational analysis, are time-consuming and can only be done in

low-throughput (Schreiber et al., 2008). In addition to simple detection of phosphorylation sites, *quantitative* studies of dynamic phosphorylation events are important to delineate and understand cell signalling pathways. Mass spectrometry is an ideal detector of phosphorylation events, fulfilling these criteria (Macek et al., 2009). Only during the last few years have mass spectrometry-based methods become sufficiently sensitive and robust to be used routinely and in large scale in cell signalling research: The recent years have witnessed a breakthrough in mass spectrometry-based phosphoproteomics, such that hundreds or thousands of phosphorylation sites can be obtained in single experiments (Ballif et al., 2004; Beausoleil et al., 2004; Ficarro et al., 2002; Kruger et al., 2008; Larsen et al., 2005; Olsen et al., 2006; Pan et al., 2008; Trost et al., 2009; Villen et al., 2007).

1.4.2 Fractionation and phosphopeptide enrichment strategies

Mass spectrometry-based proteomics usually involve the enzymatic digestion of proteins into peptides, which typically consist of six to 20 amino acid residues. To reduce sample complexity, peptide samples are separated by on-line reverse phase liquid chromatography, prior to tandem mass spectrometry (LC-MS/MS) (Aebersold and Mann, 2003). Furthermore, fractionation can be obtained by separation on a 1D SDS-polyacrylamide gradient gel (Fig. 9).

Due to the low abundance of phosphoproteins and the sub-stoichiometric nature of phosphorylation (section 1.4.1), phosphopeptides need to be enriched in addition, in order to be efficiently measured in the mass spectrometer. Many different strategies have been reported. The most successful to date have been affinity- and antibody-based methods, such as binding to phospho-specific antibodies, affinity binding to kinase domains, metal chelation and ion exchange chromatography (Macek et al., 2009). While good antibodies are available for the purification of tyrosine phosphorylated proteins and peptides, the smaller phospho-serine and -threonine residues are less immunogenic, so immunoprecipitation is commonly only done with phospho-tyrosine specific antibodies (Schreiber et al., 2008). Since MAPKs, which are an important module of the TLR signalling pathway (section 1.3.3.1), are serine/threonine kinases, an analysis targeting all three, serine, threonine and tyrosine phosphorylation, was desired. Phosphopeptide enrichment in this thesis therefore builds on a previously described strategy developed by Mann and co-

workers (Olsen et al., 2006) involving Titansphere (TiO_2) and Strong cation exchange (SCX) chromatography (Fig. 9), which are described below:

1.4.2.1 Titansphere (TiO_2) enrichment

TiO_2 particles are stable with regards to mechanical, chemical and thermal stress. Organic phosphates are effectively adsorbed to TiO_2 in acidic and desorbed in alkaline conditions, making TiO_2 suitable for selective enrichment of phosphopeptides (Ikeguchi and Nakamura, 1997). Heck and co-workers demonstrated that TiO_2 chromatography can achieve a very high enrichment efficiency (90 %) for phosphopeptides in simple samples (Pinkse et al., 2004). For complex samples, non-specific binding of acidic amino acids like glutamic and aspartic acid can be reduced by 2,5-dihydroxy benzoic acid (DHB) as a competitor (Larsen et al., 2005), because the binding strengths to TiO_2 decrease from phosphopeptide to DHB to acidic peptides (Fig. 7). This approach shows even higher affinity and selectivity for phosphopeptides than the previously described Immobilised metal affinity chromatography (IMAC), which relies on high-affinity coordination of phosphates to certain trivalent metal ions (Macek et al., 2009).

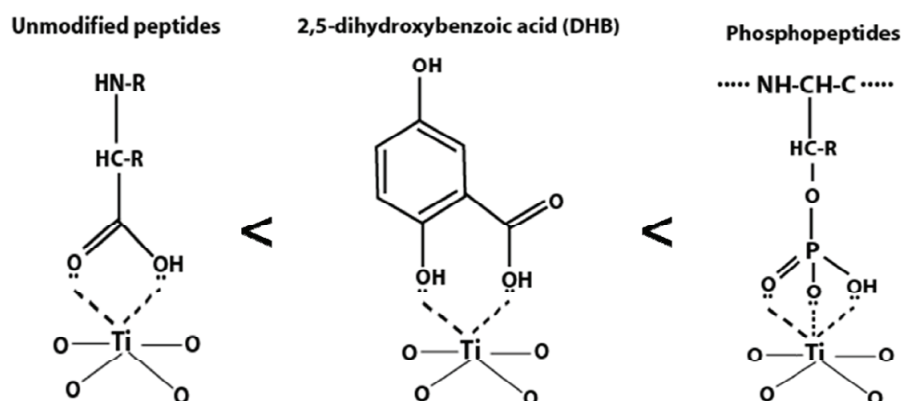


Fig. 7. Comparison of binding capacities of peptides, 2,5-dihydroxy benzoic acid (DHB) and phosphopeptides to Titansphere (TiO_2).

TiO_2 adsorbs to DHB with a higher affinity than to acidic amino acid residues but with a lower affinity than to phosphate groups. DHB therefore increases the specificity of TiO_2 in phosphopeptide enrichment. Adapted from Pan, 2008.

1.4.2.2 Strong cation exchange (SCX) chromatography

SCX is another powerful approach to enrich for phosphorylated peptides. It is based on the difference in the solution charge states of phosphorylated and non-phosphorylated peptides (Macek et al., 2009). At pH 2.7, most tryptic peptides carry

one positive charge at each peptide terminus (NH_4^+ from the N-terminal amino group and the positively charged side chain of arginine or lysine), resulting in a net charge of +2. A negatively charged phosphate group reduces the charge state by one, and therefore decreases binding to the SCX column (Fig. 8A). Peptides with different solution charge states are separated on a preparative column using a linear salt gradient: multiply phosphorylated peptides bind to the column with minimum affinity, while non-phosphorylated peptides bind strongly (Fig. 8B). Gygi and co-workers observed that the +1 SCX fractions are highly enriched in phosphopeptides, as is the SCX flow-through (net zero or negative charge) (Beausoleil et al., 2004), which is therefore analysed several times in this thesis. SCX as a first separation/enrichment step, followed by IMAC or TiO_2 chromatography (Fig. 9), is a powerful and robust combination for phosphopeptide enrichment that has proven to be very successful in large scale phosphoproteomics studies (Gruhler et al., 2005; Olsen et al., 2006; Villen et al., 2007).

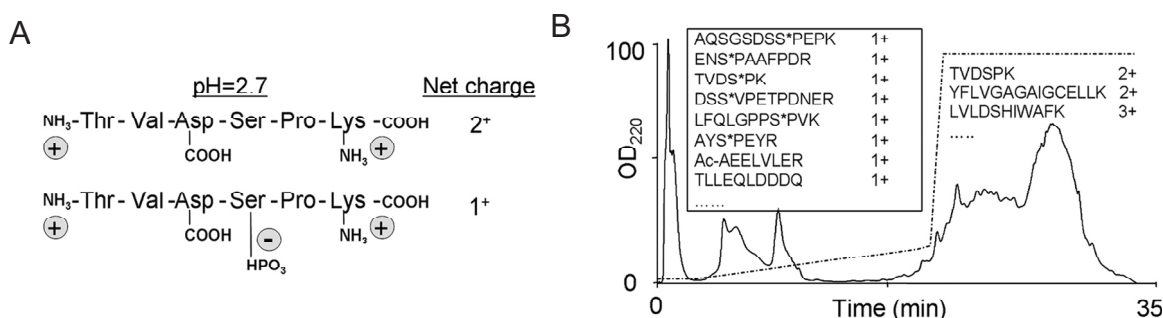


Fig. 8. Peptide fractionation and phosphopeptide enrichment by Strong cation exchange (SCX) chromatography.

(A) At pH 2.7, most peptides produced by Trypsin proteolysis have a solution charge state of +2, whereas phosphopeptides have a charge state of +1 only. (B) SCX separates the peptides using a linear salt gradient (dashed line). Early fractions and the flow through are highly enriched in phosphopeptides (box), while non-phosphorylated peptides elute at high salt concentrations. Phosphorylation sites are denoted by asterisks. Adapted from Beausoleil et al., 2004.

Alternatively to the negative charge of the phosphate group, its strong hydrophilicity may be used to enrich phosphopeptides by Hydrophilic interaction chromatography (HILIC) (McNulty and Annan, 2008). This recently discovered method is well suited for small amounts of material (sub mg) and has a higher resolution than SCX. However, very strong interactions of multiply phosphorylated peptides with the stationary phase may lead to difficulties with elution (Macek et al., 2009).

1.4.3 Phosphopeptide analysis by mass spectrometry

Mass spectrometric measurements are carried out in the gas phase on ionised analytes. By definition, a mass spectrometer consists of an ion source, a mass analyser that measures the mass-to-charge ratio (m/z) and a detector that registers the number of ions at each m/z value. Electrospray ionisation (ESI) and Matrix-assisted laser desorption/ionisation (MALDI) are the two techniques most commonly used for ionisation (Aebersold and Mann, 2003). Mass spectrometric analyses in this thesis used ESI and were carried out by Dr. Jesper Olsen in the laboratory of Prof. Dr. Matthias Mann at the Max-Planck Institute for Biochemistry, Munich, on an LTQ-Orbitrap XL instrument (Thermo Electron, Bremen).

1.4.3.1 Identification of phosphopeptides

The effluent from the liquid chromatography (LC) column (section 1.4.2) is directly electrosprayed into the mass spectrometer, which measures the mass-to-charge ratio (m/z) and intensity, indicating abundance, in a survey scan (MS or MS¹ spectrum). At the same time, the mass spectrometer also dissociates the peptides and detects the resulting fragment ions in a so-called tandem mass spectrum (MS/MS or MS² spectrum). Taking a protein database as a reference, mass spectra can be correlated to amino acid sequences and possible post-translational modifications with the aid of computer algorithms. The found peptide sequences are then assigned to proteins, which ultimately leads to protein identification (Aebersold and Mann, 2003) (Fig. 9). Phosphorylation is identified from the tandem mass spectra, and involves loss of the phosphate group (mainly from serine and threonine) as well as detection of characteristic reporter ions (resulting from cleavage at either side of stably attached phospho-tyrosine) (Macek et al., 2009).

1.4.3.2 Localisation of the phosphate group

Although phosphopeptides can be effectively fragmented and thereby identified by MS/MS, it is often difficult to localise the position of the phosphorylation site with single-amino acid resolution, especially for multiply phosphorylated peptides (Macek et al., 2009). For example, in a peptide with consecutive serines, the fragments between each of them have to be identified in the MS/MS spectrum to unambiguously place the phosphorylation on the correct one. Mann and co-workers have therefore developed a posttranslational modification (PTM) score: The

spectrum of an identified peptide is compared with theoretical spectra in which the phosphate group is placed at each possible sequence position, thereby allowing classification of phosphorylation sites (Olsen et al., 2006). Note that even with an ambiguous localisation score, the phosphorylation site is still unambiguously confined to the identified peptide.

1.4.3.3 Bioinformatic data mining

Bioinformatic approaches as a means for functional annotation and data mining can take place at the end of the workflow, leading to biologically interpretable results and insights (Fig. 9). For example, biological information can be discovered by using functional annotation schemes, such as the Gene Ontology (GO) (<http://www.geneontology.org>) or signalling pathway databases (Kumar and Mann, 2009). Also algorithms for molecular networking are emerging, for example the STRING 8.0 database (Jensen et al., 2009; <http://string.embl.de>). Furthermore, integration of mass spectrometry-based proteomics and phosphoproteomics with other “-omics” datasets like gene expression data can provide deeper insights. It is expected that integration of different large-scale studies will deliver a new kind of biological knowledge that cannot be obtained by each of the separate approaches (Kumar and Mann, 2009).

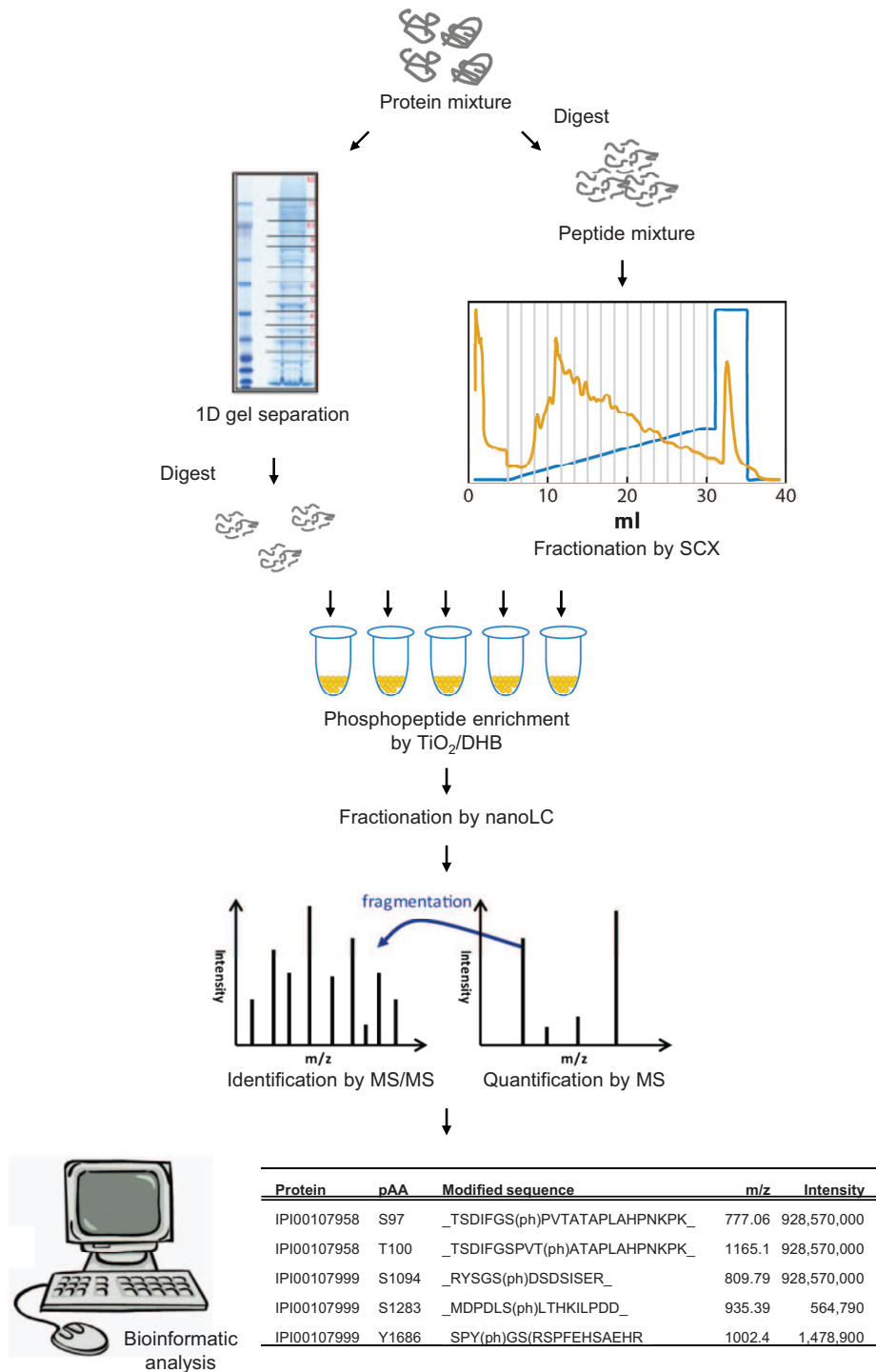


Fig. 9. Workflow of mass spectrometry-based phosphoproteomics.

Protein mixtures are separated by SDS-PAGE and digested into peptides (left), or digested and fractionated by strong cation exchange (SCX) chromatography, which also enriches for phosphopeptides (right). Phosphopeptides from peptide fractions are enriched by Titansphere (TiO_2) chromatography in the presence of 2,5-dihydroxy benzoic acid (DHB), separated by liquid chromatography (nanoLC) and directly measured in a mass spectrometer. Relative peptide quantification is based on the first stage of mass spectrometry (MS), whereas peptide identification is achieved upon gas-phase fragmentation in the second stage (MS/MS). Using a reference database and a post-translational modification (PTM) score (Olsen et al., 2006) proteins and their phosphorylation sites are identified. Bioinformatic data mining takes place at the end of the workflow. (pAA) phosphorylated amino acid. (m/z) mass-to-charge ratio. Adapted from Macek et al., 2009, and Pan, 2008.

1.4.4 Quantitative measurements using Stable isotope labelling with amino acids in cell culture (SILAC)

Mass spectrometry is not inherently quantitative, as different peptides have different mass spectrometric responses. For accurate quantification, it is therefore required to compare each individual peptide between experimental conditions (Bantscheff et al., 2007). To differentially quantify two proteomes or phosphoproteomes, stable isotopes such as deuterium (^2H), carbon-13 (^{13}C), nitrogen-15 (^{15}N) or oxygen-18 (^{18}O) can be introduced in various ways, most commonly by chemical modification or by metabolic labelling (Macek et al., 2009).

Stable isotope labelling with amino acids in cell culture (SILAC) (Fig. 10), an approach introduced by Mann and co-workers (Ong et al., 2002), allows mixing of samples before enrichment and fractionation steps, and has proved especially useful for direct comparisons of phosphopeptide abundances in time-course or treatment analyses (Kruger et al., 2008; Olsen et al., 2006; Pan et al., 2008). In the most commonly used implementations, the medium contains labelled arginine and lysine which ensures that all tryptic cleavage products of a protein carry at least one labelled amino acid (Mann, 2006). Incorporation of heavy amino acids, which are chemically identical to their non-labelled counterparts, into a protein during cell culture leads to a known mass shift of its peptides compared with the peptides that contain the light version of the amino acid. Simultaneous mass spectrometric analysis of up to three conditions (cell populations labelled light, medium and heavy; stimulation A, B and C), reveals for each peptide SILAC triplets in the MS^1 mass spectra (Fig. 10). The ratio of peak intensities directly yields the ratio of the peptides in population A versus populations B and C. To achieve complete labelling, essential amino acids, e.g. arginine and lysine, are chosen and cells are grown in their presence with dialysed serum, to avoid contamination with non-labelled counterparts, for around ten cell divisions. In some cell types, conversion of labelled arginine to proline needs to be prevented by titration of arginine or addition of non-labelled proline (Olsen, personal communication; Mann, 2006).

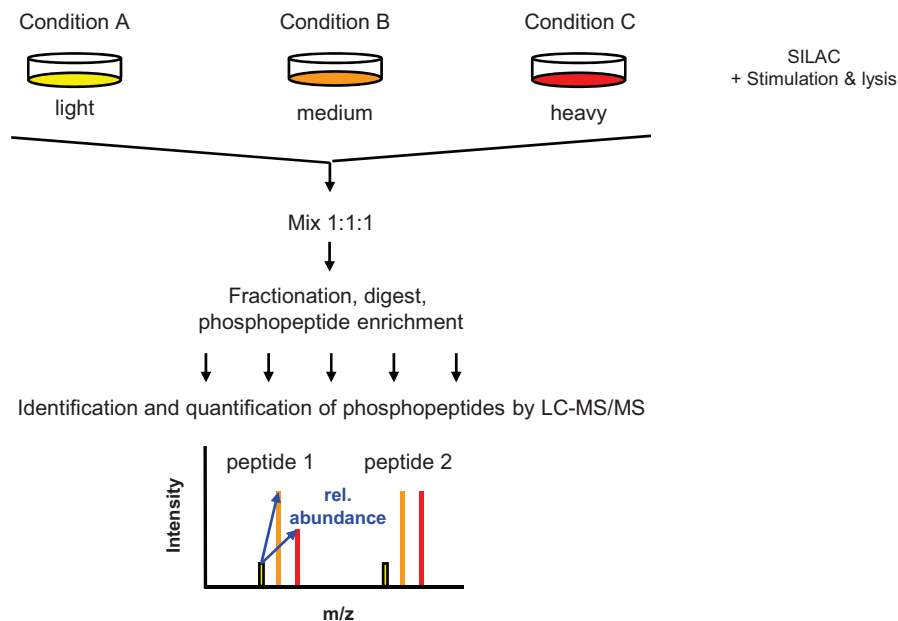


Fig. 10. Quantitative phosphoproteomics using Stable isotope labelling with amino acids in cell culture (SILAC).

Proteins are metabolically labelled during cell culture by addition of SILAC amino acids. Three SILAC states are presented. One state is labelled with light amino acids, one with medium amino acids (e.g. $^{13}\text{C}_6$ -arginine and $^2\text{D}_4$ -lysine) and one with heavy amino acids (e.g. $^{13}\text{C}_6^{15}\text{N}_4$ -arginine and $^{13}\text{C}_6^{15}\text{N}_2$ -lysine) before cells are stimulated. Samples are mixed as early as possible to avoid introducing experimental errors. Labeled peptides appear in the MS^1 mass spectrum as SILAC triplets, because incorporation of the medium and heavy amino acids leads to mass shifts. The intensities of the peaks reflect the relative abundances of each peptide in the three different conditions.

As demonstrated in the first large scale quantitative, site specific and time-resolved phosphoproteomic study, reported by Olsen et al., a combination of SILAC for quantification, SCX and TiO_2 chromatography for phosphopeptide enrichment and high-accuracy mass spectrometric characterisation is an excellent strategy for quantitative phosphoproteome analyses identifying thousands of phosphorylation sites with single amino acid accuracy (Olsen et al., 2006).

2 Aim of the study

Innate immune activation by TLRs has been extensively studied, but there lacks a systems level analysis of the phosphorylation cascades triggered by microbial stimuli in macrophages. Therefore it remains unknown whether the canonical signalling pathways comprise the main kinases, their targets and TFs, and which other biological processes are regulated by phosphorylation in activated macrophages. Recent progress in mass spectrometry-based proteomics combined with innovative experimental strategies and advances in computational methods now enable global quantitative studies of cellular proteomes and phosphoproteomes.

This study was designed to quantitatively analyse the phosphoproteome of TLR-activated primary macrophages, using the TLR4 ligand LPS as a stimulus. The first aim was to establish optimal conditions for differentiation and efficient metabolic labelling (SILAC) for primary bone marrow-derived macrophages in order to allow highly accurate quantitative comparisons of phosphoproteomes under different conditions. Second, a phosphoproteome analysis combining SILAC with 1D gel separation, Strong cation exchange (SCX) and Titansphere (TiO₂) chromatography for phosphopeptide enrichment, and high-accuracy mass spectrometry was to be carried out in resting and LPS-activated macrophages at different time points, in two independent large-scale and multi-step experiments. Third, the resulting list of phosphorylation sites was to be analysed by bioinformatic approaches in order to detect the extent and kinetics of regulation, information on activated kinases and signalling pathways, and other molecular functions and processes influenced by LPS-regulated phosphorylation. Finally, using *in-silico* promoter analysis, phosphorylation of TFs should be linked to a nascent transcriptome dataset generated under comparable conditions, to identify novel candidate regulators of TLR-activated gene expression.

3 *Material*

3.1 *Chemicals and reagents*

2,5-dihydrobenzoic acid (DHB)	Sigma-Aldrich, Taufkirchen
4-thiouridine (4sU)	Sigma-Aldrich, Taufkirchen
Acetic acid	Roth, Karlsruhe
Acetone	Sigma-Aldrich, Taufkirchen
Acetonitrile (ACN)	Merck, Darmstadt
Acrylamide/Bis, 30 % solution	Biorad, Munich
Agarose	Invitrogen, Karlsruhe
Amino acids (non-labelled)	Sigma-Aldrich, Taufkirchen
Amino acids (SILAC)	Euriso-Top, Saarbrücken
Ammonia	Sigma-Aldrich, Taufkirchen
Ammonium bicarbonate	Sigma-Aldrich, Taufkirchen
Ammonium chloride (NH ₄ Cl)	Sigma-Aldrich, Taufkirchen
Ammonium hydrogen carbonate (NH ₄ HCO ₃)	Sigma-Aldrich, Taufkirchen
Ammonium persulfate (APS)	Sigma-Aldrich, Taufkirchen
β-Glycerophosphate	Sigma-Aldrich, Taufkirchen
β-Mercaptoethanol (cell culture)	Gibco, Karlsruhe
β-Mercaptoethanol (non cell culture)	Sigma-Aldrich, Taufkirchen
Bovine serum albumine (BSA)	Sigma-Aldrich, Taufkirchen
Bromphenolblue	Sigma-Aldrich, Taufkirchen
C18 Reprosil AQUA-Pur 3 μm particles	Dr. Maisch GmbH, Ammerbach-Entringen
C8 material for STAGE tips	Varian, Darmstadt
Chloroform	Merck, Darmstadt
Citric acid monohydrate	Sigma-Aldrich, Taufkirchen
Complete protease-inhibitor cocktail tablets	Roche Applied Science, Mannheim
Coomassie Brilliant Blue R-250	Biomol GmbH, Hamburg

ddH ₂ O	Millipore device, in-house
DEPC-treated water	Ambion, Darmstadt
DirectPCR [®] Lysis Reagent (Tail)	PeqLab, Erlangen
Dithiothreitol (DTT)	Sigma-Aldrich, Taufkirchen
Deoxynucleotidtriphosphates (dNTPs)	Amersham Biosciences, Heidelberg
DMEM with stable glutamine	Biochrom AG, Berlin
DMEM, custom made with stable glutamine and deficient in L-arginine and L-lysine	Biochrom AG, Berlin
EDTA disodium salt dihydrate (Na ₂ EDTA·2H ₂ O)	Sigma-Aldrich, Taufkirchen
EDTA disodium salt monohydrate (Na ₂ EDTA·1H ₂ O)	Sigma-Aldrich, Taufkirchen
EDTA for RNA	USB Europe, Staufen
Ethanol	Roth, Karlsruhe, and in-house supply
Ethidium bromide	Roth, Karlsruhe
Ethidium monoazide (EMA)	Invitrogen, Karlsruhe
Ethylendiaminetetraacetic acid (EDTA)	Sigma-Aldrich, Taufkirchen
EZ link Biotin-HPDP	Pierce, USA
Fetal calf serum (FCS)	Biochrom AG, Berlin
Glacial acetic acid	Sigma-Aldrich, Taufkirchen
Glycerol	Roth, Karlsruhe
Glycine	Sigma-Aldrich, Taufkirchen
Hydrochloric acid (HCl)	In-house supply
Hydrogen peroxide (H ₂ O ₂)	Sigma-Aldrich, Taufkirchen
IL-3, murine recombinant	Tebu-bio, Offenbach
IL-6, murine recombinant	Tebu-bio, Offenbach
IL-10, murine recombinant	Tebu-bio, Offenbach
Iodoacetamide (IAA)	Sigma-Aldrich, Taufkirchen
Isopropanol	Sigma-Aldrich, Taufkirchen

Lipopolysaccharides from <i>Escherichia coli</i> O55:B5 (Cat. No. L2880) (LPS)	Sigma-Aldrich, Taufkirchen
MACS columns	Miltenyi, Bergisch-Gladbach
Methanol	Roth, Karlsruhe
Milk powder	Roth, Karlsruhe
NP40 (Igepal Ca-630)	Sigma-Aldrich, Taufkirchen
Orange G	Sigma-Aldrich, Taufkirchen
Paraformaldehyde (PFA)	Merck, Darmstadt
PBS Dulbecco Instamed (PBS)	Biochrom AG, Berlin
Penicillin/streptomycin	Biochrom AG, Berlin
Potassium bicarbonate (KHCO ₃)	Sigma-Aldrich, Taufkirchen
Potassium chloride (KCl)	Sigma-Aldrich, Taufkirchen
Potassium dihydrogen phosphate	Sigma-Aldrich, Taufkirchen
Ready Gel Precast Gel, 4 to 15 % Tris-HCl	Bio-Rad Laboratories, Munich
Resource S column for SCX	GE Healthcare, Munich
RPMI 1640 medium	Biochrom AG, Berlin
SCF, murine recombinant	Tebu-bio, Offenbach
Sodium chloride (NaCl)	Sigma-Aldrich, Taufkirchen
Sodium citrate	Sigma-Aldrich, Taufkirchen
Sodium deoxycholate	Sigma-Aldrich, Taufkirchen
Sodium dodecyl sulfate	Roth, Karlsruhe
Sodium fluoride (NaF)	Merck, Darmstadt
Sodium hydroxide (NaOH)	Merck, Darmstadt
Sodium orthovanadate	Sigma-Aldrich, Taufkirchen
Sodium phosphate dibasic (Na ₂ HPO ₄)	Sigma-Aldrich, Taufkirchen
Streptavidin-HRP	R&D Systems, Wiesbaden-Nordenstadt
Sucrose	Sigma-Aldrich, Taufkirchen
Sulfuric acid (H ₂ SO ₄)	Roth, Karlsruhe
Tetramethylbenzine (TMB) ELISA substrate	Sigma-Aldrich, Taufkirchen

Tetramethylethylenediamine (TEMED)	Sigma-Aldrich, Taufkirchen
Thiourea	Sigma-Aldrich, Taufkirchen
Titansphere (TiO ₂)	GL Sciences, Japan
TriFast™	PeqLab, Erlangen
Tri-fluoro acetic acid (TFA)	Merck, Darmstadt
Tris Base (Tris Ultra)	Roth, Karlsruhe
Tris hydrochloride (Tris-HCl) (pH 7.4) (RNA)	USB Europe, Staufen
Trizma hydrochloride (Tris-HCl)	Roth, Karlsruhe
Trypan blue solution	Sigma-Aldrich, Taufkirchen
Tween20	Sigma-Aldrich, Taufkirchen
Urea	Sigma-Aldrich, Taufkirchen
Western Lightning Chemiluminescence Reagent	Perkin Elmer Life Sciences Inc., Jügesheim

3.2 Kits

BCA Protein Assay Reagent Kit	Pierce, USA
DuoSet ELISA Development Systems	R&D Systems, Wiesbaden- Nordenstadt
GeneChip® Hybridisation, Wash and Stain Kit	Affymetrix, UK
GeneChip® WT cDNA Amplification Kit	Affymetrix, UK
GeneChip® WT cDNA Synthesis Kit	Affymetrix, UK
GeneChip® WT Terminal Labelling Kit	Affymetrix, UK
PhosphoScan Kit (C18 cartridges)	Cell Signaling, USA
RNA HighSense Reagents and Supplies	Bio-Rad Laboratories, Munich
RNeasy MinElute Spin Columns	Qiagen, Hilden

3.3 Primers

Primer sequences were kindly provided by Dr. A. Cato from the Forschungszentrum Karlsruhe, and oligonucleotides were purchased from Metabion, Martinsried.

Tab. 1. Primers.

Name	Target	Sequence	Application
RL300	Erp7Ilfw	CAGGTAAGTGTGTGTCGGTGGTGCTAATG	DUSP1 genotyping
RL301	Erp7Iirev	CTATATCCTCCTGGCACAATCCTCCTAG	DUSP1 genotyping
RL302	HHneo	AAATGTGTCAGTTTCATAGCCTGAAGAACG	DUSP1 genotyping

3.4 Antibodies

Tab. 2. Antibodies for Westernblot.

Antigen	Source	Dilution	Company
p38 MAPK	Rabbit, polyclonal	1 : 1,000	Cell Signalling
phospho-p38 MAPK (Thr180/Tyr182)	Rabbit, polyclonal	1 : 1,000	Cell Signalling
α -Tubulin	Mouse, IgG	1 : 5,000	Sigma-Aldrich
Anti-mouse IgG F(ab') ₂ -fragment, HRP-coupled	Goat	1 : 10,000	Dianova
Anti-rabbit IgG F(ab') ₂ -Fragment, HRP-coupled	Donkey	1 : 10,000	Dianova

Tab. 3. Antibodies for flow cytometry.

Antigen	Source	Dilution	Company
F4/80	IgG2b	FITC	AbD Serotech
CD11b	IgG2b	FITC	BD Pharmingen
CD16/CD32 (Fc block)	IgG2b	---	BD Biosciences

3.5 DNA- and protein standards

1 kb DNA ladder	Invitrogen, Karlsruhe
PageRuler™ pre-stained protein ladder	Fermentas, St. Leon-Rot

3.6 Enzymes

Accutase	PAA Laboratories, Cölbe
Benzonase	VWR, Ismaning
Endoproteinase Lys-C	Wako Chemicals, USA
pegGOLD Taq-DNA-Polymerase "all inclusive"	PeqLab, Erlangen
Proteinase K	Roche Applied Science, Mannheim

Trypsin, sequencing grade modified (mass spectrometry)	Promega, Mannheim
Trypsin-EDTA (cell culture)	PAA Laboratories, Cölbe

3.7 Consumable items

Cell culture dishes	Schubert, Leipzig
Cell scraper	Peske, Aindlingen-Arnhofen
Dispenser tips	PP, Switzerland
Film Kodak BioMax Light	Sigma-Aldrich, Taufkirchen
Filter tips	Kisker, Steinfurt
Maxisorp 96-well ELISA plates	Nunc, Wiesbaden
Mouse GeneST [®] 1.0 GeneChips	Affymetrix, UK
Optical 96-well plates	Applied Biosystems, USA
Parafilm	Roth, Karlsruhe
PCR plates 96-well	Peqlab, Erlangen
Petri dishes	Peske, Aindlingen-Arnhofen
Pipets for cell culture	Greiner, Frickenhausen
Polypropylene tubes (ultracentrifugation)	VWR, Ismaning
RNA HighSense Chips	Bio-Rad Laboratories, Munich
Sterile filter flasks	Zefa, Harthausen
Test tubes (0.5, 1.5 or 2 mL)	Eppendorf, Hamburg
Test tubes (15 or 50 mL)	Falcon, USA
Transfer membrane Protran	VWR, Ismaning
Whatman paper	Schleicher&Schuell, Dassel

3.8 Laboratory equipment

ÄKTA Purifier chromatography system	Amersham Biosciences, Heidelberg
Automated fraction collector	Amersham Biosciences, Heidelberg
Cell culture centrifuge	Heraeus, Hanau
EASY-nLC system Proxeon	Biosystems, Denmark
ELISA reader sunrise	Tecan, Switzerland

Experion automated electrophoresis station	Bio-Rad Laboratories, Munich
FACS Calibur	BD Bioscience, Heidelberg
Film cassette	Dr. Goos-Suprema, Heidelberg
Freezer -20 °C	Siemens, Munich
Freezer -80 °C	Thermo Scientific, USA
Fridge	Liebherr, Switzerland
Gel documentation system	Bio-Rad Laboratories, Munich
GeneChip® Fluidics Station 450	Affymetrix, UK
GeneChip® Scanner 3,000	Affymetrix, UK
Incubator Hera Cell 240	Heraeus, Hanau
Lab water purification system	Millipore, Schwalbach
LTQ-Orbitrap XL mass spectrometer	Thermo Electron, Bremen
Microscope Zeiss Axiovert 40 C	Zeiss, Jena
Microwave	Privileg, Munich
Multichannel pipets	Thermo Labsystems, USA
Multipipet plus	Eppendorf, Hamburg
Nanodrop® ND-1,000 Spectrophotometer	PeqLab, Erlangen
Neubauer counting chamber	Roth, Karlsruhe
Nitrogen freezing tank Espace 300	Air Liquide, Düsseldorf
PerfectBlue Maxigel system	PeqLab, Erlangen
PerfectBlue Dual Gel System Twin ExW S	PeqLab, Erlangen
pH-meter Multical	WTW, Weilheim
Pipetboy accu	Integra Biosciences, Fernwald
Pipets	Gilson, USA
Power Supply Power Pac 200	Bio-Rad Laboratories, Munich
SE250/SE260 Mighty Small II Mini vertical gel electrophoresis unit	Hofer, USA
Sealing apparatus Folio	Severin, Sundern
Shaker	PeqLab, Erlangen
Sonicator UW60	Bandelin Electronic, Berlin
Speed-vac Concentrator 5,310	Eppendorf, Hamburg
Sterile bench	Heraeus, Hanau
T3 Thermocycler	Biometra, Göttingen

Table-top centrifuge	Heraeus, Hanau
Thermomixer Comfort	Eppendorf, Hamburg
Ultra centrifuge Sorvall	Thermo Scientific, USA
Vortexer Genie 2	Scientific Industries, USA
Westernblot transfer tankt	PeqLab, Erlangen
Westernblot developer Curix60	Agfa, Köln

3.9 Databases and software

CellQuest Pro	BD Bioscience, Heidelberg
ClustalW	http://www.ebi.ac.uk/Tools/clustalw2
Cytoscape	http://www.cytoscape.org
Expasy	http://www.expasy.ch
Experion software	Bio-Rad Laboratories, Munich
Expression Console	Affymetrix, UK
FlowJo	Tree Star, USA
Gene Expression Omnibus (GEO)	http://www.ncbi.nlm.nih.gov/geo/
Gene Ontology (GO)	http://www.geneontology.org/GO
Genomatix software tools	http://www.genomatix.de
InnateDB	http://www.innateDB.ca
International protein index (IPI) database	http://www.ebi.ac.uk/IPI
Magellan	Tecan, Switzerland
Mascot search engine	Matrix Science, UK
MaxQuant	http://www.maxquant.org
NCBI-BLAST2	http://www.ebi.ac.uk/Tools/blastall/
Phosida	http://www.phosida.com
PubMed	http://www.ncbi.nlm.nih.gov/sites/entrez?db=pubmed
R	http://www.r-project.org
Spotfire DecisionSite for Functional Genomics	Tibco, Munich
STRING 8.0	http://string.embl.de
Uniprot	http://www.uniprot.org
Xcalibur 2.0	Thermo Scientific, USA

4 Methods

4.1 Mice

Wild type and *Dusp1*-deficient mice on a C3H/HeN background were bred under pathogen-free conditions at the animal facility of the Institute of Medical Microbiology, Immunology and Hygiene at Technische Universität München, Germany. Animal experiments were approved and authorised by the local government. Mice were genotyped prior to preparation of bone marrow cells as described in sections 4.4.1-4.4.3, using the primers listed in Tab. 1.

Dusp1-deficient mice, initially generated at the R. Bravo laboratory at Bristol-Myers Squibb Pharmaceutical Research Institute (Dorfman et al., 1996) were kindly provided by Dr. A. Cato from the Forschungszentrum Karlsruhe on a mixed 129Sv x C57Bl/6 background. Experiments were performed with ten to twelve week old mice backcrossed at least seven generations onto C3H/HeN. Wild type C3H/HeN mice from Harlan (Itingen) were used as controls.

4.2 Cell culture

Cells were cultured at 37 °C, 5 % CO₂ and 85 % humidity.

4.2.1 L-cell-conditioned medium (LCCM)

L-cell-conditioned medium (LCCM) was used as a source of macrophage colony stimulating factor (M-CSF) during differentiation of bone marrow cells into macrophages. LC929 cells (5×10^6 cells/tube) were thawed quickly, washed with pre-warmed RPMI complete medium (cRPMI), plated on a 15 cm cell culture dish and cultured. Nearly confluent plates were split 1:3 to 1:4: The medium was removed, adherent cells were detached with 5 mL Trypsin (37 °C, 5 min), Trypsin was inactivated by addition of 20 mL cRPMI, centrifugation (5 min, 1200 rpm) and re-suspension in cRPMI, and cells were replated. The supernatant containing secreted M-CSF was collected from cells grown again to confluence, fresh cRPMI was added, and the procedure was repeated three to four times every other day. The collected LCCM was sterile filtered and stored in 50 mL aliquots at 4 °C.

LCCM for SILAC of bone marrow-derived macrophages (BMDMs) (section 4.2.3) was subsequently filtered on 5 kDa cut-off columns (Amicon ultra, Millipore) and washed two times with LCCM wash. 50 mL Aliquots were stored at -80 °C.

cRPMI: RPMI 1640 with stable glutamine, 10 % FCS, 1 % Penicillin/Streptomycin, 0.1 % β -mercaptoethanol

LCCM wash: Custom made DMEM with stable glutamine and deficient in L-arginine and L-lysine, 1 % Penicillin/Streptomycin, 0.1 % β -mercaptoethanol

4.2.2 *Standard protocol for differentiation of bone marrow-derived macrophages (BMDMs)*

Mice were sacrificed, the hind legs were removed and bones were separated. Femora and tibiae were flushed with PBS using a 27 G syringe into a 10 mL petri dish. After erythrocyte lysis (1 mL Erythrocyte lysis buffer per mouse, 5 min RT, 5 min 1,200 rpm), bone marrow cells were taken up in cDMEM supplemented with 10 % LCCM (section 4.2.1) as a source of M-CSF and incubated overnight in 10 cm petri dishes. The next day, non-adherent cells were counted and re-plated at a density of 0.5×10^6 cells/mL in cDMEM with 10 % LCCM in 10 cm petri dishes. On day three, 5 mL of fresh cDMEM with 10 % LCCM were added. After 6 to 7 days of differentiation, cultures were nearly confluent. After removal of non-adherent cells remaining cells were detached with 4 mL accutase, diluted 1:4 in PBS, at 37 °C for 15 min. Cells were spun down, resuspended in cDMEM, counted, replated in cDMEM in cell culture dishes at a density of 1×10^6 cells/mL, and rested overnight before they were used for experiments.

Erythrocyte lysis buffer: 0.15 M NH_4Cl , 10 mM KHCO_3 , 0.1 mM $\text{Na}_2\text{EDTA} \cdot 2\text{H}_2\text{O}$

cDMEM: DMEM with stable glutamine, 10 % FCS, 1 % Penicillin/Streptomycin, 0.1 % β -mercaptoethanol

4.2.3 *SILAC of BMDMs*

4.2.3.1 *Optimised protocol*

To sufficiently label all proteins of BMDMs with stable isotope-substituted versions of the essential amino acids L-arginine and L-lysine, the standard protocol for differentiation of BMDMs was optimised for proliferation and prolonged time in culture: Bone marrow cells were isolated and cultured in SILAC medium for 17 days as follows: After overnight depletion of adherent cells non-adherent cells were expanded by addition of recombinant murine IL-3 (10 mg/L), IL-6 (10 mg/L) and SCF

(50 mg/L) in the presence of 10 % 5 kDa cut-off filtered LCCM (section 4.2.1) as a source of M-CSF on 10 cm petri dishes (Peske, Aindlingen-Arnhofen; not cell culture dishes!), starting with 1×10^7 cells per plate. Cultures were split every 2 to 3 days according to the procedure described below (section 4.2.3.1). After 13 days, cells were plated in medium with 10 % 5 kDa cut-off filtered LCCM without cytokines to complete differentiation into macrophages for 3 days. On day 16 non-adherent cells were discarded and 25×10^6 adherent cells were plated on 15 cm cell culture plates (Schubert, Leipzig) without LCCM for stimulation the next day.

SILAC medium: Custom made DMEM with stable glutamine and deficient in L-arginine and L-lysine, 10 % dialysed FCS, 1 % Penicillin/Streptomycin, 0.1 % β -mercaptoethanol, 84 g/L L-arginine·HCl $^{13}\text{C}_6$ (Arg "6") or $^{13}\text{C}_6^{15}\text{N}_4$ (Arg "10"), 146 g/L L-lysine·HCl $^2\text{D}_4$ (Lys "4") or $^{13}\text{C}_6^{15}\text{N}_2$ (Lys "8") or non-labelled counterparts (Arg "0" and Lys "0"), 30 g/L non-labelled L-proline

4.2.3.1 Splitting procedure

To split whole cultures, consisting of non-adherent progenitor cells and adherent cells that developed under the influence of M-CSF, non-adherent cells were collected in 250 mL cell culture centrifuge beakers and placed on ice. Adherent cells were detached with Accutase diluted 1:4 in sterile PBS (4 mL per 10 cm plate, 37 °C, 15 min). After dilution of Accutase with 4 mL PBS cells were collected with a cell scraper in a separate cell centrifuge beaker and plates were washed with 4 mL sterile PBS to collect as many cells as possible. Detached cells were spun down (Sorvall RC 26Plus, SLA-1500, 300 g, 4 °C, 10 min) and re-suspended in the medium with non-adherent cells plus fresh SILAC medium with cytokines and M-CSF for re-plating. Whole cultures were split 1:2 or higher, depending on cell density. On day 13 all cells were deprived of medium to remove cytokines before re-plating in medium with 10 % LCCM.

4.2.3.2 Determination of growth curves

Expansion of cell cultures was monitored by counting cells every time they were split. An aliquot of cell suspension (adherent and non-adherent cells before re-plating) was diluted with trypan blue as appropriate and counted in a Neubauer counting chamber under the microscope. For each time point the total number of cells was extrapolated from the number of cells/mL determined in two replicates and the total volume.

$$n = c \cdot v$$

$$c = \mu \cdot d \cdot 10^4$$

n	Total number of cells
c	Number of cells/mL
v	Total volume [mL]
μ	Mean number of cells per big square
d	Dilution factor

4.2.4 Stimulation

For activation of TLR4 differentiated BMDMs (section 4.2.2 or 4.2.3) were stimulated with 100 ng/mL LPS *Escherichia coli* O55:B5 (Sigma-Aldrich, Taufkirchen, Cat. No. L2880). For stimulation with IL-10 (Tebu-bio, Offenbach) 5 ng/mL were used.

4.3 Immunoassays

4.3.1 Enzyme linked immunosorbent assay (ELISA)

Cytokines in the supernatant of resting or stimulated cells were detected by DuoSet ELISA Development System (R&D Systems, Wiesbaden-Nordenstadt) following the manufacturer's protocol. Briefly, MaxiSorp 96-well ELISA plates were coated with 100 μ L per well of capture antibody (720 ng/mL) in PBS and incubated overnight at 4 °C. The next day the plate was tapped dry and subsequently incubated with 250 μ L per well of Blocking buffer for 1 h at RT or at 4 °C overnight. Afterwards, the plate was washed three times with 250 μ L Washing buffer, tapped dry, and 100 μ L per well of the samples, appropriately diluted in Reagent diluent, and standards were added. Incubation took place at RT for 2 h or at 4 °C overnight and was followed by three washing steps. The detection antibody (36 μ g/mL) was diluted in Reagent diluent and added in a volume of 100 μ L per well. After incubation for 2 h at RT the plate was washed three times. This was followed by incubation with 100 μ L per well of Streptavidin-horseradish peroxidase (HRP) (50 μ L in 10 mL reagent diluent). Finally the plate was washed three times and fresh Substrate reagent was added (100 μ L/well). The plate was incubated in the dark because the Substrate reagent contains H₂O₂, which is light sensitive. The incubation time ranged from 10 to 60 min, depending on the protein detected. To stop the reaction 50 μ L per well of

Stop solution were added and the plate was analysed in the ELISA reader at 450 nm (reference at 570 nm).

Blocking buffer:	PBS, 1 % BSA, 5 % sucrose
Reagent diluent:	PBS, 1 % BSA
Washing buffer:	PBS, 0.05 % Tween20
Phosphate citrate buffer:	25.7 mL 0.2 M Na ₂ HPO ₄ , 24.3 mL 0.1 M citric acid monohydrate (pH 5.0), 50 mL ddH ₂ O, adjust pH to 5.0 with HCl
Substrate reagent:	1 tablet tetramethylbezone (TMB) and 2 µL 30 % H ₂ O ₂ per 10 mL Phosphate citrate buffer
Stop solution:	2 M H ₂ SO ₄

4.3.2 Flow cytometry

Up to 0.2 to 1 x 10⁶ cells per staining were centrifuged at 1,200 rpm at 4 °C for 5 min in a v-shaped 96-well plate. Alternatively, staining was performed in 1.5 mL tubes (centrifugation at 3,500 rpm, table-top centrifuge). The supernatant was discarded and the cells were washed with 100 µL FACS buffer (centrifugation at 1,200 rpm, 4 °C, 5 min) and resuspended in 100 µL FACS buffer. To stain dead cells, 1 µL of Ethidium monoazide (EMA, 0.5 mg/mL) was added and cells were incubated for 10 min on ice in darkness, followed by 10 min in direct light. After washing the cells once, cell surface Fc receptors were blocked by incubation with 50 µL of unlabelled anti-CD16/CD32 antibody (Fc block), diluted 1:400 in FACS buffer, for 15 min at 4 °C, followed by a washing step with FACS buffer. Cells were resuspended in 50 µL FACS buffer supplemented with an appropriate amount of fluorescently labelled antibody (1:50 to 1:100) (Tab. 3). Staining lasted for 20 min in the dark at 4 °C and was followed by two washing steps. For eventual storage overnight at 4 °C, cells were resuspended in 150 µL 2 % paraformaldehyde (PFA). Finally, stained cells were resuspended in 200 to 350 µL FACS buffer and analyzed by flow cytometry using the FACS Calibur instrument under the CellQuest Pro software. Data analysis was performed with FlowJo.

FACS buffer: PBS, 2 % FCS

4.4 Molecular biology

4.4.1 Isolation of genomic DNA

Genomic DNA for genotyping of mice was isolated from tails using DirectPCR® Lysis Reagent (Tail) (PeqLab, Erlangen) according to the manufacturer's instructions. Briefly, tail tips were digested with 500 µL DirectPCR® Lysis Reagent (Tail) supplemented with 0.2 to 0.3 mg/mL Proteinase K under shaking (600 to 700 rpm) at 55 °C overnight. Subsequently, Proteinase K was inactivated by incubation at 85 °C for 45 min, remaining tissue was spun down and genomic DNA was stored at -20 °C.

4.4.2 Polymerase chain reaction (PCR)

Amplification of genomic DNA was performed directly from digested tail samples (section 4.4.1) using pegGOLD Taq-DNA-Polymerase “all inclusive” (PegLab, Erlangen) with the reaction mix and PCR program described below.

Tab. 4. PCR reaction mix.

Reagent	Volume
Reaction buffer (10 x)	2.5 µL
Enhancer solution (5 x)	5 µL
dNTP-Mix (10 mM)	0.5 µL
Primer 1 (100 µM)	0.2 µL
Primer 2 (100 µM)	0.2 µL
Primer 3 (100 mM)	0.2 µL
Taq-DNA-Polymerase	0.25 µL
H ₂ O	14.65 µL
Genomic DNA	1.5 µL

Tab. 5. PCR program.

Number of cycles	Program	Temperature	Time
1	Denaturation	95 °C	15 min
34	Denaturation	95 °C	30 s
	Annealing	55 °C	30 s
	Elongation	72 °C	1 min
1	Cooling	4 °C	∞

4.4.3 Agarose gel electrophoresis

Agarose gels (1 %) were used to separate DNA fragments variable in size. TAE-buffer (1 x) with ethidium bromide (100 ng/mL) was used as electrophoresis and gel buffer. Samples were mixed 4:1 with 4 x DNA loading dye and separated at 130 V. For size determination of the fragments, 5 μ L of a 1 kb ladder were used. DNA bands were visualized with UV light (254 nm).

TAE-buffer (50 x): 242 g Tris Base, 500 mL ddH₂O, 57.1 mL glacial acetic acid, 100 mL 0.5 M Na₂EDTA·1H₂O (pH 8.0), ad 1,000 mL ddH₂O

DNA Loading dye (4 x): 50 mg Orange G, 15 mL glycerol, 0.5 mL 1 M Tris-HCl, ad 50 mL ddH₂O

4.4.4 Metabolic labelling and purification of total and nascent RNA

Metabolic labelling and purification of total and nascent RNA were performed essentially as described (Dolken et al., 2008), with minor modifications for use with primary macrophages. In brief, 4 x 10⁷ BMDMs differentiated under the same conditions as for the phosphoproteome analysis (except SILAC) (section 4.2.3) were stimulated on 15 cm cell culture dishes with 100 ng/mL LPS *Escherichia coli* O55:B5 (Sigma-Aldrich, Taufkirchen, Cat. No. L2880) for 45 min or 4.5 h or were left untreated. For metabolic labelling, the medium was supplemented with 200 μ M 4-thiouridine (4sU, Sigma-Aldrich, Taufkirchen, Cat. No. T4509) during the last 35 min of stimulation. Cells were lysed by addition of 10 mL TriFast™ and total RNA was extracted, following a modified protocol (Chomczynski and Mackey, 1995): Lysates were incubated at RT for 5 min and collected in 15 mL polypropylene tubes (VWR International, Ismaning, Cat. No. 525 0253), which tolerate up to 15,000 g. Cell lysates were either stored at -80 °C or directly used for RNA extraction. Extraction was performed with 0.2 mL chloroform per millilitre TriFast™ by centrifugation at 10,000 g after vigorous shaking and incubation at RT for 5 min. Total RNA was precipitated from the upper phase in a 0.5 volume of isopropanol and 0.5 volume of a high-salt Precipitation solution at -20 °C overnight, and pelleted by centrifugation (10,000 g, 15 min, 4 °C) the next day, followed by two washing steps in 75 % ethanol and re-suspension in RNase-free water. RNA purity and concentration were assessed by spectrophotometry (Nanodrop®, PeqLab, Erlangen). The extracted total RNA was stored at -80 °C.

For purification of *de novo* transcribed labelled RNA (“nascent RNA”) from total RNA extracts, biotinylation of 4sU-labelled RNA was performed in a total volume of 1 mL containing 120 µg RNA, 10 mM Tris (pH 7.4), 1 mM EDTA and 0.2 mg/mL EZ link Biotin-HPDP (Pierce, USA) by rotation at RT for 90 min, followed by two rounds of phenol-chloroform extraction and precipitation. For separation of biotinylated nascent and pre-existing unlabelled RNA paramagnetic streptavidin-coated beads and MACS columns were used (Miltenyi, Bergisch-Gladbach). RNA and beads were mixed and incubated at RT for 15 min, transferred to the columns and washed extensively with Washing buffer. The flow-through and the first wash volume were collected for recovery of unlabelled, pre-existing RNA. Labelled RNA was eluted with two rounds of 100 µL DTT (100 mM) into buffer RLT (Qiagen, Hilden) and cleaned up using RNeasy MinElute Spin Columns. Concentration and integrity of total and labelled RNA were determined by spectrophotometry (Nanodrop®, PeqLab, Erlangen) and Experion automated electrophoresis system (Biorad, Munich).

Precipitation solution: 50 % isopropanol; 50 % 0.8 M Sodium citrate, 1.2 M NaCl

Washing buffer: 100 mM Tris-HCl (pH 7.4) and 10 mM EDTA (USB Europe, Staufen); 1 M NaCl, 0.1 % Tween20

4.4.5 Microarray analysis of gene expression

To investigate the changes in nascent and total mRNA after LPS stimulation of macrophages, RNA samples from two independent experiments were processed and hybridised to Affymetrix Mouse GeneST[®] 1.0 GeneChips according to the manufacturer’s protocols. In brief, 200 ng total RNA and 100 ng nascent RNA were reverse transcribed introducing by random priming a T7-binding site into the cDNA that allows *in vitro* transcription. The resulting cRNA was subjected to a second round of random primed cDNA synthesis in the presence of dUTP, which allows fragmentation of the cDNA with Uracil DNA glycosylase and Apurinic/aprimidinic endonuclease 1. Biotinylation of the fragmented cDNA was accomplished by incubation with Terminal deoxynucleotidyltransferase (TdT). 5 µg of biotinylated DNA were hybridized to Mouse GeneST[®] 1.0 GeneChips overnight, followed by washing and staining procedures and scanning, following Affymetrix protocols. For generation of probe set expression values, CEL files containing probe level data were normalized using Robust multi-array average (RMA) (Affymetrix Expression Console).

4.5 Biochemistry – basic tools

4.5.1 Preparation of protein lysates

Cell lysis was carried out on ice. After stimulation cells were washed twice with ice-cold PBS and lysed with 140 μ L ice-cold Lysis buffer per 1×10^6 cells for 15 min, under occasional tapping of the plate. Lysates were collected and centrifuged at 13,000 rpm for 5 min in a table-top centrifuge to remove debris. Supernatants were collected in 1.5 mL tubes, sonicated for 10 s at maximum power, cooled on ice for 5 min and stored at -80 °C. Protein concentrations were determined using the BCA Protein Assay Reagent Kit (Pierce, USA) according to manufacturer's guidelines.

RIPA buffer: 150 mL PBS, 2 g sodium deoxycholate, 2 mL 10 % SDS, 0.8 mL 0.5 M EDTA, 0.42 g NaF, 2 mL NP40 (Igepal Ca-630), ad 200 mL PBS

Lysis buffer: 10 mL RIPA buffer, supplemented freshly with 50 μ L 200 mM sodium orthovanadate and 200 μ L 50 x Complete protease-inhibitor cocktail

4.5.2 SDS-polyacrylamide gel electrophoresis (SDS-PAGE)

SDS-PAGE was carried out using gels of 1.5 mm thickness. First the resolving gel (12.5 %, Tab. 6) was poured and immediately covered with 2 mL isopropanol. After polymerisation of the resolving gel, the isopropanol was removed, the stacking gel (4 %, Tab. 6) was poured and the comb was inserted. After complete polymerisation the gel was installed, overlaid with 1 x Tank buffer and the combs were removed. Then, the wells were flushed with Tank buffer to remove residual acrylamide. Protein lysates (section 4.5.1) were mixed 1:4 with 4 x Sample buffer and incubated for 5 min at 95 °C. Depending on the comb, 25 μ L of the lysate were loaded for 20-well combs and 18 μ L for 25-well combs, respectively. For determination of protein sizes, 5 μ L of a protein standard (Fermentas, St. Leon-Rot) were loaded onto the gel. Gel electrophoresis took place at 300 V and 80 mA for big and 40 mA for small gel chambers for 1 to 2 h.

Tab. 6. SDS-PAGE gel recipes.

Reagent	Resolving gel	Stacking gel
Acrylamide/Bis solution (30%)	12.45 mL	2 mL
Resolving buffer (4 x)	7.5 mL	---
Stacking buffer (4 x)	---	3.3 mL
SDS (10 %)	300 μ L	132 μ L
ddH ₂ O	9.6 mL	9.7 mL
TEMED	10 μ L	6.6 μ L
APS (10 %)	150 μ L	66.8 μ L

Resolving buffer (4 x): 36.3 g Tris Base, ddH₂O ad 150 mL, pH 8.8 with HCl

Stacking buffer (4 x): 12 g Tris Base, ddH₂O ad 160 mL, pH 6.8 with HCl

Tank buffer (10 x): 30.28 g Tris Base, 144 g glycine, 100 mL 10 % SDS, ddH₂O ad 2 L

Laemmli buffer (4 x): 6.25 mL Tris-HCl, 2 g SDS, 50 mL glycerol, 400 μ L 0.5 M EDTA, 100 mg bromphenolblue, ad 100 mL ddH₂O

Sample buffer (4 x): 1 mL 4 x Laemmli buffer, 80 μ L β -mercaptoethanol

4.5.3 Coomassie staining of protein gels

To visualise proteins in SDS gels, gels were incubated in Coomassie staining solution for 20 to 30 min under rotation, followed by de-staining until the desired background reduction was reached.

Coomassie staining solution: 500 mL ddH₂O, 400 mL methanol, 100 mL acetic acid, 0.25 g Coomassie R-250; filter before use

De-staining solution (4 x): 500 mL ddH₂O, 400 mL methanol, 100 mL acetic acid

4.5.4 Westernblot analysis

For the transfer of proteins from SDS gels to a nitrocellulose membrane the tank blot method was carried out. Two pieces of Whatman paper, the nitrocellulose membrane and two sponges were equilibrated in Transfer buffer together with the gel for 5 min. After assembling the set in the transfer chamber (sponge, Whatman, membrane, gel, Whatman, sponge; membrane to cathode), the chamber was filled with 1 x Transfer buffer. The transfer was performed at 1 mA per cm² (e.g. 220 mA, V max for two big gels). After transfer, the membrane was incubated in water for 5 min on the shaker to remove remaining methanol. To avoid unspecific binding the membrane was blocked for 1 h in 1 x TBS-T with 5 % milk. Incubation with the primary antibody (diluted in 1 x TBS-T, 5 % milk) took place at 4 °C overnight. The next day the membrane was washed three times for 5 min in 1 x TBS-T and then

incubated with the secondary antibody (diluted in 1 x TBS-T, 5 % milk) for 1 h at RT on the shaker. After three washing steps for 20 min each, proteins were detected using Western Lightning Chemiluminescence Reagent (Perkin Elmer Life Sciences Inc., Jügesheim), according to the manufacturer's instructions.

If the membrane was subjected to incubation with a different antibody, a stripping protocol was carried out to remove previous antibodies from the membrane. Briefly, the membrane was incubated in H₂O for 5 min, followed by incubation with pre-warmed 0.2 N NaOH for 20 to 40 min and a final wash in H₂O for 5 min. All steps were performed on a shaker. The membrane was then blocked again in 1 x TBS-T with 5 % milk for 1 h for use of primary antibody.

Transfer buffer (1 x):	200 mL methanol, 720 mL ddH ₂ O, ad 1,000 mL Transfer buffer stock (10 x)
Transfer buffer stock (10 x):	48.4 g Tris Base, 216.4 g glycine, 100 mL 10 % SDS, ad 2,000 mL ddH ₂ O
TBS (10 x):	48.4 g Tris Base, 160 g NaCl, pH 7.6 with HCl, ad 2,000 mL ddH ₂ O
TBS-T (1 x):	1 L 1 x TBS, 1 mL Tween20

4.6 Phosphoproteome analysis

4.6.1 Stimulation and cell lysis

Per condition 50 x 10⁶ SILAC encoded macrophages (section 4.2.3) were left untreated or stimulated with 100 ng/mL LPS *Escherichia coli* O55:B5 (Sigma-Aldrich, Taufkirchen, Cat. No. L2880) for 15 min or 4 h. Cells were washed with PBS, lysed in ice-cold Modified RIPA buffer for 15 min and scraped. Lysates were pooled, vortexed for 2 min and centrifuged to separate soluble and chromatin pellet fractions (17,000 g, 15 min). The soluble fraction was precipitated overnight at -20 °C by adding four volumes of ice cold acetone. The acetone precipitate was re-solubilised in 8 M urea. Proteins from the in-soluble chromatin pellet were extracted by DNA digest with Benzonase (VWR, Ismaning) and re-solubilisation in 8 M urea followed by incubation with Sample buffer under rotation at 95 °C for 5 min.

Modified RIPA buffer:	1% NP40 (Igepal CA-630), 0.1 % sodium deoxycholate, 150 mM NaCl, 1 mM EDTA, 50 mM Tris Base(pH 7.5); supplied with 1 mM sodium orthovanadate, 5 mM NaCl and 5 mM β-glycerophosphate for inhibition of phosphatases, and complete protease inhibitors directly before use
8 M urea:	6 M urea, 2 M thiourea

Laemmli buffer (4 x):	6.25 mL Tris-HCl, 2 g SDS, 50 mL glycerol, 400 μ L 0.5 M EDTA, 100 mg bromphenolblue, ad 100 mL ddH ₂ O
Sample buffer (4 x):	1 mL 4 x Laemmli buffer, 80 μ L β -mercaptoethanol

4.6.2 Reduction and alkylation of protein lysates

Mixed protein lysates (section 4.6.1) were reduced at RT under shaking (1,200 rpm) for 30 min by addition of 1 M dithiothreitol (DTT) to a final concentration of 1 mM DTT and then alkylated for 30 min in the dark by addition of 550 mM iodoacetamide (IAA-) solution to final 5.5 mM.

4.6.3 In-gel digest of chromatin pellet fraction

After reduction and alkylation (section 4.6.2) proteins from the chromatin pellet fraction were resolved by SDS-PAGE on a gradient gel (4 to 15 % Tris-HCl Ready Gel Precast Gel, Bio-Rad, Munich) and stained with Coomassie (section 4.5.3). Each lane was loaded with 40 μ g of total protein and cut into five slices containing equal protein amounts. Enzymatic digestion *in-situ* was performed essentially as described (Shevchenko et al., 2006). Briefly, gel slices were minced, de-stained (20 mM NH₄HCO₃/50 % ethanol absolute, 1,200 rpm, 3 x 20 min), de-hydrated (ethanol absolute, 1,200 rpm, 2 x 10 min) and digested by saturating the gel with 12.5 ng/ μ L sequencing grade modified Trypsin (Promega, Mannheim) in 20 mM ammonium bicarbonate (500 rpm, overnight). Peptide mixtures were acidified with tri-fluoro acetic acid (TFA, final concentration 3 %) and extracted from the gel in three rounds (30 % acetonitrile (ACN)/3 % TFA, 80 % ACN/0.05 % acetic acid, 100 % ACN; 30 min, 800 rpm, take supernatant).

4.6.4 In-solution digest of proteins

After reduction and alkylation (section 4.6.2) 20 ng Endoproteinase Lys-C (Wako Chemicals, USA) per μ g protein were added to the soluble protein fraction and the lysate was digested at RT under shaking (1,200 rpm) for 4 h. The resulting peptide mixtures were diluted with water to achieve a final urea concentration below 2 M. For double-digestion, 20 ng sequencing grade modified Trypsin (Promega, Mannheim) per μ g of protein were added and the mixture was shaken at RT overnight. Trypsin activity was quenched by acidification using TFA to a final concentration of 1 %.

4.6.5 Strong cation exchange (SCX) chromatography

SCX chromatography was performed on *in-solution* digested peptide mixtures essentially as described (Olsen et al., 2006). Briefly, TFA was added to peptide mixtures to adjust their pH to 2. If conductivity of the samples was too high, samples were desalted on C18 cartridges (PhosphoScan Kit, Cell Signaling, USA) according to the manufacturer's instructions. 10 mg per sample were loaded onto a 1 mL resource S column (GE Healthcare, Munich) equilibrated with SCX buffer A using an ÄKTA Purifier chromatography system (Amersham Biosciences, Heidelberg) with a fraction collector. The peptides were separated by a linear gradient of KCl from 0 (SCX buffer A) to 350 mM (SCX buffer B) with a flow rate of 1 mL/min. 17 peptide fractions were collected including the flow through. Adjacent fractions were combined to a total of eleven fractions for enrichment of phosphopeptides.

SCX buffer A: 5 mM potassium dihydrogen phosphate, 30 % ACN, 0.1 % TFA, pH 2.5

SCX buffer B: 5 mM potassium dihydrogen phosphate, 350 mM KCl, 30 % ACN, 0.1 % TFA, pH 2.5

4.6.6 Titansphere (TiO₂) enrichment of phosphopeptides

Phosphopeptides from each fraction and the SCX flow-through were enriched by using TiO₂ chromatography columns as described (Olsen et al., 2006) with minor modifications. Phosphopeptides from the SCX flow-through were extracted in three rounds. Acidified peptide fractions (pH below 2) were incubated with approximately 5 µL TiO₂-material (GL Sciences, Japan) in TiO₂ loading buffer. Beads were washed once with 100 µL TiO₂ washing buffer 1 and twice with 100 µL TiO₂ washing buffer 2 and transferred to home-made C8-STAGE tips (Rappsilber et al., 2003) in 200 µL pipet-tips. The columns were washed once more with TiO₂ washing buffer 2. Phosphopeptides were eluted from the TiO₂-C8-STAGE tips into a 96-well plate with 2 x 20 µL of TiO₂ elution buffer and dried to 2 µL in a Speed-vac. The dried phosphopeptide mixtures were acidified with 5 % ACN in 0.3 % TFA to an end volume of 8 µL.

TiO₂ loading buffer: 3g/L 2,5-DHB, 80 % ACN, 0.1 % TFA

TiO₂ washing buffer 1: 40 % ACN, 0.1 % TFA

TiO₂ washing buffer 2: 80 % ACN, 0.1 % TFA

TiO₂ elution buffer: 40 % ACN in 15 % ammonia-water solution (pH ~11)

4.6.7 Mass spectrometric analyses

4.6.7.1 Liquid chromatography and tandem mass spectrometry (LC-MS/MS)

Phosphopeptide mixtures were analysed by online nanoflow liquid chromatography tandem mass spectrometry (nanoLC-MS/MS) as described previously (Olsen et al., 2006) with a few modifications. Briefly, all nanoLC-MS/MS-experiments were performed on an EASY-nLC™ system (Proxeon Biosystems, Denmark) connected to the LTQ-Orbitrap XL (Thermo Electron, Bremen) through a nanoelectrospray ion source. The phosphopeptides were auto-sampled directly onto the 15 cm long 75 µm-inner diameter (i.d.) analytical column packed with reversed-phase C18 Reprosil AQUA-Pur 3 µm particles at a flow rate of 500 nL/min. The flow rate was reduced to 250 nL/min after loading, and the phosphopeptides were separated with a linear gradient of ACN from 5 to 40 % in 0.5 % acetic acid for 100 min. The effluent from the column was directly electrosprayed into the mass spectrometer.

The LTQ Orbitrap XL instrument under Xcalibur 2.0 was operated in the data dependent mode to automatically switch between full scan MS and MS/MS acquisition. Survey full scan MS spectra (from m/z 300 to 2,000) were acquired in the orbitrap with resolution $R = 60,000$ at m/z 400 (after accumulation to a 'target value' of 1,000,000 in the linear ion trap). The ten most intense multiply-charged ions ($z \geq 2$) were sequentially isolated and fragmented in the linear ion trap by collisionally induced dissociation (CID) at a target value of 5,000 or a maximum ion time of 150 ms. All tandem mass spectra were acquired with the multi-stage activation (MSA) option enabled for neutral losses of m/z 32.66, 48.99 and 97.97. For all full scan measurements in the orbitrap detector a lock-mass ion from ambient air (m/z 445.120025) was used for internal calibration as described earlier (Olsen et al., 2006). Typical mass spectrometric conditions were: spray voltage 2.2 kV; no sheath and auxiliary gas flow; heated capillary temperature, 200 °C; normalized CID collision energy 40 % for MSA in LTQ. The ion selection threshold was set to 100 counts for MS/MS. An activation $q = 0.25$ and activation time of 30 ms for MSA acquisition were used.

4.6.7.2 Assigning peptide sequences using MASCOT and MaxQuant

Raw Orbitrap full-scan MS and ion trap MSA spectra were processed by MaxQuant (Cox and Mann, 2008) as described (Olsen et al., 2006). In brief, all identified SILAC triplets were quantified, accurate precursor masses determined using the entire LC elution profiles and MS/MS spectra were merged into peak-list files (*.msm), and searched against the mouse International protein index (IPI) protein database version 3.37. Peptides and proteins were identified by Mascot (Matrix Science, UK) via automated database matching of all tandem mass spectra against an in-house curated concatenated target/decoy database; a forward and reversed version of the mouse IPI sequence database (version 3.37; 102,934 forward and reversed protein sequences from EBI (<http://www.ebi.ac.uk/IPI/>)) supplemented with common contaminants such as human keratins, bovine serum proteins and porcine Trypsin was used. Tandem mass spectra were initially matched with a mass tolerance of 7 ppm on precursor masses and 0.5 Da for fragment ions, and strict Trypsin specificity and allowing for up to three missed Tryptic cleavage sites. Cysteine carbamidomethylation (Cys +57.021464 Da) was searched as a fixed modification, whereas N-acetylation of protein (N-term +42.010565 Da), N-pyro-glutamine (Gln - 17.026549), oxidized methionine (+15.994915 Da) and phosphorylation of serine, threonine and tyrosine (S/T/Y +79.966331 Da) were searched as variable modifications.

4.6.7.3 Analysis of assigned peptide sequences

The resulting Mascot result files (*.dat) were loaded into the MaxQuant software (Cox and Mann, 2008) for further processing. In MaxQuant an estimated false discovery rate (FDR) of all peptide and protein identifications was fixed at 1 %, by automatically filtering on peptide length, mass error and Mascot score of all forward and reversed peptide identifications. Finally, to pinpoint the actual phosphorylated amino acid residue(s) within all identified phosphopeptide sequences in an unbiased manner, the localisation probabilities of all putative serine, threonine and tyrosine phosphorylation sites were calculated using the PTM score algorithm as described (Olsen et al., 2006). Quantification of phosphorylation sites was done by MaxQuant software as described (Olsen et al., 2006). Data were normalised such that the median log-transformed ratio of all peptides identified were zero, to correct for

unequal sample mixing. Phosphopeptide ratios referring to un-stimulated wild type were calculated for each genotype and time point.

4.6.7.4 Exclusion of contaminating proteins

Samples can be contaminated with FCS proteins during cell culture or with human keratins during sample preparation. Exclusion of contaminating proteins is especially important for the analysis of down-regulated phosphorylation sites, since contaminating proteins do not contain labelled amino acids and are therefore often characterised by very low SILAC-ratios in all conditions. Most contaminating proteins were identified via an in-house curated database of contaminating proteins (human keratins, bovine serum proteins and porcine Trypsin) (section 4.6.7.2). Furthermore, phosphorylation sites with SILAC-ratios ≤ 0.3 in all conditions were manually checked for keratins or secreted proteins using PubMed Gene (<http://www.ncbi.nlm.nih.gov/sites/entrez?db=pubmed>). For proteins with unclear annotation, homology of the identified peptide sequences with bovine and murine proteins was analysed using NCBI-BLAST2 (<http://www.ebi.ac.uk/Tools/blastall/>). If the BLAST scores for murine and bovine proteins were equal, the protein was regarded as contaminant. Phosphorylation sites on contaminating proteins were removed from the dataset.

4.6.7.5 Calculation of labelling efficiency and arginine to proline conversion

Labelling efficiency and conversion of labelled arginine to proline were calculated after mass spectrometry had been performed according to the following formulae:

$$E = 1 - (1 / (2 R + 1))$$

- E Labelling efficiency
R Ratio of completely labelled/partially labelled peptide

$$P = 1 / (2 R^* + 1)$$

- P Arginine to proline conversion
R* Ratio of peptide with labelled proline/peptide with labelled arginine

4.7 Bioinformatic analyses

After exclusion of contaminating proteins (section 4.6.7.4), reproducibly regulated in the same direction in both experiments analyses on the phosphoprotein level were performed on all phosphorylated proteins, regardless of the probability for right localisation of the phosphate group within a peptide according to the PTM score (Olsen et al., 2006). (Note that the likelihood that such a peptide is phosphorylated is still $\geq 99\%$). Analyses on the phosphorylation site level included only sites for which the phosphate group could be localised within the peptide with single amino acid accuracy (class I sites).

4.7.1 Definition of genes expressed in macrophages

Genes expressed in macrophages were defined from a previously published genome-wide analysis of LPS tolerance in macrophages in the laboratory (Mages et al., 2007) (dataset is available in the Gene Expression Omnibus (GEO) database (<http://www.ncbi.gov/geo/>), identifier GSE8621). All genes represented by at least one probe set with present-calls on at least two of twelve microarray samples and a normalised expression value of at least 80 were considered as expressed in macrophages.

4.7.2 Contribution of gene expression changes to regulation of the phosphoproteome

Changes in gene expression on the level of total cellular RNA were correlated with changes in phosphorylation for all proteins with LPS-up-regulated phosphorylation (\log_2 ratio of mean fold-changes from two independent experiments). If several probe sets existed for one gene, the probe set with the highest expression value was selected. For 35 proteins with LPS-up-regulated phosphorylation no corresponding probe set was found or RNA expression was not above background level.

4.7.3 Gene Ontology (GO) analysis

While most GO analysis tools calculate an over-representation of GO terms over the genomic background a strategy for direct comparison of different lists against each other was developed in this thesis: Numbers of phosphoproteins associated with

each GO term were determined using the GO Browser in Spotfire DecisionSite (Tibco, Munich), using the generic GOSlim ontology file (OBO-Edit version 1.101) and the GO annotation file for mouse (version 11/7/2008), downloaded from <http://www.geneontology.org/GO>. To determine statistically significant over-representation of GO terms, odds ratios ((number of matches list A / number of non-matches list A) / (number of matches list B / number of non-matches list B)) and Fisher's exact probabilities using the R Statistics package (<http://www.r-project.org>) were calculated for each GO term, comparing proteins with LPS-regulated and non-regulated phosphorylation sites. P-values were corrected for multiple testing using the Benjamini-Hochberg method for controlling false discovery rate (FDR) (Benjamini and Hochberg, 1995). Only GO terms with at least three identified phosphoproteins were analysed. GO terms with an odds ratio ≥ 1.3 and a corrected p-value ≤ 0.05 were considered significant.

4.7.4 Kinase motifs

Phosphorylation sites were matched to the known substrate specificities (linear sequence motifs) of 33 human kinases (<http://www.phosida.com>). To determine statistically significant over-representation of a motif, the number of sites that matched the pattern was determined among LPS-up-regulated and LPS-down-regulated phosphorylation sites and among phosphorylation sites that were not regulated in response to LPS. Odds ratios and Fisher's exact probabilities, which were corrected for multiple testing, were calculated as described for the GO analysis (section 4.7.3). All enriched kinase motifs matched at least ten phosphorylation sites. Motifs with an odds ratio ≥ 1.3 and a corrected p-value ≤ 0.05 were considered significant.

4.7.5 Signalling pathways

4.7.5.1 Over-representation analysis

Phosphoproteins were assigned to signalling pathways via ENSEMBL identifiers using InnateDB (Lynn et al., 2008; <http://www.innateDB.ca>, version 29/1/2009), which provides pathway annotation from many different databases and calculates over-representation over the genomic background. For a direct comparison of LPS-regulated and non-LPS-regulated phosphoproteins, the number of phosphoproteins

associated with each pathway was determined with InnateDB, and odds ratios and Fisher's exact probabilities were calculated as described for the GO analysis (section 4.7.3). Only pathways for which at least five phosphoproteins were identified were included in the analysis. Signalling pathways with an odds ratio ≥ 1.3 and a p-value ≤ 0.05 were considered significant.

4.7.5.2 Protein interaction networks

Gene symbols of over-represented signalling pathways were extracted from InnateDB (<http://www.InnateDB.ca>; Lynn et al., 2008) and loaded into the database STRING 8.0 (Jensen et al., 2009; <http://string.embl.de>) for extraction of protein interaction networks. Reported interactions included direct (physical) and indirect (functional) interactions based on experimental evidence from high-throughput studies, co-regulation of gene expression, same genomic context or co-citation in the literature. Networks were visualised with Cytoscape v.2.6.2 (<http://www.cytoscape.org>). Only interactions with a minimum STRING combined score of 0.400, which represents the default medium confidence level in STRING, were kept.

4.7.6 Transcription factor (TF) phosphorylation and DNA binding sites

4.7.6.1 Over-representation analysis of TF binding sites

To determine over-represented TF binding sites in LPS-regulated promoters, promoter sequences of LPS-induced genes (≥ 3 -fold) and of genes not regulated by LPS (2,000 probe sets with the least regulation; to minimise background noise, only probe sets with GeneID and a maximal expression value of at least 50) were retrieved with Genomatix Gene2Promoter via GeneIDs (<http://www.genomatix.de>, large scale option, database version EIDorado 07-2008) and searched for the presence of binding sites for 50 TF families with phosphorylated members, with Genomatix RegionMiner (<http://www.genomatix.de>, matrix library version 7.1). RegionMiner determines the number of hits and calculates over-representation over the genomic background. In contrast, the number of promoters with a binding site, not the number of binding sites within a promoter was considered in this thesis and two lists were compared directly to each other: Binding site over-representation in promoters of LPS-regulated genes compared to promoters of genes not regulated

by LPS was determined by odds ratios and Fisher's exact probabilities, which were corrected for multiple testing, as described for the GO analysis (section 4.7.3). TF families with an odds ratio ≥ 1.3 and a corrected p-value ≤ 0.05 were considered significantly different.

4.7.6.2 Evolutionary conservation of TF phosphorylation sites

Amino acid sequences of murine TFs and available orthologs from other species were derived from Uniprot (<http://www.uniprot.org>), aligned with ClustalW (<http://www.ebi.ac.uk/Tools/clustalw2>) and analysed for evolutionary conservation of amino acid residues that showed LPS-regulated phosphorylation in the phosphoproteome study.

4.7.6.3 Evolutionary conservation of TF binding sites

To determine evolutionary conservation of TF binding sites, the promoters of the 20 most strongly induced genes in nascent RNA (45 min, ranked mean fold-changes from two independent experiments) were compared to orthologous vertebrate promoters (retrieved with Genomatix Gene2Promoter (<http://www.genomatix.de>), database version EIDorado 12-2009) with Genomatix MatInspector (Cartharius et al., 2005), and similar positions of TF binding sites relative to the transcriptional start sites were determined by eye in Genomatix-aligned promoters.

5 Results

5.1 Quantitative phosphoproteome analysis of primary macrophages

The global and quantitative analysis of macrophage phosphorylation sites in response to TLR4 ligation with LPS in this thesis builds on a previously described strategy combining Stable isotope labelling with amino acids in cell culture (SILAC) for quantification, Strong-cation-exchange (SCX) and Titansphere (TiO₂) chromatography for phosphopeptide enrichment and high-accuracy mass spectrometric characterisation (Fig. 14) (Olsen et al., 2006), which was optimised for use with primary bone marrow-derived macrophages (BMDMs) as described below:

5.1.1 Optimised protocol for SILAC of primary BMDMs

SILAC (section 1.4.4) allows highly accurate quantification of peptides from different samples relative to each other. However, metabolic labelling of primary cells is not a trivial task. First, SILAC requires sufficient time of cell culture for full labelling of all proteins with heavy isotope versions of essential amino acids. For cell lines with high proliferation rates, for example for HeLa cells, labelling takes around ten cell divisions (Olsen, personal communication). The rate of cell division during the standard 7-day protocol for generation of BMDMs (section 4.2.2) is unknown, but was not expected to be sufficient. Second, to prevent contamination with non-labelled counterparts of the SILAC amino acids, fetal calf serum (FCS) needs to be replaced with dialysed FCS, which might not contain all factors required for culture of primary cells. Third, since Trypsin, which is used to generate peptides for mass spectrometric analyses (section 1.4.2), cuts after arginine and lysine, these essential amino acids are used for SILAC to ensure labelling of all Tryptic peptides, but conversion of labelled arginine to proline can impede quantification of proline-containing peptides. The amount of arginine therefore needs to be reduced as far as possible, without limiting cell growth and metabolism.

The use of dialysed FCS within the standard protocol for generation of BMDMs (section 4.2.2) did not alter the number of cells obtained per mouse, macrophage surface marker expression or MAPK activation and cytokine production in response

to LPS (data not shown). Subsequently, the standard protocol was adapted to longer time of culture in the presence of SILAC medium, containing labelled arginine and lysine amino acids (Fig. 11A): After overnight depletion of adherent cells from bone marrow, expansion of progenitor cells was induced with cytokines (IL-3, IL-6, and SCF) in the presence of L-cell conditioned medium (LCCM) (section 4.2.1) as a source of M-CSF, which was before filtered three times using 5 kDa cut-off columns to remove non-labelled amino acids. IL-3, IL-6 and SCF are cytokines with a role in macrophage development *in vivo* (section 1.2.1) and have been used to stimulate proliferation of bone marrow cells for retroviral infections (e.g. Holst et al., 2006). Following 13 days expansion, cells were differentiated into macrophages with M-CSF only in the absence of cytokines for 3 days. Adherent *and* non-adherent cells were kept during the whole expansion and differentiation process, while only adherent cells were plated for stimulation. A detailed description is given in the Methods section (4.2.3). This 17-day protocol yielded large numbers of cells (Fig. 11B).

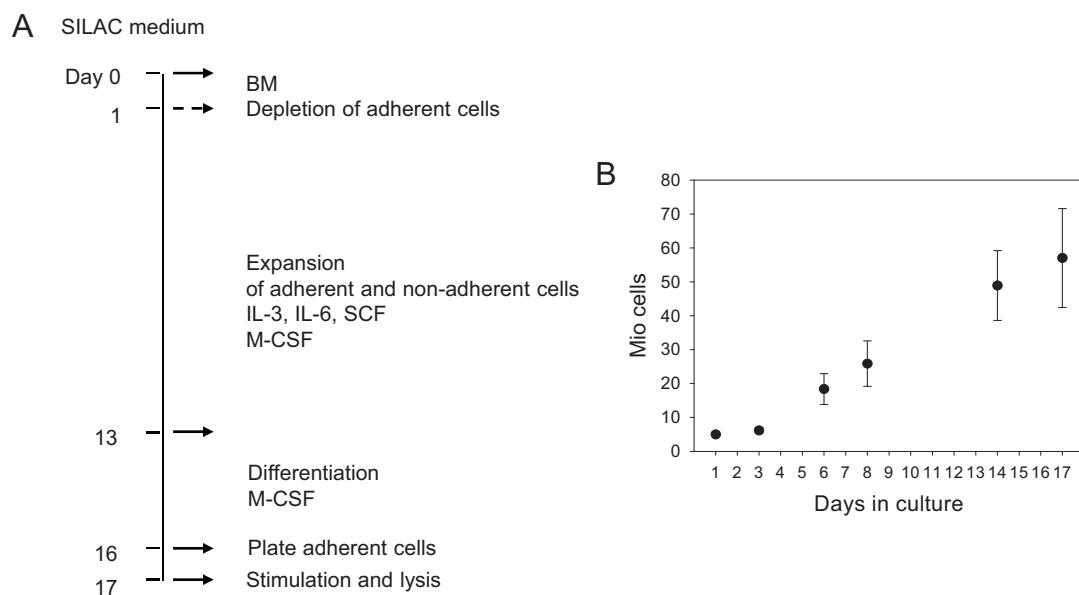


Fig. 11. Optimised protocol for SILAC of bone marrow-derived macrophages (BMDMs).

(A) Cells were cultured in SILAC medium containing labelled arginine and lysine amino acids and dialysed FCS during the whole time in culture. Details are given in the Methods section (4.2.3). (B) Cell proliferation under the SILAC protocol. Depicted are total numbers of cells at different time points during SILAC labelling (means \pm standard deviations from two independent experiments).

Best labelling efficiency (90 to 95 %, Fig. 12A, B) and minimal conversion of labelled arginine to proline (below 5 %, Fig. 12A, C) were reached at high concentrations of labelled lysine (146 mg/L) and arginine (84 mg/L) in the presence of non-labelled proline (30 mg/L).

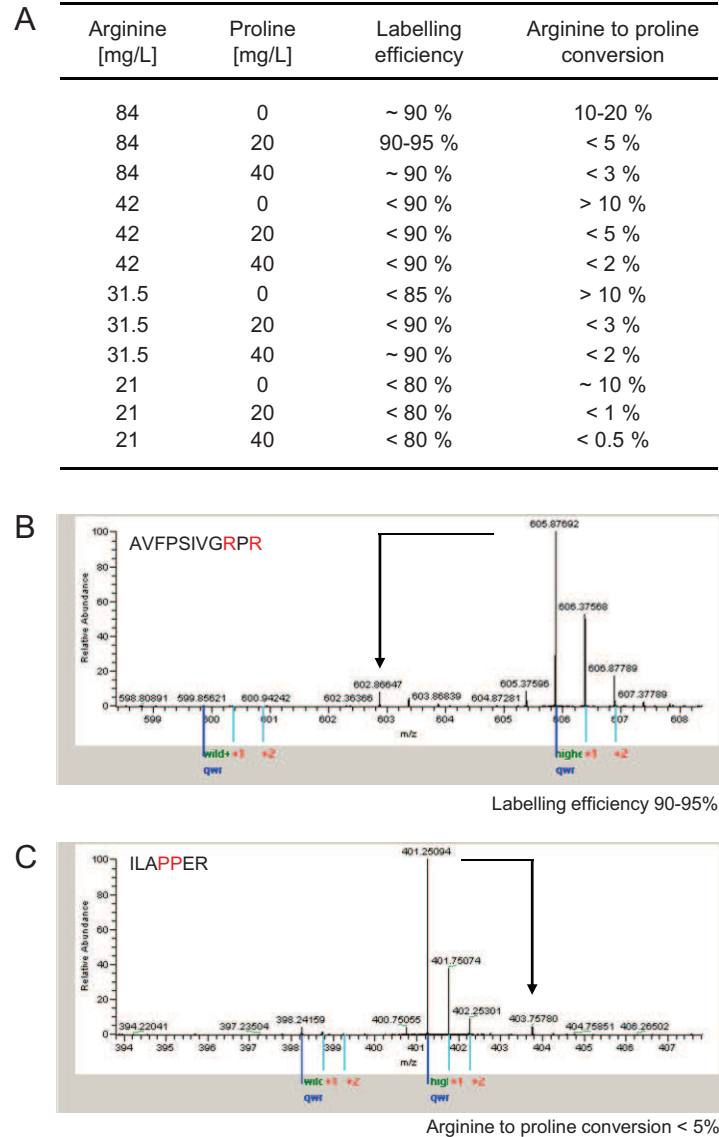


Fig. 12. Labelling efficiency and arginine to proline conversion.

(A) Titration of labelled arginine and non-labelled proline to optimise labelling efficiency and arginine to proline conversion, using the optimised protocol depicted in Fig. 11A. (B) Labelling efficiency. Representative peptide containing two arginine residues. The arrow indicates the position of partially labelled peptide. (C) Arginine to proline conversion. Representative proline-containing peptide. The arrow indicates the position of peptide with labelled proline. Labelling efficiency and arginine to proline conversion were calculated as described in the Methods section (4.6.7.5).

Macrophages obtained by the 17-day protocol showed increased auto-fluorescence, which is a common phenomenon during long term culture, likely caused by incorporation of flavonoids from the medium (Fig. 13A, left panel). Expression of the macrophage surface marker CD11b was similar and expression of F4/80 was slightly reduced compared to normal macrophages (Fig. 13A, middle and right panels). As macrophages obtained by the standard or SILAC-adapted protocols were comparable in terms of functional readouts in response to LPS stimulation, such as activation of p38 MAPK and production of inflammatory cytokines (CCL3, CCL4, IL-6, IL-12p40, IL-10) (Fig. 13B-D and data not shown), the 17-day protocol was used to SILAC-label cells for the phosphoproteome study.

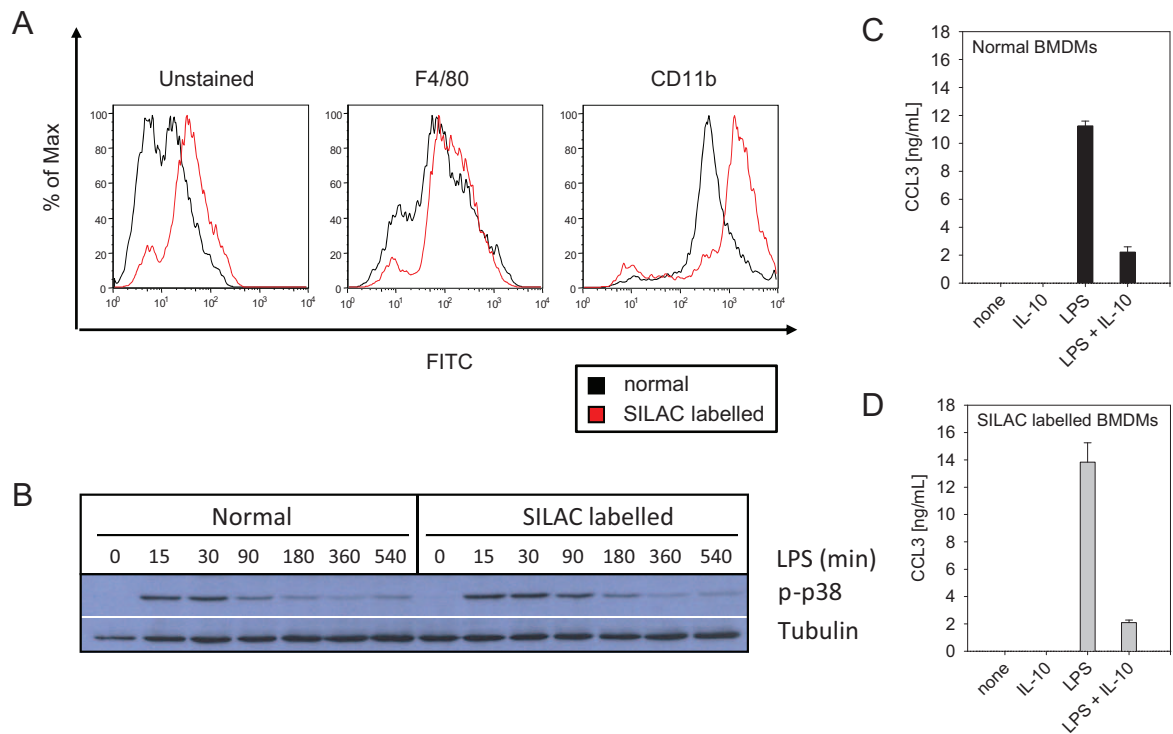


Fig. 13. Quality control of macrophages obtained by the SILAC-adapted protocol.

(A) Surface marker expression of macrophages differentiated with the normal or SILAC-adapted protocols, as analysed by flow cytometry. (B) Western blot for phosphorylation of p38 MAPK after stimulation with 100 ng/mL LPS for the indicated times. (C) Cytokine expression in response to overnight stimulation with 100 ng/mL LPS and/or 5 ng/mL IL-10 was measured by ELISA (means \pm standard deviations from two technical replicates). Data are representative for two independent experiments.

5.1.2 Experimental setup

The aim of this study was to analyse the phosphoproteome of resting and LPS-activated macrophages. As the MAPK phosphatase DUSP1 had been shown to negatively regulate LPS-induced signalling in our laboratory and elsewhere (section 1.3.5), macrophages from *Dusp1*-deficient mice were also included in this study. Based on the kinetics of p38 activation in response to LPS (Fig. 13B), it was decided to compare phosphorylation in un-stimulated macrophages to phosphorylation observed 15 min and 4 h after LPS stimulation.

Macrophages from wild type and *Dusp1*-deficient mice were SILAC-encoded with both arginine and lysine, using three distinct isotopic forms (Fig. 14). Cells were stimulated with LPS for 15 min, 4 h or were left un-treated and lysed in the presence of protease- and phosphatase-inhibitors (section 4.6.1). Cell lysates were pooled as indicated in Fig. 14. Pooling samples for further preparation ensures equal sample treatment and highly accurate quantification. Comparison of more than three conditions can be achieved by including a common reference lysate, here un-stimulated wild type, in several pools, which is used as a reference point for calculation of phosphopeptide ratios. Mixed protein lysates were separated into a soluble and a chromatin pellet fraction. The soluble fraction was digested into peptides *in-solution* using Lys-C and Trypsin, and peptides were fractionated by SCX chromatography. Proteins from the chromatin pellet were re-solubilised, separated by 1D SDS-PAGE, the gel was cut into pieces and proteins were digested *in-gel* with Trypsin. Each fraction was enriched for phosphopeptides on TiO_2 and analysed by online LC-MS/MS as described in the Methods section (section 4.6.). Serine, threonine and tyrosine phosphorylation were searched as variable modifications. Phosphate groups were localised within the peptide sequences according to the PTM score (Olsen et al., 2006). Data were normalised to correct for unequal sample mixing (section 4.6.7.3), and fold-changes relative to un-stimulated wild type were calculated for each phosphopeptide and condition. Two independent experiments were performed.

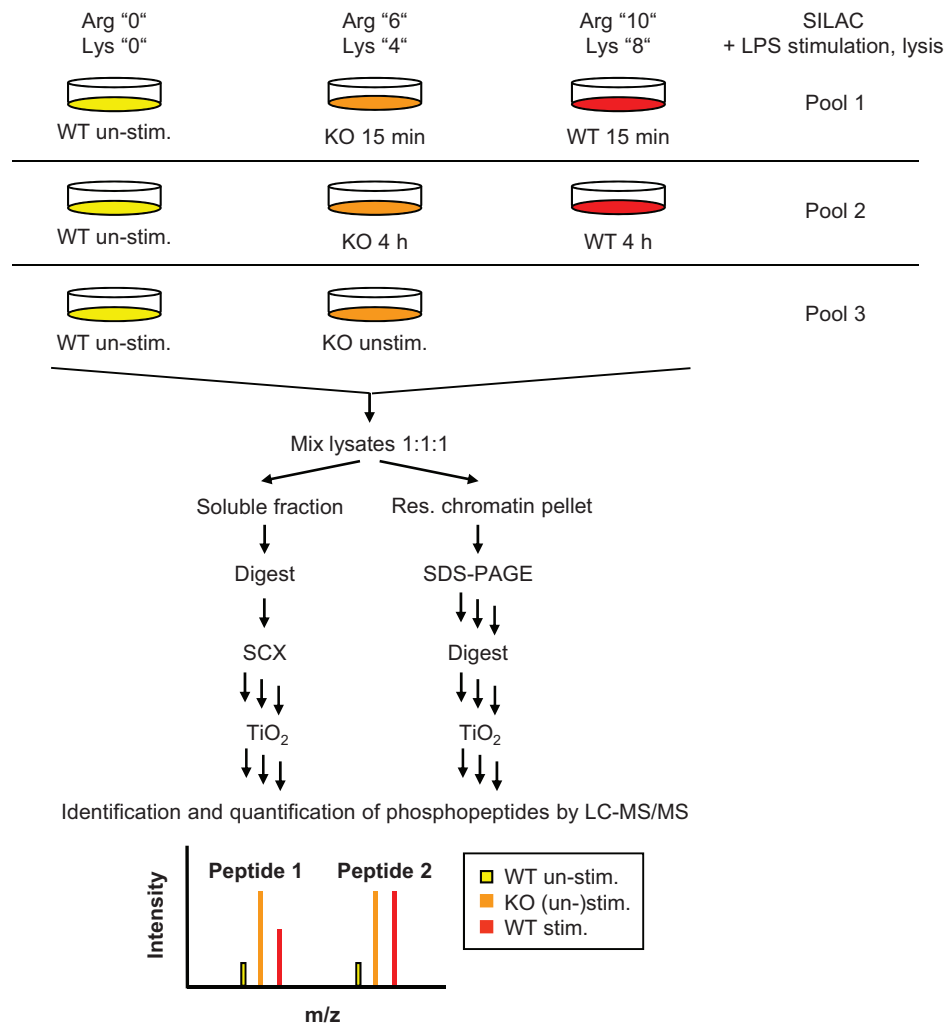


Fig. 14. Strategy for global and quantitative analysis of LPS-regulated phosphorylation.

Bone marrow cells from wild type (WT) and *Dusp1*-deficient (KO) mice were SILAC encoded with normal and stable isotope-substituted arginine and lysine amino acids, creating three states distinguishable by mass. Each population was stimulated with 100 ng/mL LPS for 15 min or 4 h or left un-treated. Un-stimulated wild type cells were included in all three pools as a common reference point. Cell lysates to be directly compared were pooled, fractionated, and enzymatically digested into peptides, and phosphopeptides were enriched on TiO₂ and analysed by online liquid chromatography tandem mass spectrometry (LC-MS/MS). Due to the mass shifts introduced by the SILAC amino acids mass spectra of labelled peptides revealed SILAC triplets (same peptide from the three cell populations of a pool), with the intensities of the peaks reflecting the relative amounts of a peptide in the three conditions. This SILAC-based approach allowed high-accuracy quantification of phosphopeptides and, in most cases, localisation of the phosphate group with single amino acid accuracy. Two independent experiments were performed. (m/z) mass-to-charge ratio, (SCX) Strong cation exchange. SILAC amino acids: L-arginine-HCl ¹³C₆ (Arg "6") or ¹³C₆¹⁵N₄ (Arg "10"), L-lysine-HCl ²D₄ (Lys "4") or ¹³C₆¹⁵N₂ (Lys "8") or non-labelled counterparts (Arg "0" and Lys "0").

5.1.3 Macrophage phosphorylation sites and proteins

6,956 phosphorylation sites on 1,850 proteins were reproducibly identified with single amino acid accuracy ("class I" according to the PTM score (Olsen et al., 2006), Appendix, Tab. S1). More than 60 % were novel with respect to the

phosphorylation site database Expasy (containing all Swiss-Prot/TrEMBL entries; <http://www.expasy.ch>) and a recent phosphoproteome study in the mouse liver cell line Hepa1 to 6 (Pan et al., 2008) (Appendix, Tab. S1). The overlap between the two independent experiments was 63 to 89 %, depending on the experiment referred to (Fig. 15). All following bioinformatic analyses were focused on these reproducibly identified phosphorylation sites and phosphoproteins, if not indicated otherwise (section 4.7).

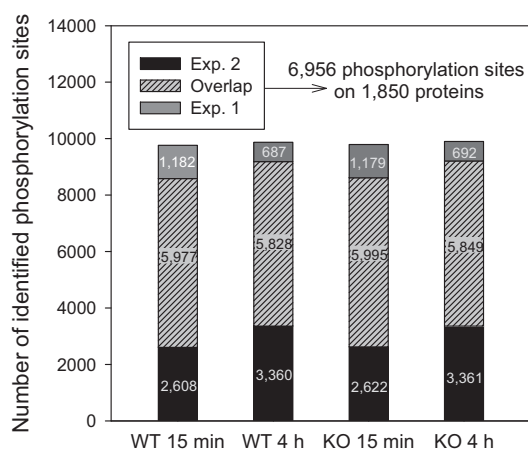


Fig. 15. Overlap of phosphorylation sites identified in two independent experiments.

Depicted are phosphorylation sites which could be quantified in the indicated conditions relative to un-stimulated wild type. All following bioinformatic analyses focus on reproducibly identified phosphorylation sites and phosphoproteins, if not indicated otherwise.

In accordance with previous reports from other cellular systems (Olsen et al., 2006; Pan et al., 2008; Villen et al., 2007) most phosphorylation sites were on serine (84 %) and threonine residues (14 %), while tyrosine phosphorylation occurred only in 2 % of the cases (Fig. 16).

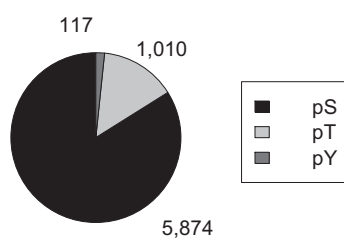


Fig. 16. Distribution of phosphorylated amino acids.

Total numbers of serine (pS), threonine (pT), tyrosine (pY) phosphorylation sites.

The detected phosphoproteins were derived from all cellular compartments: A comparison of the Gene Ontology (GO) annotation for cellular component (<http://www.geneontology.org/GO>) between the identified phosphoproteins and genes expressed in macrophages on the mRNA level (section 4.7.1) showed an overall similar distribution (Fig. 17). GO terms with odds ratio ≥ 1.3 or ≤ 0.67 and Fisher's exact probability ≤ 0.05 after correction for multiple testing were considered significantly different (section 4.7.3). As expected, extracellular proteins were under-represented among phosphoproteins. Also, among phosphoproteins a relative paucity of proteins from mitochondria, ribosomes, endoplasmic reticulum and lysosomes was observed. This is in line with previous observations of low phosphorylation (Olsen et al., 2006) and protein kinase expression (Pagliarini et al., 2008) in mitochondria. Surprisingly, the plasma membrane was well represented among phosphoproteins, indicating that the under-representation of phosphoproteins from cellular organelles is unlikely to be caused by technical reasons. Of note, among phosphoproteins over-representation of the terms "nucleus", "chromosome" and "cytoskeleton" was observed.

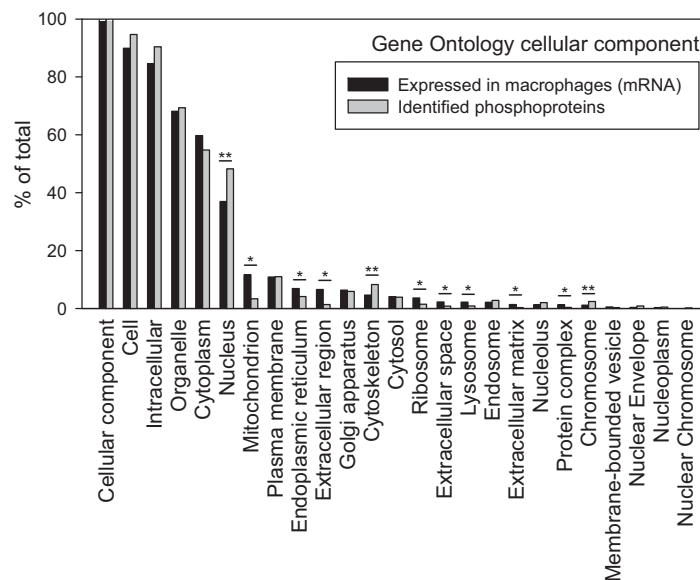


Fig. 17. Distribution of phosphorylated proteins in cellular compartments.

Genes expressed in macrophages (definition in section 4.7.1) and identified phosphoproteins were assigned to GOSlim Gene Ontology terms (<http://www.geneontology.org/GO>) for cellular component using the GO browser of Spotfire DecisionSite. The number of proteins associated with each GO term is referred to the total number of proteins in the respective list (% of total). Significantly over- and under-represented GO terms are marked (odds ratio ≥ 1.3 (**)) or ≤ 0.76 (*), respectively, and corrected p-value ≤ 0.05 .

5.2 Dynamics of the phosphoproteome after TLR4 activation

Next, changes in phosphorylation dependent on LPS stimulation, time, gene expression dynamics and the MAPK phosphatase DUSP1 were investigated:

5.2.1 Minor effect of DUSP1-deficiency on global phosphorylation

Deletion of DUSP1 had only a small impact on the phosphoproteome, with less than 1.3 % of all phosphopeptides hyper-phosphorylated in resting (data not shown) and 2 % in LPS-activated (Appendix, Tab. S1) *Dusp1*-deficient macrophages more than 1.5-fold in both experiments, suggesting a limited role of DUSP1 in the control of phosphorylation downstream of TLR4 (definition of cut-off see below, section 5.2.2). However, in contrast to the strong and reproducible effects of LPS in wild type cells described below (section 5.2.2), a high degree of variability between experiments was observed, regarding the expected influence of DUSP1 on phosphorylation of its main target p38 MAPK:

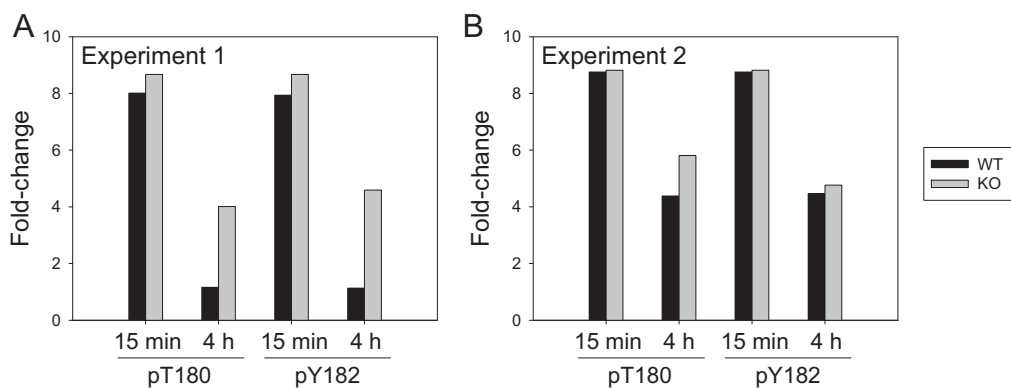


Fig. 18. Influence of DUSP1 on phosphorylation of p38 MAPK.

p38 MAPK phosphorylation relative to un-stimulated wild type is depicted for phosphorylated threonine 180 (pT180) and tyrosine 182 (pY182), which are known target sites for DUSP1 action on p38, in wild type (WT) and *Dusp1*-deficient (KO) macrophages. (A) Experiment 1. (B) Experiment 2.

Only in one of the two experiments had the level of p38 MAPK phosphorylation returned to base line in wild type cells 4 h after stimulation, while it was still 3-fold stronger in the absence of DUSP1 (Fig. 18A). In the other experiment, reduction of phosphorylation in wild type cells was only achieved to the same level observed in *Dusp1*-deficient cells (Fig. 18B). This indicated that DUSP1-dependent down-regulation of phosphorylation took only place in the first experiment. Because of the

lack of a good antibody to assess expression of DUSP1 in the phosphoproteome samples, and the observed variability in DUSP1-dependent de-phosphorylation of its most prominent target p38, it was decided to focus for further analyses on the effect of LPS on the phosphoproteome in wild type cells.

5.2.2 Strong and dynamic regulation by LPS stimulation

Stimulation with LPS strongly affected the phosphoproteome at both time points. Overall, phosphorylation of 24 % of all sites was up-regulated and 9 % down-regulated more than 1.5-fold in both experiments in response to LPS in wild type cells (Fig. 19A and B). These criteria can be considered very stringent, as less than 0.5 % of the identified non-phosphorylated peptides were found to change more than 1.5-fold in both experiments within 15 min after stimulation, a time frame too short to expect considerable changes in protein expression (data not shown). For following bioinformatic analyses, phosphorylation sites regulated as defined above were compared to non-regulated phosphorylation sites with changes between 0.67- and 1.5-fold in both experiments.

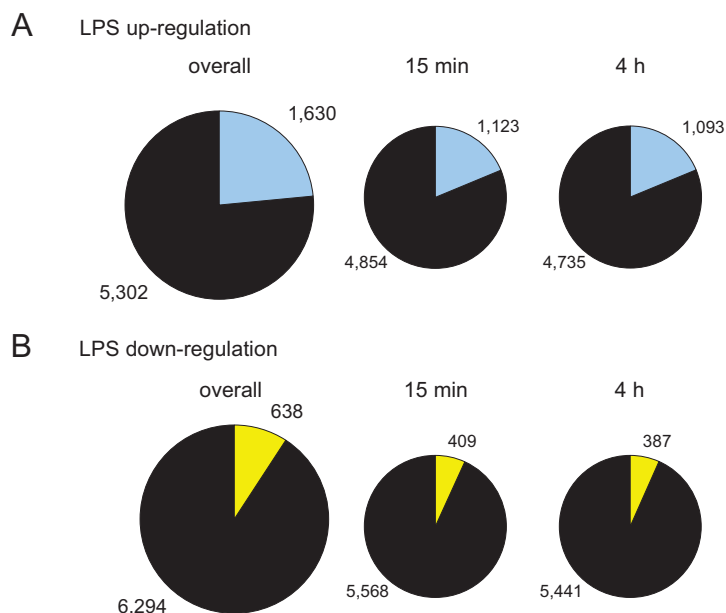


Fig. 19. Extent of regulation by LPS.

A fold-change relative to un-stimulated wild type of at least 1.5 in both experiments was used as threshold to define (A) up- and (B) down-regulated phosphorylation sites in wild type cells. Phosphorylation sites up-regulated in both experiments are indicated in blue, phosphorylation sites down-regulated in both experiments in yellow. All other phosphorylation sites are indicated in black.

The extent of regulation by LPS was very similar between short and prolonged stimulation (Fig. 19A and B). This could, in principle, result either from sustained phosphorylation and de-phosphorylation or from dynamic regulation of different phosphorylation sites. Analysis of the kinetic profiles (Fig. 20A) revealed that the phosphorylation status was sustained over time for only 36 % of up-regulated and 25 % of down-regulated phosphorylation sites (Fig. 20A and B, black bars). All other sites changed their phosphorylation status over time (Fig. 20A and B, light grey bars) or were detected at one of the time points only (Fig. 20B, dark grey bars), arguing against presence at the other time point in high amounts. Consequently, the changes in phosphorylation were of a highly dynamic nature for a large fraction of regulated phosphorylation sites.

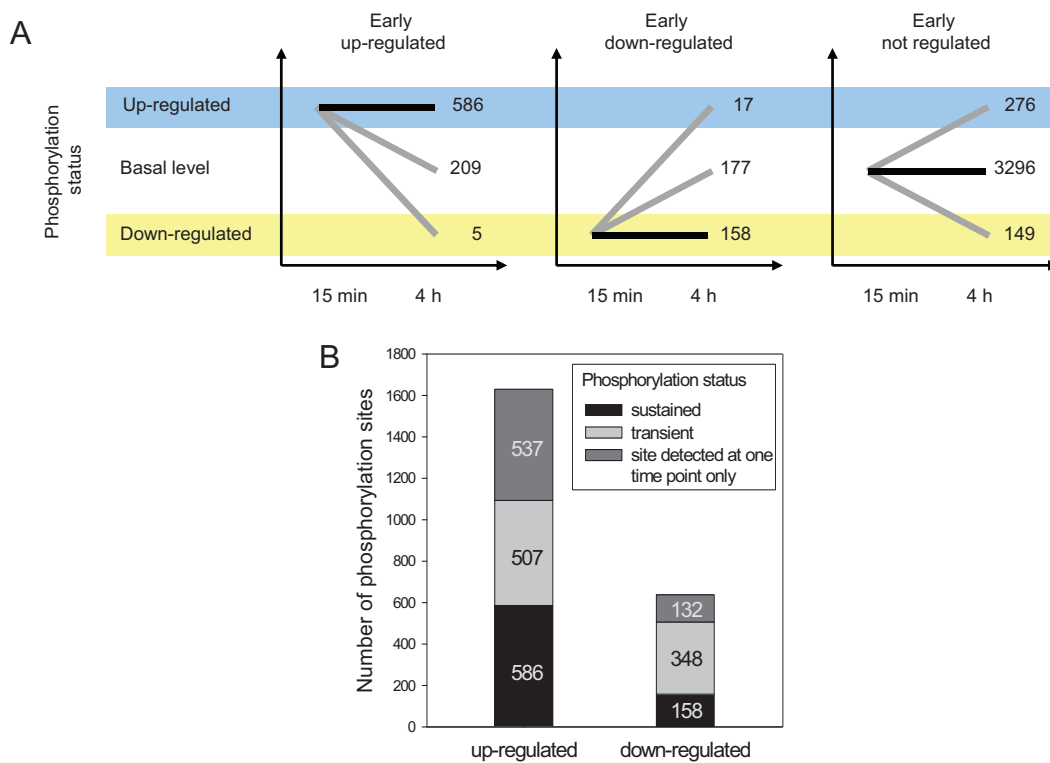


Fig. 20. Kinetics of regulation.

(A) Kinetic profiles of phosphorylation sites identified in wild type cells at both time points. (B) Kinetic status of phosphorylation for LPS-regulated sites. Phosphorylation sites were detected at one of the time points only (dark grey) or at both time points, with either sustained (black) or transient phosphorylation status (light grey).

5.2.3 Limited contribution of gene expression changes to the regulation of the phosphoproteome

To estimate the contribution of LPS-induced changes in gene expression to the observed changes in phosphorylation, transcriptome analyses were performed on macrophages cultured under identical conditions as for the phosphoproteome experiments (except SILAC), which were stimulated with LPS for 45 min or 4.5 h or left un-treated. Early after stimulation only two genes with up-regulated protein phosphorylation showed stronger increases in total mRNA levels than in phosphorylation (Fig. 21A). At the late time point regulation of gene expression was more common, but more than 90 % of all up-regulated phosphorylation sites had stronger changes in phosphorylation than in gene expression (Fig. 21B), indicating that induction of gene expression, in most cases, does not account for the increased phosphorylation.

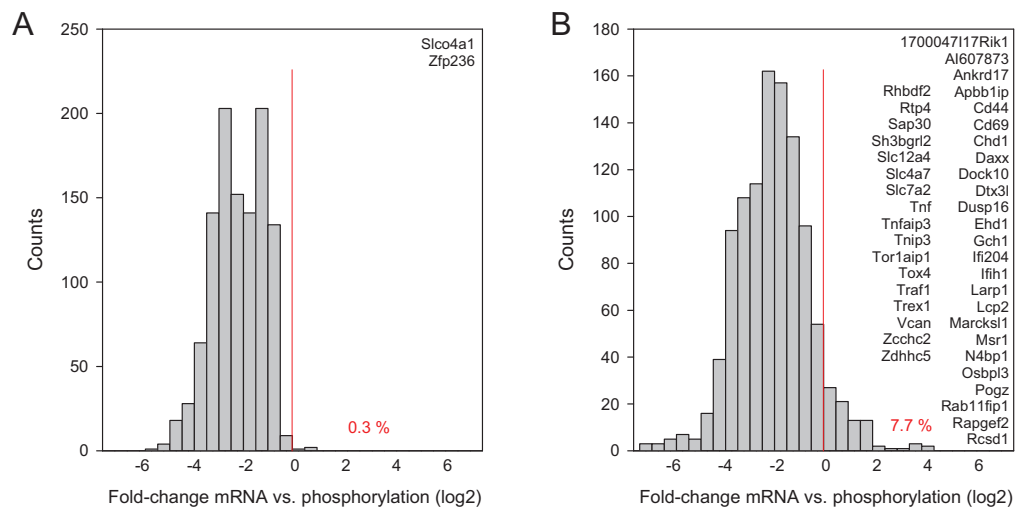


Fig. 21. Contribution of gene expression changes to the regulation of the phosphoproteome.

Transcriptome analyses using Affymetrix Mouse GeneST[®] 1.0 microarrays were performed on LPS treated macrophages cultured under identical conditions as for the phosphoproteome experiments (except SILAC). Changes in gene expression (total RNA; 45 min and 4.5 h, 100 ng/mL LPS treatment) relative to changes in phosphorylation (15 min, 4 h) are shown for LPS up-regulated phosphorylation sites (A) early and (B) late after stimulation (log₂ ratio of mean fold-changes from two independent experiments, 0.5-bins). The percentage of phosphorylation sites with stronger changes in gene expression than in phosphorylation and gene symbols of affected proteins are indicated.

5.3 Kinase activity induced by LPS

Each of the phosphorylation sites identified here is the substrate of one or more kinases. To obtain footprints of kinase activation in response to TLR ligation, the phosphopeptide sequences were searched for the known substrate specificities of 33 human kinases (<http://www.phosida.com>), which have been shown to match well with murine phosphorylation sites (Pan et al., 2008). Motifs enriched among LPS-up-regulated or down-regulated compared to non-regulated phosphorylation sites were determined by calculation of odds ratios and Fisher's exact probabilities corrected for multiple testing as described in the Methods section (section 4.7.4). Motifs with an odds ratio of at least 1.3 *and* a corrected p-value below 0.05 were considered significantly different between LPS-regulated and non-regulated conditions. 15 min after stimulation the strongest over-representation was observed for the Extracellular signal regulated kinase (ERK)/MAPK motif, which is in accordance with the known role of the MAPK module in TLR signalling (Tab. 7). Other over-represented motifs were associated with kinases recently described in the context of TLR signalling: Protein kinase D (PKD) plays a role in TLR9 and TLR5 signalling (Ivison et al., 2007; Park et al., 2009b); activation of AKT and its targets GSK3 and mTOR has recently been shown in response to TLR stimulation (Cao et al., 2008; Schmitz et al., 2008); Ca²⁺-dependent activation of Calmodulin kinase 2 (CAMK2) is required for the expression of many LPS target genes (Liu et al., 2008b). Other kinases, among them the DNA damage-activated kinases Ataxia-telangiectasia mutated (ATM) and ATM and Rad 3-related (ATR) and the cell cycle-associated kinases AURORA and Checkpoint kinases 1 and 2 (CHK1/2), have not been linked to the response to LPS before. 4 h after stimulation over-representation could only be detected for few motifs, among them the ERK/MAPK motif (Tab. 7) (discussed in section 6.1.2). All kinases associated with over-represented motifs were expressed in macrophages in the corresponding microarray study, and some had LPS-regulated phosphorylation sites themselves, potentially modulating kinase activity (Tab. 7). Interestingly, over-representation of several motifs, including the ERK/MAPK motif, was also observed for down-regulated phosphorylation sites (Tab. 7), suggesting that TLR signalling also triggers down-regulation of this type of phosphorylation by activation of phosphatases or degradation of the

phosphorylated proteins. Furthermore, regulation of kinase and phosphatase activity or degradation could also be restricted to different cellular compartments, e.g. cytoplasm versus nucleus, explaining over-representation of a motif among up- and down-regulated phosphorylation sites at the same time point.

Tab. 7. Kinase activation during TLR4 signalling.

Time	Kinase motif	Enrichment (odds ratio) up	Enrichment (odds ratio) down	Kinase expression	Kinase phosphorylation
15 min	ERK/MAPK	3.7	3.5	Mapk1, 3, 4, 6-9, 11-15	Mapk3**, 6,9,10**,14**
	ATM/ATR	3.5	---	Atm, Atr	---
	PKD	3.4	---	Pkd1, Pkd1-3, Pkd2	---
	CHK1	3.2	---	Chka*, Chkb-cpt1b	---
	AURORA	2.5	---	Aurka-c, Aurkaip1	---
	CAMK2	2.1	---	Camk2a, b, d, g, n1, n2	Camk2d, Camkk2
	PLK	1.9	---	Plk1, 2*, 3, 4	---
	NEK6	1.7	2.2	Nek1-9	Nek3, 9
	PKA	1.6	---	Prkaa1-2, -b1-2, -ca-b, -g1-3, -r1a-b, -r2a-b	Prkaa1**, -b1**, -g2**, -r1a, -r2a, -r2b
	CK1	1.6	1.8	Ckb, Ckm, Ckmt1-2	---
	GSK3	1.6	1.7	Gsk3a, Gsk3b	Gsk3a, Gsk3b**
	AKT (PKB)	1.4	---	Akt1, Akt2, Akt3, Akts1, Aktip	Akt, Akt1s1, Aktip
	CDK	---	1.9	Cdk2-9, Cdk2ap1-2, Cdk5rap1-3, Cdkal1, Cdkl1-5	Cdk7, Cdk5rap2
	4 h	PKD	2.0	---	Pkd1, Pkd1-3, Pkd2
CHK1		1.9	---	Chka, Chkb-cpt1b	---
ERK/MAPK		1.8	1.7	Mapk1, 3, 4, -6-9, 11-15	Mapk3**, 6, 9, 10, 14
AURORA		---	2.7	Aurka-c, Aurkaip1	---

* expression regulated (≥ 2 -fold), ** phosphorylation regulated (≥ 1.5 -fold) at respective time point

Kinase motifs (<http://www.phosida.com>) over-represented among LPS-up- or down-regulated compared to non-regulated phosphorylation sites (odds ratio ≥ 1.3 and corrected p-value ≤ 0.05 ; only motifs meeting both criteria are shown), suggesting kinase activation or site-specific down-regulation of phosphorylation in response to LPS, respectively. Each motif matched at least ten identified phosphorylation sites. Expression of associated kinases determined in the corresponding microarray experiments, and identification of phosphopeptides from the kinases themselves at the respective time points are indicated.

5.4 Association of LPS-regulated phosphoproteins with signalling pathways and functional annotation

To test in an unbiased way whether TLR4-induced phosphorylation preferentially targets specific signalling pathways and cellular processes, two annotation systems were used: InnateDB, a database integrating pathway information from several other sources (<http://www.innateDB.ca>; Lynn et al., 2008) and the GOSlim GO annotation (<http://www.geneontology.org/GO>), providing high level GO terms, for molecular functions and biological processes. Over-represented signalling pathways and GO terms were determined as described in the Methods section (sections 4.7.5 and 4.7.3, respectively).

5.4.1 Signalling pathways

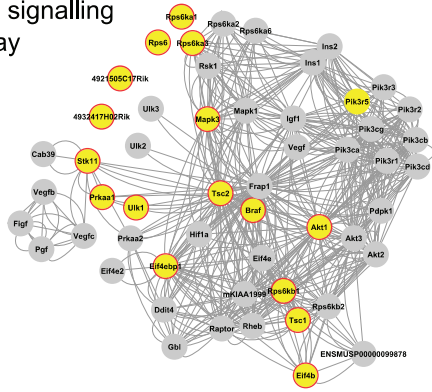
48 identified phosphoproteins were annotated as members of the TLR, MAPK or NF- κ B signalling pathways in InnateDB or on the innate immunity signalling poster compiled by Latz and Fitzgerald (Latz, 2008), 65 % of them were novel, and 31 showed LPS-regulated phosphorylation (Appendix, Tab. S2). In the over-representation analysis for InnateDB signalling pathways the pathway name “TLR signalling” showed a trend for enrichment among LPS-regulated phosphoproteins compared to non-regulated phosphoproteins (odds ratio 2.4; p-value 0.15). Significant over-representation was found for MAPK signalling members and pathways recently described as activated downstream of TLRs, e.g. the AKT and mTOR pathways (Cao et al., 2008; Schmitz et al., 2008) and the Rho GTPase cycle (Ruse and Knaus, 2006) (Tab. 8). To graphically illustrate the coverage of enriched signalling pathways with identified and LPS-regulated phosphoproteins, protein interaction networks were extracted from the STRING 8.0 database (Jensen et al., 2009; <http://string.embl.de>) and visualised with Cytoscape (<http://www.cytoscape.org>) (Fig. 22).

Tab. 8. Signalling pathways targeted by LPS-regulated phosphorylation.

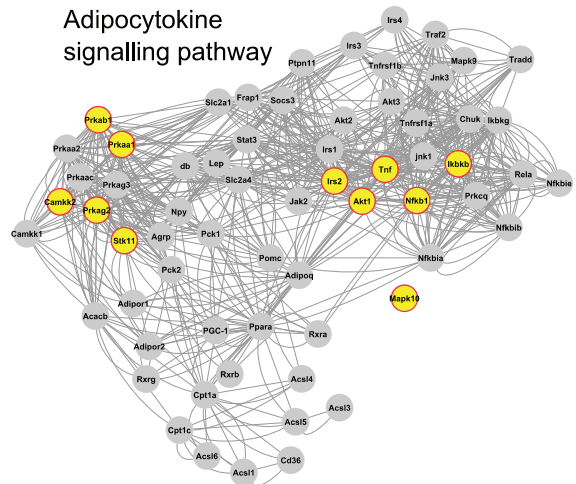
Pathway name	Enrichment (odds ratio)		
	Overall	15 min	4 h
mTOR signalling pathway	> 16.0	>17.9	6.5
Adipocytokine signalling pathway	> 11.0		> 8.0
AKT phosphorylates targets in the cytosol	> 8.0		> 6.0
AKT (PKB)-Bad signalling	2.5		
EGFR1	> 8.0		
Caspase-mediated cleavage of cytoskeletal proteins	> 8.0	8.5	7.8
TGF-beta signalling pathway	> 7.0		
TNF-alpha	> 7.0		
Insulin signalling pathway	3.0		2.6
MAPK signalling pathway	2.0		
Rho GTPase cycle		2.8	
<i>below cut-off:</i>			
Toll-like receptor signalling pathway	2.4	1.4	3.3

Signalling pathways (<http://www.innateDB.ca>; Lynn et al., 2008) with at least five identified phosphoproteins were analysed for over-representation among LPS-regulated phosphoproteins compared to non-regulated phosphoproteins (odds ratio ≥ 1.3 and p -value ≤ 0.05 ; *below cut-off*: p -value criterion not met, details see text). Depicted are over-represented pathways which did not show more than 75 % overlap with MAPK, AKT and mTOR signalling.

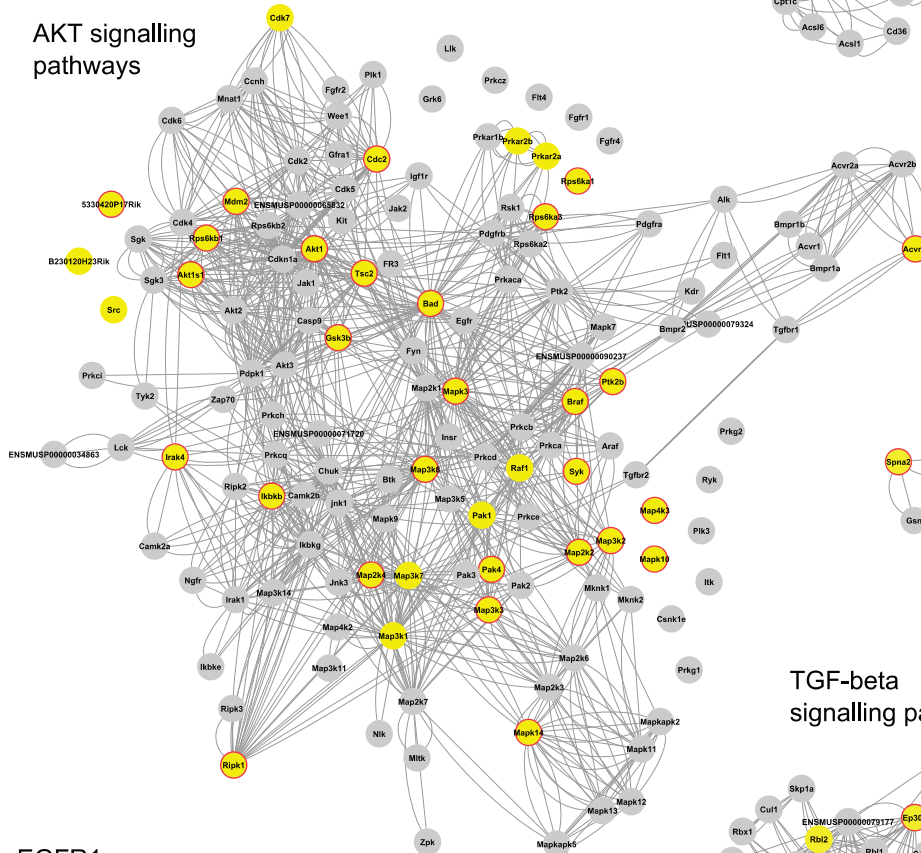
mTOR signalling pathway



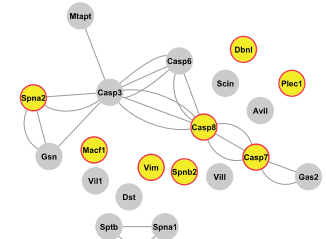
Adipocytokine signalling pathway



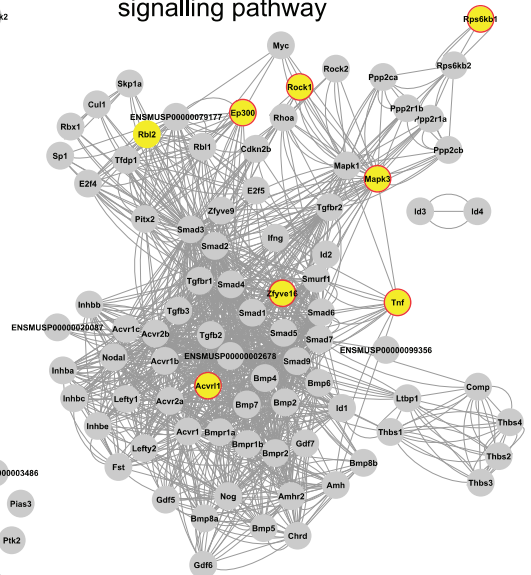
AKT signalling pathways



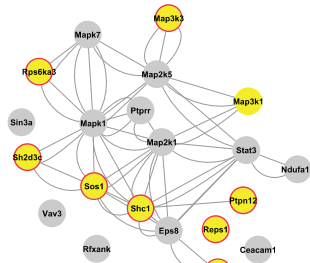
Caspase-mediated cleavage of cytoskeletal proteins



TGF-beta signalling pathway



EGFR1



TNF-alpha

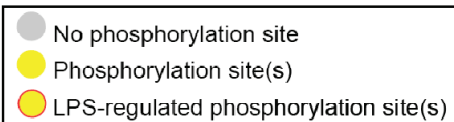
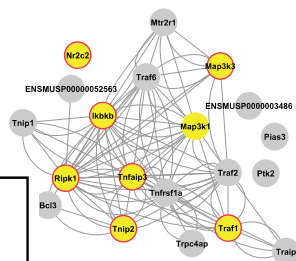


Fig. 22. Protein interaction networks of over-represented signalling pathways.

Protein interaction networks for InnateDB pathways enriched among LPS-regulated phosphoproteins were analysed with the STRING 8.0 database (<http://string.embl.de>; Jensen et al., 2009) and visualised with Cytoscape (<http://www.cytoscape.org>). Networks include direct (physical) and indirect (functional) interactions, based on experimental evidence from high-throughput studies, co-regulation of gene expression, same genomic context or co-citation in the literature. Only interactions with a minimum STRING combined score of 0.400, which represents the default medium confidence level in STRING 8.0, were kept. Depicted are over-represented pathways which did not show more than 75 % overlap with MAPK, AKT and mTOR signalling.

5.4.2 Gene Ontology (GO) analysis

GO analysis comparing LPS-regulated to non-regulated phosphoproteins showed enrichment of the terms “signal transduction”, “cell communication” and “kinase activity” (Tab. 9). Interestingly, functional annotation terms associated with the cytoskeleton were also significantly enriched among LPS-regulated phosphoproteins (“cytoskeletal protein binding”, “actin binding”). “Cell proliferation” showed a trend for over-representation (odds ratio 4.6, corrected p-value 0.12), consistent with over-representation of motifs for cell cycle associated kinases observed above (section 5.3). An overview of phosphoproteins with LPS-regulated phosphorylation sites associated with enriched GO terms is given in the Appendix (Tab. S3).

Tab. 9. Molecular functions and biological processes targeted by LPS-regulated phosphorylation.

Gene Ontology (GO) term	Enrichment (odds ratio)		
	Overall	15 min	4 h
Signal transduction*	3.1	2.6	1.9
Cell communication*	2.8	2.6	2.1
Actin binding**	2.3	2.9	
Cytoskeletal protein binding**	2.3	2.4	
Kinase activity**	1.7		
<i>below cut-off:</i>			
Cell proliferation*	4.6	2.1	3.0

* biological process, ** molecular function

Phosphoproteins were assigned to GOSlim GO terms for molecular functions and biological processes (<http://www.geneontology.org/GO>), and over-representation among LPS-regulated phosphoproteins compared to non-regulated phosphoproteins was determined (odds ratio ≥ 1.3 and corrected p-value ≤ 0.05 ; *below cut-off*: p-value criterion not met, details see text) for terms with at least three identified phosphoproteins.

In summary, un-biased statistical analyses of kinase motifs, signalling pathways and functional GO annotation consistently highlighted known and novel players of TLR signalling and linked TLR activation to the cytoskeleton and cell cycle regulation (see overview in Fig. 27).

5.5 Connecting TF phosphorylation with LPS-induced transcriptional activation

One major function of signal transduction is regulation of gene expression. In this study, 187 phosphoproteins annotated as transcriptional regulators (<http://www.genomatix.de>, Matrix Library 7.1) with 668 phosphorylation sites were detected, 25 % of which were regulated by LPS (Fig. 23A). Phosphorylation controls TF translocation, association with binding partners, binding to DNA or transcriptional activation capacity (Karin, 1991). Thus, LPS-induced genes were likely to be regulated by TFs with LPS-regulated phosphorylation. It was therefore hypothesised that the frequencies of binding sites for phosphorylated TFs could be increased in promoters of transcriptionally LPS-regulated genes. The strategy for testing this hypothesis is shown in Fig. 23B.

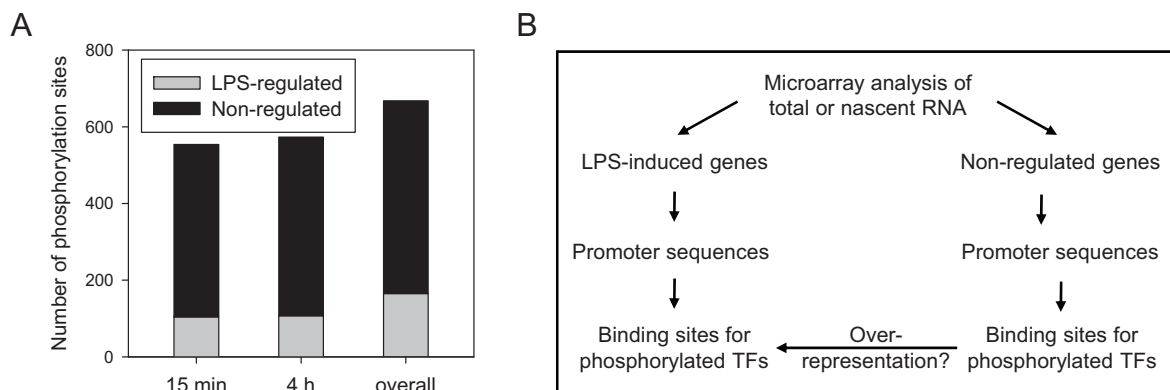


Fig. 23. TF phosphorylation - strategy for detection of over-represented binding sites in promoters of LPS-induced genes.

(A) Phosphorylation sites on TFs. Phosphorylation sites up- or down-regulated more than 1.5-fold in both experiments are indicated in grey. (B) Workflow for integration of phosphoproteome and transcriptome data. Microarray analyses of metabolically labelled nascent RNA and of total cellular RNA were performed on macrophages cultured under identical conditions as for the phosphoproteome experiments (except SILAC). Promoter sequences of LPS-regulated genes (induction ≥ 3 -fold) and of genes the expression of which was not altered in response to LPS (2,000 least regulated probe sets) were retrieved with Genomatix Gene2Promoter (<http://www.genomatix.de>). Promoters were analysed for the presence of binding sites for all identified phosphorylated TF families with Genomatix RegionMiner, and significant over-representation in LPS-regulated promoters was determined (odds ratio ≥ 1.3 and corrected p-value ≤ 0.05).

5.5.1 Identification of transcriptionally regulated genes in metabolically labelled nascent RNA

To identify transcriptionally regulated genes with high sensitivity, an analysis of RNA synthesised *de novo* after LPS stimulation (nascent RNA) was carried out by Katja Frühauf, a Master student in this laboratory. Macrophages cultured under the same conditions as for the phosphoproteome experiments (except SILAC) were stimulated with LPS for 45 min or 4.5 h or were left un-treated. Nascent RNA was isolated following metabolic labelling with 4-thiouridine (4sU) during the last 35 min before cell harvest, as recently described (Dolken et al., 2008) (experimental details are given in the Methods sections 4.4.4 and 4.4.5).

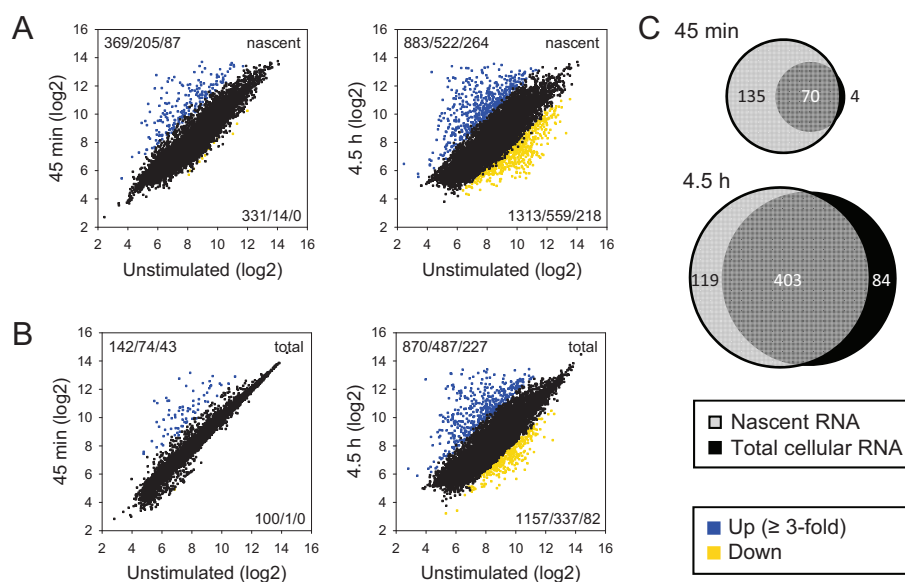


Fig. 24. Nascent transcriptome analysis for detection of transcriptionally LPS-induced genes.

Microarray analysis of (A) nascent and (B) total cellular RNA from two independent experiments. Macrophages were left un-treated or stimulated with LPS for 45 min or 4.5 h. Nascent RNA was labelled by addition of 4sU during the last 35 min of stimulation, purified after extraction of total cellular RNA and nascent and total cellular RNA were analysed on Affymetrix Mouse GeneST[®] 1.0 microarrays, as described in the Methods section (sections 4.4.4 and 4.4.5). For each comparison, the number of probe sets induced at least 2-/3-/5-fold is represented in the upper left corner, the number of probe sets repressed at least 2-/3-/5-fold in the lower right corner. (C) Venn diagrams illustrate the increased sensitivity for early changes in transcription. At least 3-fold induced probe sets of nascent compared to total RNA are shown.

Microarray analyses of nascent RNA identified substantially more probe sets as up-regulated after 45 min of LPS stimulation than parallel analyses of total cellular RNA (Fig. 24A to C). In contrast, 4.5 h after stimulation, up-regulated genes in total and nascent RNA largely overlapped (Fig. 24C). This approach therefore allowed a much

more sensitive detection of early changes in transcription, and the respective genes were likely to be direct targets of LPS-regulated TFs. The promoters of transcriptionally LPS-regulated genes were therefore used for integration of phosphoproteome and transcriptome data in this thesis.

5.5.2 Integration of phosphoproteome and nascent transcriptome data by *in-silico* promoter analysis

In-silico promoter scanning for binding sites for all 50 TF families with phosphorylated members was used to test for binding site enrichment in transcriptionally induced genes (≥ 3 -fold) compared to non-regulated genes (Appendix, Tab. S4). Promoter sequences were retrieved with Genomatix Gene2Promoter and the presence or absence of TF binding sites was determined with Genomatix RegionMiner using TF matrix families (<http://www.genomatix.de>) (section 4.7.6). 45 min after LPS treatment, significant over-representation was found for binding sites for NF- κ B, an established mediator of LPS-induced transcription; two other canonical LPS-activated TF families, CREB and IRFF, showed a trend for enrichment (odds ratio 1.3, corrected p-values 0.10 and 0.08, respectively). Significant enrichment for C/EBP, Myocyte enhancing factor 2 (MEF2), Nuclear factor of activated T cells (NFAT), and Heat shock factor family (HEAT) binding sites suggested a more genuine role for the associated TFs, which have been described as activators of individual LPS-target genes (Han et al., 1997; Inouye et al., 2007; Inouye et al., 2004; Matsumoto et al., 1999; Tanaka et al., 1995; Zhu et al., 2003). In addition, Octamer binding protein (OCT1) and Homeobox (HOXC) family members, which to date have not been assigned a role in LPS-induced transcription, were significantly enriched (Tab. 10). Binding sites for AP-1 TFs as defined by Genomatix (see also sections 1.3.4.2 and 1.3.4.3) were not enriched (odds ratio 1.2, corrected p-value 0.32). In contrast, analysis of promoters of genes induced in total cellular RNA after 45 min did not reveal any significant over-representation (data not shown). For IRFF, C/EBP, MEF2, NFAT, OCT1 and HOXC overrepresentation was still observed at 4.5 h in genes regulated on nascent and total RNA levels (Tab. 10 and data not shown), suggesting an enduring role for these factors, while NF- κ B binding sites were not enriched any more.

Tab. 10. TF families with over-represented binding sites in the promoters of transcriptionally LPS-regulated genes.

Time	TF family	Enrichment (odds ratio)	Phosphorylated TFs
45 min (RNA)	HEAT	1.5	Hsf1*
	15 min (phosphorylation)		
	MEF2	1.4	Mef2a*, Mef2c*, Mef2d*
	NFAT	1.4	Ilf3, Nfat5, Nfatc1*, Nfatc3*
	NFKB	1.4	Nfkb1*, Nfkb2*
	CEBP	1.4	Cebpd*, Cebpz*
	OCT1	1.3	Pou2f1
	HOXC	1.3	Pbx2
	<i>below cutoff:</i>		
	CREB	1.3	Atf2*, Atf3*, Atf7*, Nfil3
	IRFF	1.3	Irf3*
4.5 h (RNA)	SORY	1.8	Cic*, Hmga1, Hmga2
4 h (phosphorylation)	FKHD	1.7	Foxk1, Foxp1*
	OCT1	1.7	Pou2f1
	MEF2	1.6	Mef2a*, Mef2c*, Mef2d*
	RBIT	1.5	Arid3a
	HOXC	1.5	Pbx2*
	GATA	1.5	Trps1
	IRFF	1.4	Irf3*
	NFAT	1.4	Ilf3, Nfat5, Nfatc1*, Nfatc3
	CEBP	1.4	Cebpd*, Cebpz
	BCL6	1.4	Bcl6*
	STAT	1.3	Stat5b*

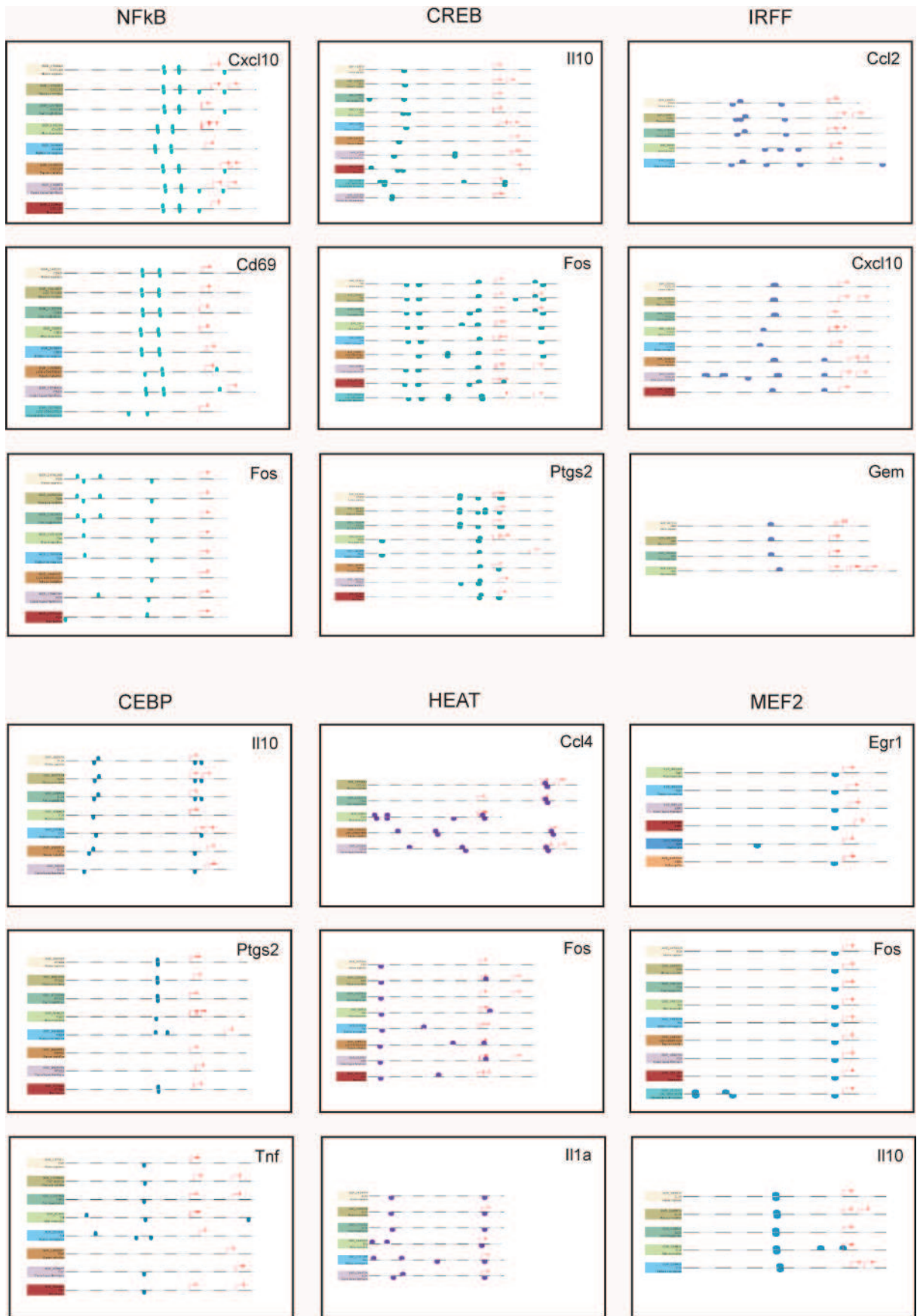
In-silico promoter analysis of genes regulated on the level of nascent RNA for binding sites of phosphorylated TFs with Genomatix Gene2Promoter and RegionMiner (<http://www.genomatix.de>). TF families with over-represented binding sites in at least 3-fold LPS-up-regulated compared to non-regulated promoters (odds ratio ≥ 1.3 and corrected p-value ≤ 0.05 ; *below cut-off*: p-value criterion not met, details see text) and gene symbols of associated TFs are shown. TFs detected in at least one experiment and with LPS-regulated phosphorylation at the respective time point (see text, section 5.5.3) are indicated by asterisks.

5.5.3 Evolutionary conservation of TF phosphorylation sites and DNA binding sites

Phosphorylation sites on many TF family members with binding site enrichment were LPS-regulated and more than half of them were novel (Tab. 10 and Appendix, Tab. S5). While the technically complex extraction of proteins from chromatin pellet fractions allowed detection of several TF phosphorylation sites in one of the experiments only, potential functional relevance was suggested by evolutionary conservation of (i) phosphorylation sites and (ii) DNA binding sites of TFs: Alignment of orthologous protein sequences from Uniprot (<http://www.uniprot.org>) with ClustalW (<http://www.ebi.ac.uk/Tools/clustalw2>) revealed that at 15 min 89 %, and

at 4 h 96 % of all amino acid residues with regulated phosphorylation on TFs in the phosphoproteome experiment were conserved in several, sometimes distantly related species (Appendix, Tab. S5). Conservation of DNA binding sites was assessed by analysing orthologous promoters of the 20 genes most strongly induced by LPS on the level of transcription with Genomatix MatInspector (<http://www.genomatix.de>, Matrix Library 7.1). For each TF with LPS-regulated phosphorylation and binding site enrichment, evolutionary conserved DNA binding sites could be identified in promoters of several of the top 20-induced genes. Selected examples are depicted in Fig. 25.

Taken together, the *in-silico* integration of phosphoproteome and nascent transcriptome data confirmed canonical and identified a number of novel candidate TFs driving TLR-induced gene expression.



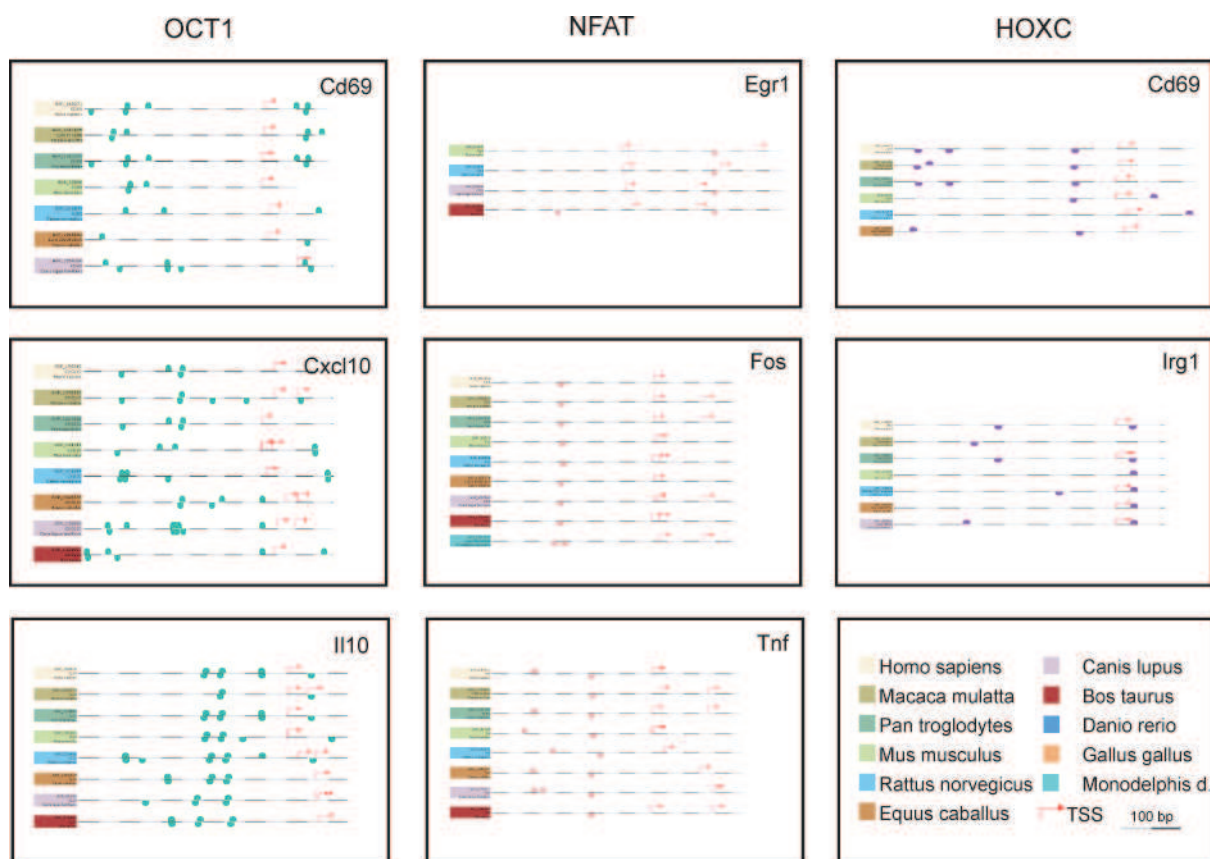


Fig. 25. Evolutionary conservation of TF binding sites in promoters of LPS-induced genes.

Promoter sequences of the 20 genes that were most strongly and rapidly induced in nascent RNA (45 min after LPS stimulation) and orthologous vertebrate promoters were analysed for evolutionary conservation of TF binding sites with Genomatix MatInspector (<http://www.genomatix.de>) (similar position relative to transcriptional start site (TSS) in Genomatix-aligned promoters). Each TF family with observed phosphorylation (15 min) and over-representation of binding sites in LPS-regulated promoters (45 min) had several target genes with evolutionary conserved binding sites, indicating potential functional relevance. Depicted are selected examples.

6 Discussion

6.1 TLR-induced phosphorylation – the global picture

6.1.1 First global and quantitative study reveals extent of regulation comparable to transcriptional reprogramming

This study provides the first unbiased and quantitative investigation of the macrophage phosphoproteome and its dynamic changes in response to TLR activation. In contrast to high-throughput techniques relying on phosphoepitope-specific antibodies like protein microarrays (Chan et al., 2004), phosphoproteomics by mass spectrometry represents an approach capable of monitoring cellular phosphorylation events in the absence of *a priori* knowledge. Yoshimura and co-workers analysed in 2005 tyrosine-phosphorylated proteins in the resting and LPS-activated macrophage-like cell line RAW 264.7 by a mass spectrometry-based approach using anti-phospho-tyrosine immunoprecipitation and 1D gel separation (Aki et al., 2005). However, the study did not provide a global picture of the macrophage phosphoproteome: It was restricted to tyrosine phosphorylation, could not localise phosphorylation sites within proteins in high-throughput, was performed in a cell line, and was further limited by its non-quantitative nature. In contrast, in this thesis, the metabolic labelling approach SILAC was adapted to *primary* macrophages. Coupled with 1D gel separation, SCX chromatography- and TiO₂-based phosphopeptide enrichment and high-accuracy mass spectrometry, this enabled reproducible identification and *quantification* of a *large number* of phosphorylation sites on *serine, threonine and tyrosine* residues with *single amino acid accuracy* and high confidence. SILAC-based quantification allowed sensitive detection of *dynamic changes*, revealing extent and kinetics of TLR-induced phosphorylation as well as potential regulation of gene expression through *phosphorylation of TFs*.

The substantial phosphoproteome regulation upon LPS stimulation is comparable in extent to the transcriptional reprogramming of macrophages (Foster et al., 2007; Mages et al., 2007; data from this study), and reflects the important role of phosphorylation cascades in TLR signalling. The parallel phosphoproteome and

transcriptome analyses in this thesis underline the notion that widespread phosphorylation precedes the massive transcriptional changes in response to TLR ligation.

6.1.2 Dynamic regulation of phosphorylation

Although the extent of regulated phosphorylation was similar early and late after stimulation, the dynamic nature of phosphorylation cascades in TLR-stimulated macrophages is evident from the kinetic differences.

Induction of phosphorylation occurred rapidly through activation of numerous kinases, the footprints of which were revealed by the analysis for over-represented kinase motifs. In addition, this allowed identification of kinase substrates under physiological conditions. Interestingly, most kinase motifs were only enriched at the 15 min time point and not at 4 h, although dynamic regulation of different phosphorylation sites rather than sustained phosphorylation had been observed. It is possible, that early after stimulation a limited set of kinases phosphorylates a large number of substrate proteins, while at the late time point activation has spread to such a large set of kinases that individual motifs are not over-represented above background level.

All over-represented motifs are targets of serine/threonine kinases (<http://www.phosida.com>), which have relatively high target sequence specificities (Olsen, personal communication). This is in contrast to tyrosine phosphorylation, where specificity is mainly accomplished by sequence-specific binding of proteins with Src-homology 2 (SH2) and Phospho-tyrosine-binding (PTB) domains (Yaffe, 2002). Serine/threonine phosphorylation is traditionally believed to largely regulate protein function through conformational changes leading to activation or deactivation of substrate proteins. Meanwhile, although with lower specificities than phospho-tyrosine binding proteins, binding partners for phospho-serine/threonine such as 14-3-3 proteins, WW domains, Forkhead-associated (FHA) domains, WD40 domains, and Leucine-rich repeat (LRR) domains of F-box proteins have been identified, which are/belong to proteins with highly diverse functions (Yaffe and Elia, 2001; Yaffe and Smerdon, 2001) (Fig. 26). This suggests that TLR stimulation influences multiple aspects of cell biology. The GO analysis in an unbiased way

revealed interesting molecular functions and biological processes influenced by TLR-regulated phosphorylation of substrate proteins - beyond signal transduction and kinase activation - including the cytoskeleton and cell proliferation, which are discussed below (sections 6.1.6 and 6.1.5, respectively).

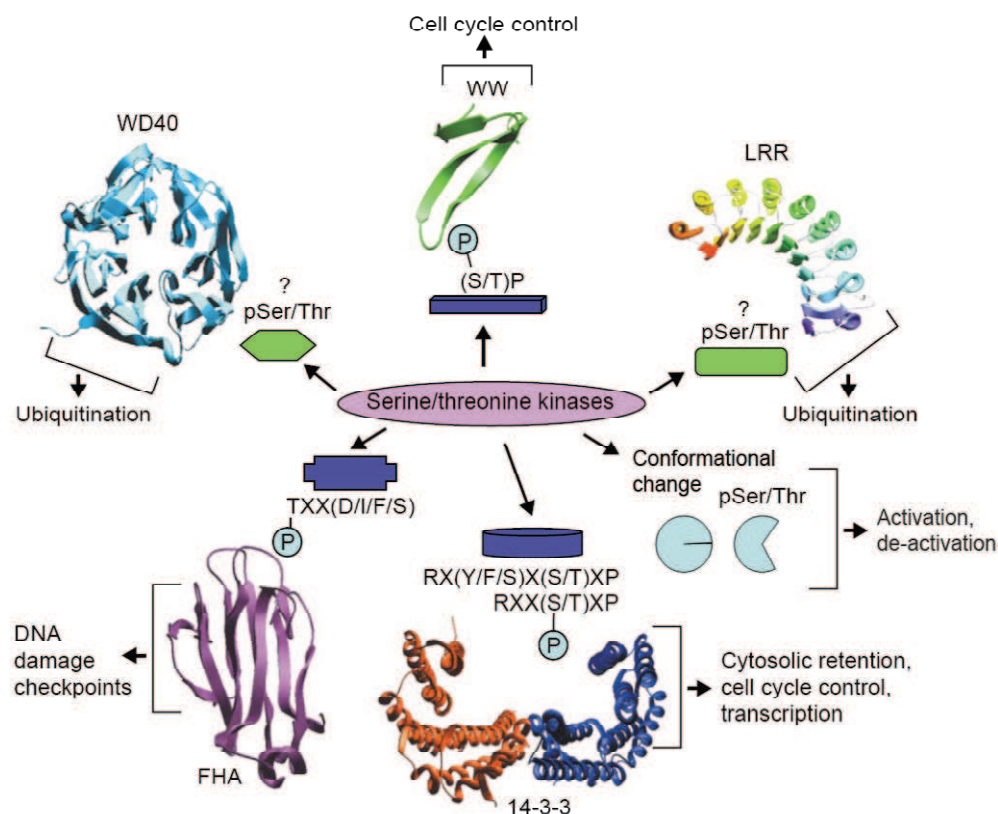


Fig. 26. Functions of serine/threonine phosphorylation.

Phosphorylation of proteins on serine and threonine residues has traditionally been thought to regulate protein function largely through allosteric modifications, inducing activation or de-activation of protein function. In addition, a variety of signalling molecules and modular domains have been identified to date that specifically bind to short phospho-serine/threonine (pSer/Thr)-containing motifs, although sequence specificity is less stringent compared to phospho-tyrosine binding domains (not depicted). Phospho-serine/threonine binding partners include 14-3-3 proteins, WW domains, Forkhead-associated (FHA) domains, WD40 domains, and leucine-rich repeat (LRR) domains of F-box proteins, which are/belong to proteins with a variety of functions. Adapted from Yaffe and Elia, 2001.

Decreased phosphorylation in response to LPS, or return of increased phosphorylation after an early peak, may be caused by protein degradation or through phosphatase activity. The M-CSF receptor (CSF1R) is an example for the first mechanism, with decreases in a phosphorylated peptide (Appendix, Tab. S1) as well as in three non-phosphorylated peptides (data not shown), consistent with earlier reports on LPS- and IFN- γ -induced M-CSF receptor degradation (Baccarini et al., 1992; Sester et al., 1999; Trost et al., 2009). Evidence for phosphatase activity is

provided by the observation that for many phosphoproteins with a down-regulated site other phosphopeptides were unchanged or increased (Appendix, Tab. S1). Furthermore, over-representation of kinase motifs among LPS-down-regulated phosphorylation sites argues for kinase de-activation or sequence-specific de-phosphorylation. Progress in mass spectrometry should allow generating quantitative proteome data in the near future to definitively determine which changes in phosphorylation are influenced by differences in protein levels (Cox and Mann, 2007). However, the parallel transcriptome analysis included in the present study already suggests that only a minor fraction of induced phosphorylation results from increased expression of the protein.

6.1.3 Variability in the effect of DUSP1-deficiency

In the present study, the influence of the MAPK phosphatase DUSP1 on the TLR-induced phosphorylation pattern was rather limited. However, this might be underestimated, since differences in phosphorylation of the known target p38 between wild type and *Dusp1*-deficient macrophages were only observed in one of the two experiments (Fig. 18). This is in contrast to the increased lethality of LPS-challenged *Dusp1*-deficient mice caused by excessive cytokine production due to prolonged MAPK activation, which is highly reproducible, and to a previous genome wide gene expression study carried out in this laboratory, identifying three times more genes uniquely up-regulated in *Dusp1*-deficient mice compared to wild type after LPS challenge (Hammer et al., 2006). On the one hand, the discrepancy could be due to different conditions *in vitro* versus *in vivo*. As suggested by Hume et al. the phenotype of an activated macrophage population depends not only on the activating stimulus but also the microenvironment of neighbouring cells and the cytokine milieu (Hume et al., 2002). The *in vitro* activation of macrophages in this thesis was solely induced by LPS and could not provide any other co-stimulatory signals of other immune cells present *in vivo*. On the other hand, a number of reports have shown a non-redundant role for DUSP1 in de-phosphorylation of MAPKs in macrophages also *in vitro* (Chi et al., 2006; Hammer et al., 2006; Salojin et al., 2006; Zhao et al., 2006). *Dusp1*-deficient mice in this thesis had a different genetic background (C3H/HeN) than the ones used in previous *in vitro* studies in this laboratory (mixed 129Sv x C57BL/6). This could account for variability in DUSP1

expression, since a comparison of the influence of genetic background on the responses of murine macrophages to LPS demonstrated variations in number, amplitude and rate of gene induction between mouse strains (Wells et al., 2003).

6.1.4 Signalling pathways

6.1.4.1 Identification of trademark TLR pathway components by unbiased statistical testing

Bioinformatic analyses of the regulated phosphorylation sites and proteins for over-representation of kinase motifs, signalling pathways and functional annotation found the major canonical TLR-activated molecular players - including the kinases IRAK2, IRAK4, MAPKs and up-stream kinases, the NF- κ B activating kinase IKK β , and over-represented binding sites for phosphorylated canonical LPS-activated TFs in the promoters of LPS-induced genes. In addition, a number of less well appreciated and novel signalling components were revealed, as discussed below (sections 6.1.4.2, 6.1.5, 6.1.6, 6.2.3). Furthermore, 65 % novel phosphorylation sites on known TLR pathway components (Appendix, Tab. S2) point to novel regulatory aspects of TLR signalling. While functional investigation of individual phosphorylation sites on single molecules was beyond the scope of this global study, the macrophage phosphoproteome dataset is now publicly available and should become a valuable resource to the scientific community of TLR signalling researchers. Importantly, identification of trademark TLR pathway modules by unbiased statistical testing strengthens the validity of the experimental data obtained in this study, which are summarised in form of a model in Fig. 27.

6.1.4.2 The PI3K/AKT pathway signalling through GSK3 and mTOR

The PI3K/AKT pathway, together with its diverging downstream kinases GSK3 and mTOR, was prominently enriched among LPS-regulated phosphoproteins. As mentioned earlier (section 1.3.3.3), PI3K activation in response to TLR-ligation has previously been assigned a negative regulatory role (Fukao and Koyasu, 2003).

In this study, up-regulated phosphorylation of S9 and T7 on GSK3 β was observed. S9 phosphorylation of GSK3 leads to in-activation of the enzyme, increased production of IL-10 (Hu et al., 2006) and reduced production of inflammatory cytokines (Martin et al., 2005), and may thereby mediate the described negative

regulatory role of PI3K/AKT activation (Fukao and Koyasu, 2003). GSK3 kinase motif-bearing phosphoproteins identified in this thesis may therefore contribute to regulation of macrophage activity. T7 phosphorylation of GSK3 has only been reported in high-throughput studies so far (Daub et al., 2008; Dephoure et al., 2008; Oppermann et al., 2009). Whether this has any stimulating or de-activating influence on the kinase activity of GSK3 remains to be investigated. Future studies may also reveal if GSK3 activity is differentially regulated in distinct cellular compartments, as suggested by the observed over-representation of the kinase motif among LPS-up-regulated as well as down-regulated phosphorylation sites.

On the other hand, the strong enrichment of mTOR pathway proteins highlights the prominence of this pathway in innate immune signalling, consistent with recent reports demonstrating its important role in pro- as well as anti-inflammatory responses: mTOR is required for efficient IFN type I production in plasmacytoid DCs (Cao et al., 2008), and for IL-10 expression (Ohtani et al., 2008; Weichhart et al., 2008) and Stat3-dependent control of Caspase-1 in myeloid DCs and macrophages (Schmitz et al., 2008). How exactly mTOR controls these effects is unclear at present, but an mTOR-dependent increase in translational efficiency is involved in the regulation of IRF7 expression (Colina et al., 2008). The regulated phosphorylation of the translation initiation factors EIF4B and EIF4EBP, and of multiple ribosomal proteins after LPS observed in this thesis may be linked to mTOR activation.

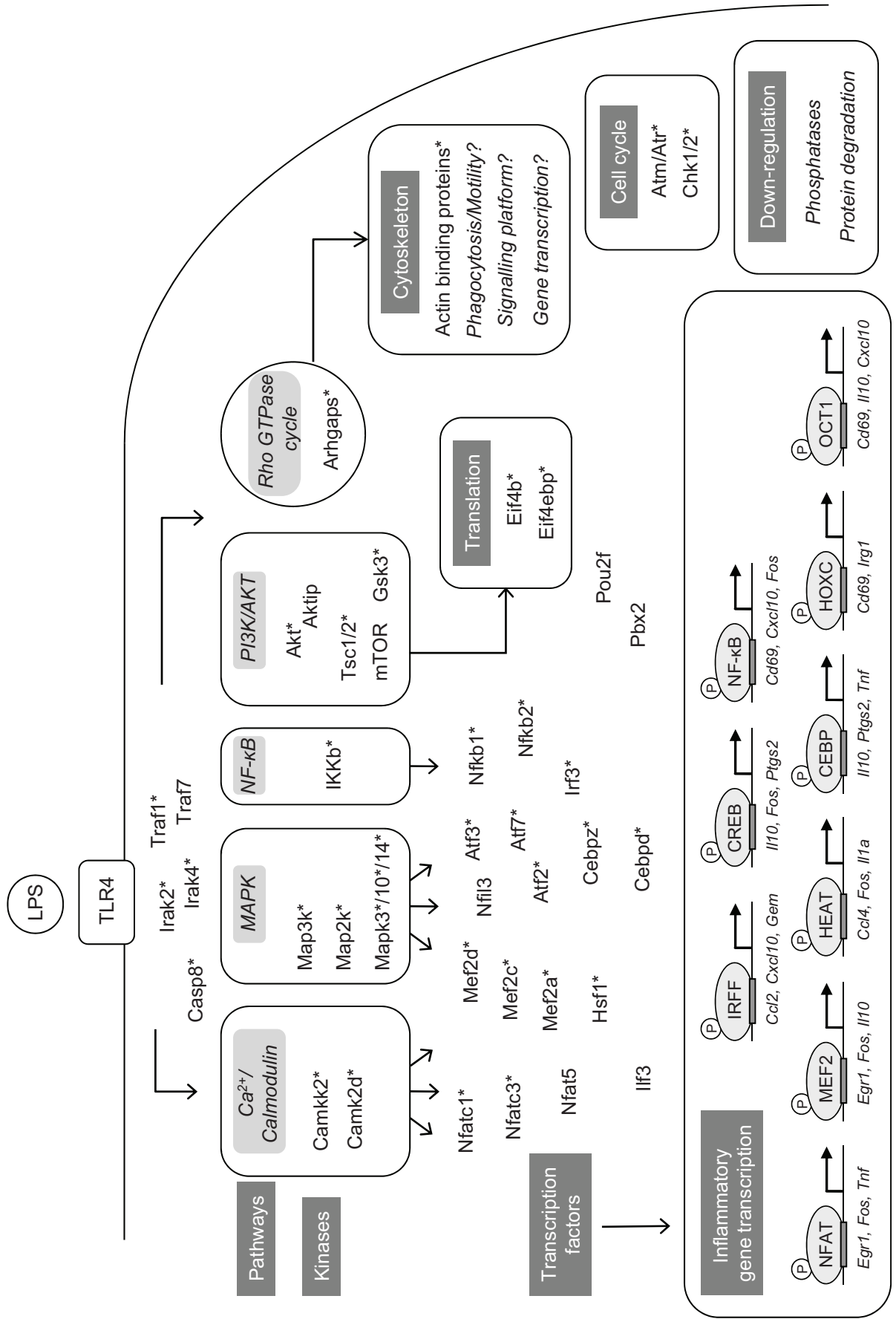


Fig. 27. The phosphoproteome of LPS-activated macrophages - overview.

Hotspots of TLR4-induced phosphorylation on the levels of pathways, kinases, biological processes and TFs are summarised. Various signalling modules, cytoskeletal rearrangement, cell cycle proteins and the translation machinery use the reversible protein modification for controlled activation that is both rapid and transient, as accomplished by phosphatase activity and phosphoprotein degradation. Most importantly, changes in phosphorylation activate TFs followed by inflammatory gene transcription indispensable for host defence. Selected examples of phosphoproteins are shown for each process. Depicted TFs have enriched evolutionary conserved binding sites in the promoters of highly and rapidly induced LPS target genes (selected examples). Asterisks indicate LPS-regulated phosphorylation on a protein or kinase target.

6.1.5 The cell cycle

Already 20 years ago it was described that microbial stimuli block macrophage proliferation by arresting the cells in G1 phase (Hume et al., 1987). Enrichment of the GO term “cell proliferation” among LPS-regulated phosphoproteins (odds ratio 4.6, corrected p-value 0.122), and evidence for activation of the cell cycle relevant kinases ATM/ATR and CHK1/2 among the LPS-regulated phosphorylation sites, suggest a potential phosphorylation-dependent mechanism for inhibition of proliferation. ATM and ATR are usually activated by genotoxic stress, phosphorylate the cell cycle checkpoint kinases CHK1 and CHK1, respectively, and other substrates, for example p53 and its regulator MDM2, leading to cell cycle arrest or apoptosis (Abraham, 2001). The present study revealed LPS-regulated phosphorylation sites on MDM2 and Tp53bp1, although they do not match the ATM/ATR or CHK1/2 kinase motifs.

A potential role of the ATM/ATR and CHK1/2 pathway in TLR-activated macrophages has not been investigated and raises the question, how bacterial stimuli might activate a signalling pathway, which is normally triggered by DNA damage. On the one hand, cytoplasmic localisation of ATM in certain cell types suggests extranuclear functions and activation mechanisms (Barlow et al., 2000). Activation of ATM by TLR-induced oxidative burst in macrophages is conceivable, as cytoplasmic ATM responds to ROS with checkpoint activation in neurons (Abraham, 2001). On the other hand, ATM and ATR belong to the PIKK family of kinases, which also encompasses mTOR (Abraham, 2001), another kinase that had been observed as activated in this study (section 6.1.4.2). While substrate specificities of mTOR and ATM/ATR are different, PIKK family kinases share kinase domains related to PI3Ks and a common structure of regulatory domains, which could provide a basis for common activation mechanisms. Cooperation of mTOR

and ATM in phosphorylation-dependent in-activation of the translational repressor EIF4EBP has been suggested in insulin signalling (Yang and Kastan, 2000). Interestingly, the p38-activated kinase MK2 (Mapkap kinase 2) has a very similar kinase motif and is a functional analogue of CHK1/2 (Manke et al., 2005); therefore, it is possible that the enrichment for the CHK1/2 kinase motif observed here is the footprint of LPS-induced, p38-dependent MK2 activation, alternatively to or in parallel with CHK1/2 activation.

6.1.6 The cytoskeleton

That cytoskeletal and actin binding proteins are targeted by TLR4-induced phosphorylation was unexpected, as the cytoskeleton is usually not part of TLR pathway models (Latz, 2008; Oda and Kitano, 2006). However, two key features of macrophages, motility and phagocytosis, depend on cytoskeletal remodelling (section 1.2.2). Likewise, Trost et al. found enrichment for cytoskeletal proteins in their proteome analysis of the IFN- γ activated phagosome (Trost et al., 2009). Enhancement of phagocytosis by TLR stimulation through MAPK-dependent pathways has been described by Medzhitov and co-workers, including increased internalisation and phagosome maturation (Blander, 2007; Blander and Medzhitov, 2004, 2006), although Russel and colleagues claim that phagosome maturation is independent of TLR stimulation (Russell and Yates, 2007a, b; Yates and Russell, 2005). An important role of TLR signalling in phagocytosis is further supported by the fact that the largest proportion (32 %) of LPS-induced genes in macrophages is components of the cytoskeleton or phagosome (Wells et al., 2003). Furthermore, Watts and co-workers described enhanced motility and antigen uptake in TLR stimulated DCs (West et al., 2004). The identification of multiple and novel phosphorylation sites on cytoskeletal proteins in this thesis should be useful in the investigation of cytoskeletal remodelling and phagocytosis under the influence of TLR ligands.

Rho family GTPases play a major role in actin remodelling (Aderem and Underhill, 1999; Greenberg and Grinstein, 2002). In the present study enrichment of the pathway term “Rho GTPase cycle” was observed, and among the proteins assigned to the GO term “signal transduction” was a large proportion of Rho GTPase activating proteins (17 % Arhgaps; Appendix, Tab. S3). How exactly Rho GTPases

are activated by TLRs is not clear yet (Ruse and Knaus, 2006). TLR2-mediated gene transcription has been shown to be mediated by association of RhoA with PKC ζ , inducing phosphorylation of NF- κ B p65 (Teusch et al., 2004). Another possible link between TLR stimulation and cytoskeletal reorganisation would be the second arm of the mTOR pathway signalling through mTORC2, which triggers actin organisation via Rho GTPases (Thomson et al., 2009). mTOR signalling was strongly activated by LPS in the present study; however, the LPS-regulated phosphoproteins assigned to the mTOR pathway (Fig. 22) suggest activation of mTORC1 rather than mTORC2 in response to LPS, arguing against a connection between mTOR activation and cytoskeletal rearrangements in LPS-activated macrophages.

Besides the potential role in TLR-induced motility and phagocytosis, the prominence of LPS-regulated actin binding protein phosphorylation could also indicate a genuine function of the cytoskeleton in providing a platform for recruitment and spatial targeting of signalling molecules; reversible phosphorylation could be a control switch for this process. If this is the case, pharmacological blockade of actin rearrangement is expected to inhibit a spectrum of TLR-induced macrophage responses. Furthermore, actin has been shown to play a role in regulation of transcription: Nuclear actin and actin-related proteins are components of chromatin remodelling machines, such as the SWI/SNF-like mammalian BAF complexes and histone acetyl transferases, nascent pre-mRNA is complexed with hnRNP proteins and actin, and even without the chromatin context naked DNA templates require actin to be transcribed by all three RNA polymerases (Grummt, 2006). In addition, actin has been shown to regulate the localisation and activity of two TFs: the Myocardin-related TF MAL, and Serum response factor (SRF), respectively (Pipes et al., 2006; Posern and Treisman, 2006; Stern et al., 2009). Interestingly, SRF is closely related to the MEF2 family (Pipes et al., 2006), which was one of the TF families highlighted by the present phosphoproteome and nascent transcriptome studies (section 6.2.3.3). A role of TLR-induced cytoskeletal changes in signal transduction and/or gene transcription is therefore conceivable.

6.2 Integration of TF phosphorylation and transcriptional activation

6.2.1 First study combining promoter motif scanning with regulated phosphorylation on TFs

The study presented in this thesis is the first analysis integrating TF phosphorylation and nascent transcriptome data through *in-silico* promoter analysis of DNA binding site enrichment. Computational approaches for the inference of transcriptional networks from microarray gene expression have used a combination of hierarchical clustering of time course transcriptome data and promoter motif scanning to associate TFs with groups of co-expressed genes (Nilsson et al., 2006; Ramsey et al., 2008). These approaches have led to the identification of large lists of candidate regulators, some of which indeed play important roles in innate immune regulation, as shown for example by Aderem and colleagues for Atf3 (Gilchrist et al., 2006). However, the fact that TF binding site motifs usually are recognised by more than one TF protein and the tendency of TF binding sites to co-occur impede the unambiguous identification of TFs from enrichment analyses. Furthermore, many TFs are regulated not on the level of expression but post-translationally, and are therefore missed by these approaches. The global phosphorylation data on TF activation in response to LPS collected in the present study helped to fill these gaps and allowed to implicate novel phosphorylated regulators of macrophage transcriptional responses through binding site enrichment analyses in the promoters of induced genes.

6.2.2 Transcriptional target identification by biosynthetic mRNA labelling

It is noteworthy that at the early time point of 45 minutes, when most direct target genes of LPS-activated TFs are up-regulated, only the use of expression data on nascent RNA but not on total RNA found TF binding sites with significant enrichment in promoters of up-regulated genes. This higher discriminative power of nascent transcription data is likely due to two effects limiting the informative value of gene regulation on total RNA level: first, the lower number of regulated genes in the dataset from total RNA renders statistical analysis less powerful, and second, a substantial fraction of LPS-induced gene expression changes is due to effects on

mRNA stability rather than *de novo* transcription. The results in this thesis therefore illustrate the suitability of the biosynthetic labelling method for identification of transcriptional target genes with high sensitivity (Dolken et al., 2008).

6.2.3 Identification of known and novel candidate regulators of the transcriptional response to TLR ligation

The combination of nascent transcriptome and phosphoproteome data by *in-silico* promoter analysis for TF binding sites identified a number of less established (C/EBP, HEAT, MEF2, NFAT) and in the context of TLR-signalling novel transcriptional regulators, such as OCT and HOXC family proteins. The fact that the best characterized LPS-activated TFs in macrophages (NF- κ B, CREB, IRFF) were recognised gives confidence that also the other TFs will soon be validated as true regulators of LPS-induced transcription.

6.2.3.1 CCAAT enhancer binding protein (C/EBP) family

In fact, for the phosphorylated C/EBP family member C/EBP δ , Aderem and colleagues recently reported a regulatory role in gene expression in response to LPS (Litvak et al., 2009): C/EBP δ is part of a regulatory circuit including NF- κ B and ATF3 and discriminates between transient and persistent TLR4-induced signals. Persistent stimulation (6 h) leads to recruitment of C/EBP δ to the promoters of 63 LPS-induced genes, and 80 % of C/EBP δ -deficient mice succumb to persistent peritoneal infection with *Escherichia coli*. While phosphorylation plays a key role in modulating the function of C/EBP β , hardly anything is known about regulation of the other isoforms by phosphorylation so far (Ramji and Foka, 2002). The two novel phosphorylation sites on C/EBP δ (S10, S167) observed in this thesis were strongly up-regulated at the late time point (4 h) and could be important in this context.

6.2.3.2 Heat shock factor (HEAT) family

IL-6 has been shown to be a direct target gene of Heat shock factor 1 (HSF1) in LPS-treated macrophages, and HSF1 is required for full IL-6 induction (Inouye et al., 2004). While in response to stress stimuli like heat, HSF1 nuclear translocation and trimerisation induces expression of heat shock genes by binding to heat shock elements in their promoters (Holmberg et al., 2002), a novel mechanism was shown for the IL-6 promoter, where HSF1 partially opens the chromatin structure for an

activator (e.g. NF- κ B) or a repressor (e.g. ATF3) to bind to it in unstressed conditions (Inouye et al., 2007). In this thesis, four-fold induced phosphorylation of S326 was observed, which plays a critical role in the induction of the factor's transcriptional competence by heat or chemical stress (Guettouche et al., 2005). On the other hand, S303 phosphorylation, which was also induced, is known to promote sumoylation of K298, which inhibits HSF1-induced transcription (Yang and Gregoire, 2006). This phospho-sumoyl switch occurs also in other proteins, for example in MEF2, which is activated when the phosphatase Calcineurin removes the phosphate group from the switch motif (Yang and Gregoire, 2006). It will be interesting to investigate the relative contribution of these two important phosphorylation sites to HSF1 activation in TLR-stimulated macrophages, particularly in the context of LPS-triggered activation of CAMK2 (see also sections 6.2.3.3 and 6.2.3.4. on MEF2 and NFAT).

6.2.3.3 Myocyte enhancing factor 2 (MEF2) family

MEF2 family TFs have been studied extensively in muscle cell differentiation, but are also involved in neuronal survival and T cell apoptosis (McKinsey et al., 2002). *Nur77*, a mediator of negative thymocyte selection, is activated by a cooperation of MEF2, NFAT and p300 in T cells (Blaeser et al., 2000), and is also a target gene of MEF2 in macrophages in activation-induced cell death (Kim et al., 2003). Both, MEF2 and NFAT, had regulated phosphorylation sites and over-represented binding sites in LPS-regulated promoters in the present study. Interestingly, both are activated in a Ca²⁺-dependent manner (Macian, 2005; McKinsey et al., 2002) (see also section 6.2.3.4 on NFAT). In 1997, Ulevitch and co-workers described MEF2C as a target for p38 MAPK in RAW 264.7 macrophages: LPS-induced phosphorylation of T293, T300 and S387 on MEF2C leads to increased *c-jun* transcription (Han et al., 1997). The described p38 target sites were not identified in this thesis. While the phosphoproteome study is not expected to cover the phosphoproteome completely, differences between the RAW 264.7 cell line and the primary BMDMs used in the present study could be a potential reason. In contrast, several novel regulated phosphorylation sites were identified here on MEF2A, -C and -D. Interestingly, S226 on MEF2C, which is transiently induced, lies less than 20 amino acids upstream of the second transcriptional activation domain (TAD2) in a

region that is acetylated by p300, which increases DNA binding (Ma et al., 2005). MEF2 is also known to bind histone deacetylases (HDACs) and p300 for regulating nucleosome acetylations (McKinsey et al., 2001). It would therefore be interesting to investigate, if chromatin remodelling depends on the identified phosphorylation sites on MEF2.

6.2.3.4 Nuclear factor of activated T cells (NFAT) family

NFAT is a key TF in T cells. There, kinases like GSK3 and Casei-kinase 1 (CK1) contribute to maintaining NFAT in the cytosol in a phosphorylated state and to expose a nuclear-export signal. Upon de-phosphorylation by the Ca²⁺-stimulated phosphatase Calcineurin, NFAT translocates to the nucleus and interacts with other TFs like AP-1. In contrast, the regulated phosphorylation sites identified in the present study in macrophages were up-regulated by LPS (Nfatc1 S402, S404, T406, T766, T761; Nfatc3 S345). They have not been described previously, but a stimulatory role is possible, and one activating phosphorylation site has also been described in T cells (Macian, 2005). Only recently, a requirement for NFAT activation in DCs and macrophages was shown for Dectin-1-dependent gene expression (Goodridge et al., 2007). Of note, binding of NFATC1 to a site in the IL-12p40 promoter has been demonstrated after TLR stimulation (Zhu et al., 2003). The identification of NFAT family TFs with LPS-regulated phosphorylation together with binding site enrichment in promoters of TLR4-activated genes in the present study suggests a broader role for the Calcineurin/NFAT pathway also in macrophages. This is in line with the observed pronounced enrichment of the CAMK2 motif among LPS-regulated phosphoproteins, and with previously reported NFAT-mediated activation of MEF2 TFs (Blaeser et al., 2000).

6.2.3.5 Homeo-domain and Octamer binding protein families (HOXC and OCT1)

Binding site enrichment was also observed for HOXC and OCT1 families, which have previously not been implicated in the transcriptional response to LPS: HOX family TFs are master regulators of developmental processes controlling the diversification of segments along the anterior-posterior axis of animals and have roles in the morphogenesis of various organs (Hombria and Lovegrove, 2003). Most known target genes are signalling pathway components or TFs (Graba et al., 1997).

Target genes are usually expressed cell type-specifically only in a subset of the cells expressing the *Hox* genes, implying that HOX proteins must interact with other proteins to confer the positional specificity of target regulation (Hombria and Lovegrove, 2003). The OCT1 family comprises POU TFs (Pituitary-specific, Octamer TF, Unc-86 comprising), which also have important developmental functions (Andersen and Rosenfeld, 2001). Interestingly, interactions between CREB, POU and HOX factors - all of which had enriched binding sites in LPS-regulated promoters (CREB: odds ratio 1.3, corrected p-value 0.10) - have been described in the immune response: Hoffmann and co-workers report the presence of a module consisting of these three binding sites in ten of 14 promoters of genes synergistically induced by IFN- γ and *Yersinia enterocolitica* infection in BMDMs (van Erp et al., 2006). Although the phosphorylation sites identified in the present study on PBX2 and POU2F1 are not altered in response to stimulation, the observed binding site enrichment in the promoters of LPS-induced genes and the preferential interaction of HOX and POU family TFs with other factors in multi-protein complexes described in the literature (Andersen and Rosenfeld, 2001; Hombria and Lovegrove, 2003) strongly suggest that HOXC and OCT1 might act in concert with yet to identify partners also for regulating TLR-induced target gene expression.

6.2.3.6 Basis for mechanistic insights into pathophysiologic consequences of deregulated Ca^{2+} signalling

An interesting observation is that several of the identified families of transcriptional regulators (MEF2, NFAT and possibly HEAT) are activated in a Ca^{2+} -dependent manner. This is particularly striking in the context of profound enrichment of the CAMK2 motif among LPS-regulated phosphoproteins observed in this study, and is further supported by recent reports showing LPS-triggered increase in Ca^{2+} levels and activation of CAMK2 (Liu et al., 2008b) and Ca^{2+} /Calmodulin-dependent expression of many LPS target genes (Lai et al., 2009). During sepsis, elevated cytosolic Ca^{2+} has been demonstrated to be an early event, which contributes to increased cellular injury in veins and multiple organs (Cuschieri et al., 2003). Ca^{2+} antagonists (Hotchkiss and Karl, 1994) or *in vivo* blockade of CAMK2 (Liu et al., 2008b) can improve survival in septic animals, suggesting that interference with Ca^{2+} /CAMK2 signalling may be a useful approach to treat inflammatory disorders. Lai et al. report Calmodulin binding and activation of the BAF chromatin remodelling

complex in LPS-regulated promoters (Lai et al., 2009). As BAF binds to LPS target genes also in the absence of Ca^{2+} signalling and can activate gene expression independently of Ca^{2+} in other cell types, they speculate that Ca^{2+} -dependent removal of repressors might be required in LPS-activated macrophages (Lai et al., 2009). Regarding the data in the present study, Ca^{2+} -dependent activation of additional TFs is another option. Thereby, the phosphoproteome and nascent transcriptome studies might provide a basis for further mechanistic insights into the roles of Ca^{2+} -dependent TLR-induced gene expression, which could be relevant for understanding disease.

7 Outlook

This study provides a novel, global perspective on innate immune activation by TLR signalling. A large number of novel site specific phosphorylation events and genes regulated on nascent transcription level were detected quantitatively and are now publicly available. The highlighted processes and phosphorylation sites on involved proteins allow the formulation of novel hypotheses about TLR signalling and macrophage biology. For example the data suggest that the PI3K/AKT and related GSK3 and mTOR pathways, cell cycle regulation mechanisms and Ca²⁺-dependent signalling play important roles in TLR-induced macrophage responses. Beyond this, we propose a number of novel functions for cytoskeletal proteins in response to TLR activation. Finally, several novel and less appreciated TF families (C/EBP, MEF2, NFAT, HEAT, HOXC, OCT1) were identified, which could be responsible for LPS-induced gene transcription.

These conjectures should be addressed experimentally in the future. For instance, it would be interesting to analyse the relative contribution of the highlighted signalling pathways and molecules to TLR-induced gene expression, most importantly to cytokine production, but also to cytoskeleton-associated phenotypes (see below). This can be done by pharmacological blockage of individual pathways. Furthermore, the recent years have witnessed the development of tools suitable for high-throughput functional analyses of single signalling components, for example RNA interference (RNAi) libraries (e.g. Root et al., 2006), which can be used to knock down TLR-regulated phosphoproteins. Combined with readouts suitable for large scale analyses, this global approach seems appropriate to follow up consequences of the observed changes in phosphorylation.

The identified TFs could additionally be analysed regarding their capacities to bind to and transactivate promoters of LPS-induced genes by chromatin-immunoprecipitation (ChIP) and promoter-reporter gene studies, using the candidate target genes identified in this thesis. Beyond that, further target genes could be discovered by ChIP-on-chip analysis – an approach combining ChIP with microarray analysis for whole genome DNA – on a systems level. Other important questions are whether or not the identified LPS-regulated phosphorylation sites influence TF

localisation, stability and association with partners, for example with chromatin remodelling factors.

Future work will also focus on the role of TLR-induced cytoskeletal changes in macrophage motility and phagocytosis, in gene transcription and/or as a platform for signal integration, as suggested by various studies in other systems (section 6.1.6). Using the actin polymerisation inhibitor Cytochalasin D in combination with analyses of cell morphology, phagocytosis, TF localisation and gene expression, we want to further dissect these novel aspects of TLR-induced macrophage responses.

Taken together, the combination of quantitative measurements of phosphorylation with unbiased statistical analyses by state-of-the art bioinformatic tools has provided a global view on innate immune signalling induced by TLRs, and has highlighted important pathways, processes and transcriptional regulators that operate at the core of host defence against microbes. Understanding such processes should finally yield novel molecular insights into human diseases such as sepsis and might help to pinpoint potential therapeutic targets.

References

- Abraham, R.T. (2001). Cell cycle checkpoint signaling through the ATM and ATR kinases. *Genes Dev* 15, 2177-2196.
- Aderem, A., and Underhill, D.M. (1999). Mechanisms of phagocytosis in macrophages. *Annu Rev Immunol* 17, 593-623.
- Aebersold, R., and Mann, M. (2003). Mass spectrometry-based proteomics. *Nature* 422, 198-207.
- Aki, D., Mashima, R., Saeki, K., Minoda, Y., Yamauchi, M., and Yoshimura, A. (2005). Modulation of TLR signalling by the C-terminal Src kinase (Csk) in macrophages. *Genes Cells* 10, 357-368.
- Akira, S., and Takeda, K. (2004). Toll-like receptor signalling. *Nat Rev Immunol* 4, 499-511.
- Akira, S., Uematsu, S., and Takeuchi, O. (2006). Pathogen recognition and innate immunity. *Cell* 124, 783-801.
- Andersen, B., and Rosenfeld, M.G. (2001). POU domain factors in the neuroendocrine system: lessons from developmental biology provide insights into human disease. *Endocr Rev* 22, 2-35.
- Baccarini, M., Dello Sbarba, P., Buscher, D., Bartocci, A., and Stanley, E.R. (1992). IFN-gamma/Lipopolysaccharide activation of macrophages is associated with protein kinase C-dependent down-modulation of the colony-stimulating factor-1 receptor. *J Immunol* 149, 2656-2661.
- Ballif, B.A., Villen, J., Beausoleil, S.A., Schwartz, D., and Gygi, S.P. (2004). Phosphoproteomic analysis of the developing mouse brain. *Mol Cell Proteomics* 3, 1093-1101.
- Bantscheff, M., Schirle, M., Sweetman, G., Rick, J., and Kuster, B. (2007). Quantitative mass spectrometry in proteomics: a critical review. *Anal Bioanal Chem* 389, 1017-1031.
- Barlow, C., Ribaut-Barassin, C., Zwingman, T.A., Pope, A.J., Brown, K.D., Owens, J.W., Larson, D., Harrington, E.A., Haerberle, A.M., Mariani, J., *et al.* (2000). ATM is a cytoplasmic protein in mouse brain required to prevent lysosomal accumulation. *Proc Natl Acad Sci U S A* 97, 871-876.
- Beausoleil, S.A., Jedrychowski, M., Schwartz, D., Elias, J.E., Villen, J., Li, J., Cohn, M.A., Cantley, L.C., and Gygi, S.P. (2004). Large-scale characterization of HeLa cell nuclear phosphoproteins. *Proc Natl Acad Sci U S A* 101, 12130-12135.
- Benjamini, Y., and Hochberg, Y. (1995). Controlling the false discovery rate - a practical and powerful approach to multiple testing. *J Roy Stat Soc B Met* 57, 289-300.

- Beutler, B. (2004). Inferences, questions and possibilities in Toll-like receptor signalling. *Nature* *430*, 257-263.
- Blaeser, F., Ho, N., Prywes, R., and Chatila, T.A. (2000). Ca(2+)-dependent gene expression mediated by MEF2 transcription factors. *J Biol Chem* *275*, 197-209.
- Blander, J.M. (2007). Signalling and phagocytosis in the orchestration of host defence. *Cell Microbiol* *9*, 290-299.
- Blander, J.M., and Medzhitov, R. (2004). Regulation of phagosome maturation by signals from toll-like receptors. *Science* *304*, 1014-1018.
- Blander, J.M., and Medzhitov, R. (2006). On regulation of phagosome maturation and antigen presentation. *Nat Immunol* *7*, 1029-1035.
- Blume-Jensen, P., and Hunter, T. (2001). Oncogenic kinase signalling. *Nature* *411*, 355-365.
- Bradley, M.N., Zhou, L., and Smale, S.T. (2003). C/EBPbeta regulation in Lipopolysaccharide-stimulated macrophages. *Mol Cell Biol* *23*, 4841-4858.
- Cao, W., Manicassamy, S., Tang, H., Kasturi, S.P., Pirani, A., Murthy, N., and Pulendran, B. (2008). Toll-like receptor-mediated induction of type I Interferon in plasmacytoid dendritic cells requires the rapamycin-sensitive PI(3)K-mTOR-p70S6K pathway. *Nat Immunol*.
- Cartharius, K., Frech, K., Grote, K., Klocke, B., Haltmeier, M., Klingenhoff, A., Frisch, M., Bayerlein, M., and Werner, T. (2005). MatInspector and beyond: promoter analysis based on transcription factor binding sites. *Bioinformatics* *21*, 2933-2942.
- Chan, S.M., Ermann, J., Su, L., Fathman, C.G., and Utz, P.J. (2004). Protein microarrays for multiplex analysis of signal transduction pathways. *Nat Med* *10*, 1390-1396.
- Chi, H., Barry, S.P., Roth, R.J., Wu, J.J., Jones, E.A., Bennett, A.M., and Flavell, R.A. (2006). Dynamic regulation of pro- and anti-inflammatory cytokines by MAPK phosphatase 1 (MKP-1) in innate immune responses. *Proc Natl Acad Sci U S A* *103*, 2274-2279.
- Chomczynski, P., and Mackey, K. (1995). Short technical reports. Modification of the TRI reagent procedure for isolation of RNA from polysaccharide- and proteoglycan-rich sources. *Biotechniques* *19*, 942-945.
- Chuang, T., and Ulevitch, R.J. (2001). Identification of hTLR10: a novel human Toll-like receptor preferentially expressed in immune cells. *Biochim Biophys Acta* *1518*, 157-161.
- Colina, R., Costa-Mattioli, M., Dowling, R.J., Jaramillo, M., Tai, L.H., Breitbach, C.J., Martineau, Y., Larsson, O., Rong, L., Svitkin, Y.V., *et al.* (2008). Translational control of the innate immune response through IRF-7. *Nature* *452*, 323-328.

- Cook, D.N., Pisetsky, D.S., and Schwartz, D.A. (2004). Toll-like receptors in the pathogenesis of human disease. *Nat Immunol* 5, 975-979.
- Cox, J., and Mann, M. (2007). Is proteomics the new genomics? *Cell* 130, 395-398.
- Cox, J., and Mann, M. (2009). MaxQuant enables high peptide identification rates, individualized p.p.b.-range mass accuracies and proteome-wide protein quantification. *Nat Biotechnol* 26, 1367-1372.
- Cuschieri, J., Gourlay, D., Garcia, I., Jelacic, S., and Maier, R.V. (2003). Modulation of endotoxin-induced endothelial function by calcium/calmodulin-dependent protein kinase. *Shock* 20, 176-182.
- Daub, H., Olsen, J.V., Bairlein, M., Gnad, F., Oppermann, F.S., Korner, R., Greff, Z., Keri, G., Stemmann, O., and Mann, M. (2008). Kinase-selective enrichment enables quantitative phosphoproteomics of the kinome across the cell cycle. *Mol Cell* 31, 438-448.
- De Meyts, P., and Whittaker, J. (2002). Structural biology of insulin and IGF1 receptors: implications for drug design. *Nat Rev Drug Discov* 1, 769-783.
- Deane, J.A., and Fruman, D.A. (2004). Phosphoinositide 3-kinase: diverse roles in immune cell activation. *Annu Rev Immunol* 22, 563-598.
- Dengjel, J., Akimov, V., Olsen, J.V., Bunkenborg, J., Mann, M., Blagoev, B., and Andersen, J.S. (2007). Quantitative proteomic assessment of very early cellular signaling events. *Nat Biotechnol* 25, 566-568.
- Dephoure, N., Zhou, C., Villen, J., Beausoleil, S.A., Bakalarski, C.E., Elledge, S.J., and Gygi, S.P. (2008). A quantitative atlas of mitotic phosphorylation. *Proc Natl Acad Sci U S A* 105, 10762-10767.
- Dolken, L., Ruzsics, Z., Radle, B., Friedel, C.C., Zimmer, R., Mages, J., Hoffmann, R., Dickinson, P., Forster, T., Ghazal, P., *et al.* (2008). High-resolution gene expression profiling for simultaneous kinetic parameter analysis of RNA synthesis and decay. *Rna* 14, 1959-1972.
- Dorfman, K., Carrasco, D., Gruda, M., Ryan, C., Lira, S.A., and Bravo, R. (1996). Disruption of the *erp/mkp-1* gene does not affect mouse development: normal MAP kinase activity in ERP/MKP-1-deficient fibroblasts. *Oncogene* 13, 925-931.
- Eferl, R., and Wagner, E.F. (2003). AP-1: a double-edged sword in tumorigenesis. *Nat Rev Cancer* 3, 859-868.
- Ficarro, S.B., McClelland, M.L., Stukenberg, P.T., Burke, D.J., Ross, M.M., Shabanowitz, J., Hunt, D.F., and White, F.M. (2002). Phosphoproteome analysis by mass spectrometry and its application to *Saccharomyces cerevisiae*. *Nat Biotechnol* 20, 301-305.
- Flannagan, R.S., Cosio, G., and Grinstein, S. (2009). Antimicrobial mechanisms of phagocytes and bacterial evasion strategies. *Nat Rev Microbiol* 7, 355-366.

- Foster, S.L., Hargreaves, D.C., and Medzhitov, R. (2007). Gene-specific control of inflammation by TLR-induced chromatin modifications. *Nature* 447, 972-978.
- Fruman, D.A., and Bismuth, G. (2009). Fine tuning the immune response with PI3K. *Immunol Rev* 228, 253-272.
- Fukao, T., and Koyasu, S. (2003). PI3K and negative regulation of TLR signaling. *Trends Immunol* 24, 358-363.
- Gao, H., Leaver, S.K., Burke-Gaffney, A., and Finney, S.J. (2008). Severe sepsis and Toll-like receptors. *Semin Immunopathol* 30, 29-40.
- Gilchrist, M., Thorsson, V., Li, B., Rust, A.G., Korb, M., Roach, J.C., Kennedy, K., Hai, T., Bolouri, H., and Aderem, A. (2006). Systems biology approaches identify ATF3 as a negative regulator of Toll-like receptor 4. *Nature* 441, 173-178.
- Goodridge, H.S., Simmons, R.M., and Underhill, D.M. (2007). Dectin-1 stimulation by *Candida albicans* yeast or zymosan triggers NFAT activation in macrophages and dendritic cells. *J Immunol* 178, 3107-3115.
- Gordon, S. (2003). Alternative activation of macrophages. *Nat Rev Immunol* 3, 23-35.
- Gordon, S., Lawson, L., Rabinowitz, S., Crocker, P.R., Morris, L., and Perry, V.H. (1992). Antigen markers of macrophage differentiation in murine tissues. *Curr Top Microbiol Immunol* 181, 1-37.
- Gordon, S., and Taylor, P.R. (2005). Monocyte and macrophage heterogeneity. *Nat Rev Immunol* 5, 953-964.
- Graba, Y., Aragnol, D., and Pradel, J. (1997). *Drosophila* Hox complex downstream targets and the function of homeotic genes. *Bioessays* 19, 379-388.
- Greenberg, S., and Grinstein, S. (2002). Phagocytosis and innate immunity. *Curr Opin Immunol* 14, 136-145.
- Gruhler, A., Olsen, J.V., Mohammed, S., Mortensen, P., Faergeman, N.J., Mann, M., and Jensen, O.N. (2005). Quantitative phosphoproteomics applied to the yeast pheromone signaling pathway. *Mol Cell Proteomics* 4, 310-327.
- Grummt, I. (2006). Actin and myosin as transcription factors. *Current Opinion in Genetics & Development* 16, 191-196.
- Guettouche, T., Boellmann, F., Lane, W.S., and Voellmy, R. (2005). Analysis of phosphorylation of human heat shock factor 1 in cells experiencing a stress. *BMC Biochem* 6, 4.
- Hammer, M., Mages, J., Dietrich, H., Servatius, A., Howells, N., Cato, A.C., and Lang, R. (2006). Dual specificity phosphatase 1 (DUSP1) regulates a subset of LPS-induced genes and protects mice from lethal endotoxin shock. *J Exp Med* 203, 15-20.

- Han, J., Jiang, Y., Li, Z., Kravchenko, V.V., and Ulevitch, R.J. (1997). Activation of the transcription factor MEF2C by the MAP kinase p38 in inflammation. *Nature* 386, 296-299.
- Hao, S., and Baltimore, D. (2009). The stability of mRNA influences the temporal order of the induction of genes encoding inflammatory molecules. *Nat Immunol* 10, 281-288.
- Hashimoto, C., Hudson, K.L., and Anderson, K.V. (1988). The Toll gene of *Drosophila*, required for dorsal-ventral embryonic polarity, appears to encode a transmembrane protein. *Cell* 52, 269-279.
- Henson, P.M., and Hume, D.A. (2006). Apoptotic cell removal in development and tissue homeostasis. *Trends Immunol* 27, 244-250.
- Herzog, K.H., Chong, M.J., Kapsetaki, M., Morgan, J.I., and McKinnon, P.J. (1998). Requirement for *Atm* in ionizing radiation-induced cell death in the developing central nervous system. *Science* 280, 1089-1091.
- Hirose, N., Maekawa, T., Shinagawa, T., and Ishii, S. (2009). ATF-2 regulates Lipopolysaccharide-induced transcription in macrophage cells. *Biochem Biophys Res Commun* 385, 72-77.
- Holmberg, C.I., Tran, S.E., Eriksson, J.E., and Sistonen, L. (2002). Multisite phosphorylation provides sophisticated regulation of transcription factors. *Trends Biochem Sci* 27, 619-627.
- Holst, J., Szymczak-Workman, A.L., Vignali, K.M., Burton, A.R., Workman, C.J., and Vignali, D.A. (2006). Generation of T-cell receptor retrogenic mice. *Nat Protoc* 1, 406-417.
- Hombria, J.C., and Lovegrove, B. (2003). Beyond homeosis--HOX function in morphogenesis and organogenesis. *Differentiation* 71, 461-476.
- Honda, K., and Taniguchi, T. (2006). IRFs: master regulators of signalling by Toll-like receptors and cytosolic pattern-recognition receptors. *Nat Rev Immunol* 6, 644-658.
- Hopkins, P.A., and Sriskandan, S. (2005). Mammalian Toll-like receptors: to immunity and beyond. *Clin Exp Immunol* 140, 395-407.
- Hotchkiss, R.S., and Karl, I.E. (1994). Dantrolene ameliorates the metabolic hallmarks of sepsis in rats and improves survival in a mouse model of endotoxemia. *Proc Natl Acad Sci U S A* 91, 3039-3043.
- Hu, X., Paik, P.K., Chen, J., Yarilina, A., Kockeritz, L., Lu, T.T., Woodgett, J.R., and Ivashkiv, L.B. (2006). IFN-gamma suppresses IL-10 production and synergizes with TLR2 by regulating GSK3 and CREB/AP-1 proteins. *Immunity* 24, 563-574.
- Huang, Q., Liu, D., Majewski, P., Schulte, L.C., Korn, J.M., Young, R.A., Lander, E.S., and Hacohen, N. (2001). The plasticity of dendritic cell responses to pathogens and their components. *Science* 294, 870-875.

- Hume, D.A., Allan, W., Fabrus, B., Weidemann, M.J., Hapel, A.J., and Bartelmez, S. (1987). Regulation of proliferation of bone marrow-derived macrophages. *Lymphokine Res* 6, 127-139.
- Hume, D.A., and Gordon, S. (1983). Optimal conditions for proliferation of bone marrow-derived mouse macrophages in culture: the roles of CSF-1, serum, Ca²⁺, and adherence. *J Cell Physiol* 117, 189-194.
- Hume, D.A., Ross, I.L., Himes, S.R., Sasmono, R.T., Wells, C.A., and Ravasi, T. (2002). The mononuclear phagocyte system revisited. *J Leukoc Biol* 72, 621-627.
- Ikeguchi, Y., and Nakamura, H. (1997). Determination of organic phosphates by column-switching high performance anion-exchange chromatography using on-line preconcentration on titania. *Anal Sci* 13, 479-485.
- Inouye, S., Fujimoto, M., Nakamura, T., Takaki, E., Hayashida, N., Hai, T., and Nakai, A. (2007). Heat shock transcription factor 1 opens chromatin structure of interleukin-6 promoter to facilitate binding of an activator or a repressor. *J Biol Chem* 282, 33210-33217.
- Inouye, S., Izu, H., Takaki, E., Suzuki, H., Shirai, M., Yokota, Y., Ichikawa, H., Fujimoto, M., and Nakai, A. (2004). Impaired IgG production in mice deficient for heat shock transcription factor 1. *J Biol Chem* 279, 38701-38709.
- Iverson, S.M., Graham, N.R., Bernales, C.Q., Kifayet, A., Ng, N., Shobab, L.A., and Steiner, T.S. (2007). Protein kinase D interaction with TLR5 is required for inflammatory signaling in response to bacterial flagellin. *J Immunol* 178, 5735-5743.
- Janeway, C.A., Jr., Travers, P., Walport, M., Shlomchik, M. J. (2005). *Immunobiology*, 6 edn (New York, Garland Science Publishing).
- Jensen, L.J., Kuhn, M., Stark, M., Chaffron, S., Creevey, C., Muller, J., Doerks, T., Julien, P., Roth, A., Simonovic, M., *et al.* (2009). STRING 8--a global view on proteins and their functional interactions in 630 organisms. *Nucleic Acids Res* 37, D412-416.
- Jin, M.S., Kim, S.E., Heo, J.Y., Lee, M.E., Kim, H.M., Paik, S.G., Lee, H., and Lee, J.O. (2007). Crystal structure of the TLR1-TLR2 heterodimer induced by binding of a tri-acylated lipopeptide. *Cell* 130, 1071-1082.
- Jin, M.S., and Lee, J.O. (2008). Structures of the toll-like receptor family and its ligand complexes. *Immunity* 29, 182-191.
- Kagan, J.C., Su, T., Horng, T., Chow, A., Akira, S., and Medzhitov, R. (2008). TRAM couples endocytosis of Toll-like receptor 4 to the induction of Interferon-beta. *Nat Immunol* 9, 361-368.
- Kamijo, R., Harada, H., Matsuyama, T., Bosland, M., Gerecitano, J., Shapiro, D., Le, J., Koh, S.I., Kimura, T., Green, S.J., *et al.* (1994). Requirement for transcription factor IRF-1 in NO synthase induction in macrophages. *Science* 263, 1612-1615.

- Karin, M. (1991). Signal transduction and gene control. *Curr Opin Cell Biol* 3, 467-473.
- Kim, H.M., Park, B.S., Kim, J.I., Kim, S.E., Lee, J., Oh, S.C., Enkhbayar, P., Matsushima, N., Lee, H., Yoo, O.J., *et al.* (2007). Crystal structure of the TLR4-MD-2 complex with bound endotoxin antagonist Eritoran. *Cell* 130, 906-917.
- Kim, S.O., Ono, K., Tobias, P.S., and Han, J. (2003). Orphan nuclear receptor Nur77 is involved in caspase-independent macrophage cell death. *J Exp Med* 197, 1441-1452.
- Koyasu, S. (2003). The role of PI3K in immune cells. *Nat Immunol* 4, 313-319.
- Kruger, M., Kratchmarova, I., Blagoev, B., Tseng, Y.H., Kahn, C.R., and Mann, M. (2008). Dissection of the insulin signaling pathway via quantitative phosphoproteomics. *Proc Natl Acad Sci U S A* 105, 2451-2456.
- Kumar, C., and Mann, M. (2009). Bioinformatics analysis of mass spectrometry-based proteomics data sets. *FEBS Lett* 583, 1703-1712.
- Lai, D., Wan, M., Wu, J., Preston-Hurlburt, P., Kushwaha, R., Grundstrom, T., Imbalzano, A.N., and Chi, T. (2009). Induction of TLR4-target genes entails calcium/calmodulin-dependent regulation of chromatin remodeling. *Proc Natl Acad Sci U S A* 106, 1169-1174.
- Lai, L., Alaverdi, N., Maltais, L., and Morse, H.C., 3rd (1998). Mouse cell surface antigens: nomenclature and immunophenotyping. *J Immunol* 160, 3861-3868.
- Lang, R. (2005). Tuning of macrophage responses by Stat3-inducing cytokines: molecular mechanisms and consequences in infection. *Immunobiology* 210, 63-76.
- Lang, R., Hammer, M., and Mages, J. (2006). DUSP meet immunology: dual specificity MAPK phosphatases in control of the inflammatory response. *J Immunol* 177, 7497-7504.
- Lang, R., Patel, D., Morris, J.J., Rutschman, R.L., and Murray, P.J. (2002). Shaping gene expression in activated and resting primary macrophages by IL-10. *J Immunol* 169, 2253-2263.
- Larsen, M.R., Thingholm, T.E., Jensen, O.N., Roepstorff, P., and Jorgensen, T.J. (2005). Highly selective enrichment of phosphorylated peptides from peptide mixtures using titanium dioxide microcolumns. *Mol Cell Proteomics* 4, 873-886.
- Latz, E.a.F., K. A. (2008). Innate immunity: sensing and signalling. *Nat Rev Immunol* 8, Poster.
- Lee, F.D. (1992). The role of interleukin-6 in development. *Dev Biol* 151, 331-338.
- Leibovich, S.J., and Wiseman, D.M. (1988). Macrophages, wound repair and angiogenesis. *Prog Clin Biol Res* 266, 131-145.

- Lemaitre, B., Nicolas, E., Michaut, L., Reichhart, J.M., and Hoffmann, J.A. (1996). The dorsoventral regulatory gene cassette *spatzle/Toll/cactus* controls the potent antifungal response in *Drosophila* adults. *Cell* 86, 973-983.
- Liew, F.Y., Xu, D., Brint, E.K., and O'Neill, L.A. (2005). Negative regulation of toll-like receptor-mediated immune responses. *Nat Rev Immunol* 5, 446-458.
- Litvak, V., Ramsey, S.A., Rust, A.G., Zak, D.E., Kennedy, K.A., Lampano, A.E., Nykter, M., Shmulevich, I., and Aderem, A. (2009). Function of C/EBPdelta in a regulatory circuit that discriminates between transient and persistent TLR4-induced signals. *Nat Immunol* 10, 437-443.
- Liu, L., Botos, I., Wang, Y., Leonard, J.N., Shiloach, J., Segal, D.M., and Davies, D.R. (2008a). Structural basis of toll-like receptor 3 signaling with double-stranded RNA. *Science* 320, 379-381.
- Liu, X., Yao, M., Li, N., Wang, C., Zheng, Y., and Cao, X. (2008b). CaMKII promotes TLR-triggered proinflammatory cytokine and type I Interferon production by directly binding and activating TAK1 and IRF3 in macrophages. *Blood* 112, 4961-4970.
- Liu, Y., Shepherd, E.G., and Nelin, L.D. (2007). MAPK phosphatases--regulating the immune response. *Nat Rev Immunol* 7, 202-212.
- Lu, Y.C., Yeh, W.C., and Ohashi, P.S. (2008). LPS/TLR4 signal transduction pathway. *Cytokine* 42, 145-151.
- Lynn, D.J., Winsor, G.L., Chan, C., Richard, N., Laird, M.R., Barsky, A., Gardy, J.L., Roche, F.M., Chan, T.H., Shah, N., *et al.* (2008). InnateDB: facilitating systems-level analyses of the mammalian innate immune response. *Mol Syst Biol* 4, 218.
- Ma, K., Chan, J.K., Zhu, G., and Wu, Z. (2005). Myocyte enhancer factor 2 acetylation by p300 enhances its DNA binding activity, transcriptional activity, and myogenic differentiation. *Mol Cell Biol* 25, 3575-3582.
- Macek, B., Mann, M., and Olsen, J.V. (2009). Global and site-specific quantitative phosphoproteomics: principles and applications. *Annu Rev Pharmacol Toxicol* 49, 199-221.
- Macian, F. (2005). NFAT proteins: key regulators of T-cell development and function. *Nat Rev Immunol* 5, 472-484.
- Mages, J., Dietrich, H., and Lang, R. (2007). A genome-wide analysis of LPS tolerance in macrophages. *Immunobiology* 212, 723-737.
- Manke, I.A., Nguyen, A., Lim, D., Stewart, M.Q., Elia, A.E., and Yaffe, M.B. (2005). MAPKAP kinase-2 is a cell cycle checkpoint kinase that regulates the G2/M transition and S phase progression in response to UV irradiation. *Mol Cell* 17, 37-48.
- Mann, M. (2006). Functional and quantitative proteomics using SILAC. *Nat Rev Mol Cell Biol* 7, 952-958.

- Martin, M., Rehani, K., Jope, R.S., and Michalek, S.M. (2005). Toll-like receptor-mediated cytokine production is differentially regulated by glycogen synthase kinase 3. *Nat Immunol* 6, 777-784.
- Martinez, F.O., Helming, L., and Gordon, S. (2009). Alternative activation of macrophages: an immunologic functional perspective. *Annu Rev Immunol* 27, 451-483.
- Matsumoto, M., Tanaka, T., Kaisho, T., Sanjo, H., Copeland, N.G., Gilbert, D.J., Jenkins, N.A., and Akira, S. (1999). A novel LPS-inducible C-type lectin is a transcriptional target of NF-IL6 in macrophages. *J Immunol* 163, 5039-5048.
- Mayr, B., and Montminy, M. (2001). Transcriptional regulation by the phosphorylation-dependent factor CREB. *Nat Rev Mol Cell Biol* 2, 599-609.
- McKinsey, T.A., Zhang, C.L., and Olson, E.N. (2001). Control of muscle development by dueling HATs and HDACs. *Curr Opin Genet Dev* 11, 497-504.
- McKinsey, T.A., Zhang, C.L., and Olson, E.N. (2002). MEF2: a calcium-dependent regulator of cell division, differentiation and death. *Trends Biochem Sci* 27, 40-47.
- McNulty, D.E., and Annan, R.S. (2008). Hydrophilic interaction chromatography reduces the complexity of the phosphoproteome and improves global phosphopeptide isolation and detection. *Mol Cell Proteomics* 7, 971-980.
- Medzhitov, R. (2007). Recognition of microorganisms and activation of the immune response. *Nature* 449, 819-826.
- Medzhitov, R., Preston-Hurlburt, P., and Janeway, C.A., Jr. (1997). A human homologue of the *Drosophila* Toll protein signals activation of adaptive immunity. *Nature* 388, 394-397.
- Metcalf, D. (1989). The molecular control of cell division, differentiation commitment and maturation in haemopoietic cells. *Nature* 339, 27-30.
- Metcalf, D. (1997). The molecular control of granulocytes and macrophages. *Ciba Found Symp* 204, 40-50; discussion 50-46.
- Miyake, K. (2006). Roles for accessory molecules in microbial recognition by Toll-like receptors. *J Endotoxin Res* 12, 195-204.
- Mosser, D.M., and Edwards, J.P. (2008). Exploring the full spectrum of macrophage activation. *Nat Rev Immunol* 8, 958-969.
- Nau, G.J., Richmond, J.F., Schlesinger, A., Jennings, E.G., Lander, E.S., and Young, R.A. (2002). Human macrophage activation programs induced by bacterial pathogens. *Proc Natl Acad Sci U S A* 99, 1503-1508.
- Nilsson, R., Bajic, V.B., Suzuki, H., di Bernardo, D., Bjorkegren, J., Katayama, S., Reid, J.F., Sweet, M.J., Gariboldi, M., Carninci, P., *et al.* (2006). Transcriptional network dynamics in macrophage activation. *Genomics* 88, 133-142.

- O'Neill, L.A., and Bowie, A.G. (2007). The family of five: TIR-domain-containing adaptors in Toll-like receptor signalling. *Nat Rev Immunol* 7, 353-364.
- Oda, K., and Kitano, H. (2006). A comprehensive map of the toll-like receptor signaling network. *Mol Syst Biol* 2, 2006 0015.
- Ohtani, M., Nagai, S., Kondo, S., Mizuno, S., Nakamura, K., Tanabe, M., Takeuchi, T., Matsuda, S., and Koyasu, S. (2008). Mammalian target of rapamycin and glycogen synthase kinase 3 differentially regulate Lipopolysaccharide-induced interleukin-12 production in dendritic cells. *Blood* 112, 635-643.
- Ohto, U., Fukase, K., Miyake, K., and Satow, Y. (2007). Crystal structures of human MD-2 and its complex with antiendotoxic lipid IVa. *Science* 316, 1632-1634.
- Olsen, J.V., Blagoev, B., Gnäd, F., Macek, B., Kumar, C., Mortensen, P., and Mann, M. (2006). Global, in vivo, and site-specific phosphorylation dynamics in signaling networks. *Cell* 127, 635-648.
- Ong, S.E., Blagoev, B., Kratchmarova, I., Kristensen, D.B., Steen, H., Pandey, A., and Mann, M. (2002). Stable isotope labeling by amino acids in cell culture, SILAC, as a simple and accurate approach to expression proteomics. *Mol Cell Proteomics* 1, 376-386.
- Oppermann, F.S., Gnäd, F., Olsen, J.V., Hornberger, R., Greff, Z., Keri, G., Mann, M., and Daub, H. (2009). Large-scale proteomics analysis of the human kinome. *Mol Cell Proteomics* 8, 1751-1764.
- Pagliarini, D.J., Calvo, S.E., Chang, B., Sheth, S.A., Vafai, S.B., Ong, S.E., Walford, G.A., Sugiana, C., Boneh, A., Chen, W.K., *et al.* (2008). A mitochondrial protein compendium elucidates complex I disease biology. *Cell* 134, 112-123.
- Palsson-McDermott, E.M., and O'Neill, L.A. (2004). Signal transduction by the Lipopolysaccharide receptor, Toll-like receptor-4. *Immunology* 113, 153-162.
- Pan, C. (2008). Phosphoproteomics and proteomic phenotyping to assess signal transduction in cancer cells. In Max-Planck Institute for Biochemistry/Faculty for Chemistry and Pharmacy (Ludwig-Maximilians University Munich).
- Pan, C., Gnäd, F., Olsen, J.V., and Mann, M. (2008). Quantitative phosphoproteome analysis of a mouse liver cell line reveals specificity of phosphatase inhibitors. *Proteomics* 8, 4534-4546.
- Park, B.S., Song, D.H., Kim, H.M., Choi, B.S., Lee, H., and Lee, J.O. (2009a). The structural basis of Lipopolysaccharide recognition by the TLR4-MD-2 complex. *Nature* 458, 1191-1195.
- Park, J.E., Kim, Y.I., and Yi, A.K. (2009b). Protein kinase D1 is essential for MyD88-dependent TLR signaling pathway. *J Immunol* 182, 6316-6327.
- Park, J.M., Greten, F.R., Wong, A., Westrick, R.J., Arthur, J.S., Otsu, K., Hoffmann, A., Montminy, M., and Karin, M. (2005). Signaling pathways and genes that inhibit

pathogen-induced macrophage apoptosis--CREB and NF-kappaB as key regulators. *Immunity* 23, 319-329.

Pinkse, M.W., Uitto, P.M., Hilhorst, M.J., Ooms, B., and Heck, A.J. (2004). Selective isolation at the femtomole level of phosphopeptides from proteolytic digests using 2D-NanoLC-ESI-MS/MS and titanium oxide precolumns. *Anal Chem* 76, 3935-3943.

Pipes, G.C.T., Creemers, E.E., and Olson, E.N. (2006). The myocardin family of transcriptional coactivators: versatile regulators of cell growth, migration, and myogenesis. *Genes & Development* 20, 1545-1556.

Poltorak, A., He, X., Smirnova, I., Liu, M.Y., Van Huffel, C., Du, X., Birdwell, D., Alejos, E., Silva, M., Galanos, C., *et al.* (1998). Defective LPS signaling in C3H/HeJ and C57BL/10ScCr mice: mutations in Tlr4 gene. *Science* 282, 2085-2088.

Posern, G., and Treisman, R. (2006). Actin' together: serum response factor, its cofactors and the link to signal transduction. *Trends Cell Biol* 16, 588-596.

Raetz, C.R. (1990). Biochemistry of endotoxins. *Annu Rev Biochem* 59, 129-170.

Raetz, C.R., and Whitfield, C. (2002). Lipopolysaccharide endotoxins. *Annu Rev Biochem* 71, 635-700.

Ramji, D.P., and Foka, P. (2002). CCAAT/enhancer-binding proteins: structure, function and regulation. *Biochem J* 365, 561-575.

Ramsey, S.A., Klemm, S.L., Zak, D.E., Kennedy, K.A., Thorsson, V., Li, B., Gilchrist, M., Gold, E.S., Johnson, C.D., Litvak, V., *et al.* (2008). Uncovering a macrophage transcriptional program by integrating evidence from motif scanning and expression dynamics. *PLoS Comput Biol* 4, e1000021.

Rappsilber, J., Ishihama, Y., and Mann, M. (2003). Stop and go extraction tips for matrix-assisted laser desorption/ionization, nanoelectrospray, and LC/MS sample pretreatment in proteomics. *Anal Chem* 75, 663-670.

Reinders, J., and Sickmann, A. (2005). State-of-the-art in phosphoproteomics. *Proteomics* 5, 4052-4061.

Ridley, A.J. (2008). Regulation of macrophage adhesion and migration by Rho GTP-binding proteins. *J Microsc* 231, 518-523.

Root, D.E., Hacohen, N., Hahn, W.C., Lander, E.S., and Sabatini, D.M. (2006). Genome-scale loss-of-function screening with a lentiviral RNAi library. *Nat Methods* 3, 715-719.

Ruse, M., and Knaus, U.G. (2006). New players in TLR-mediated innate immunity: PI3K and small Rho GTPases. *Immunol Res* 34, 33-48.

Russell, D.G., and Yates, R.M. (2007a). TLR signalling and phagosome maturation: an alternative viewpoint. *Cell Microbiol* 9, 849-850.

- Russell, D.G., and Yates, R.M. (2007b). Toll-like receptors and phagosome maturation. *Nat Immunol* 8, 217; author reply 217-218.
- Salojin, K.V., Owusu, I.B., Millerchip, K.A., Potter, M., Platt, K.A., and Oravec, T. (2006). Essential role of MAPK phosphatase-1 in the negative control of innate immune responses. *J Immunol* 176, 1899-1907.
- Sasmono, R.T., and Hume, D.A. (2004). The Biology of Macrophages. In *The Innate Immune Response to Infection*, S.E. Kaufmann, R. Medzhitov, and S. Gordon, eds. (Washington, DC, USA, ASM Press), pp. 71-94.
- Schmitz, F., Heit, A., Dreher, S., Eisenacher, K., Mages, J., Haas, T., Krug, A., Janssen, K.P., Kirschning, C.J., and Wagner, H. (2008). Mammalian target of rapamycin (mTOR) orchestrates the defense program of innate immune cells. *Eur J Immunol* 38, 2981-2992.
- Schreiber, T.B., Mausbacher, N., Breitkopf, S.B., Grundner-Culemann, K., and Daub, H. (2008). Quantitative phosphoproteomics--an emerging key technology in signal-transduction research. *Proteomics* 8, 4416-4432.
- Sester, D.P., Beasley, S.J., Sweet, M.J., Fowles, L.F., Cronau, S.L., Stacey, K.J., and Hume, D.A. (1999). Bacterial/CpG DNA down-modulates colony stimulating factor-1 receptor surface expression on murine bone marrow-derived macrophages with concomitant growth arrest and factor-independent survival. *J Immunol* 163, 6541-6550.
- Shaulian, E., and Karin, M. (2002). AP-1 as a regulator of cell life and death. *Nat Cell Biol* 4, E131-136.
- Shevchenko, A., Tomas, H., Havlis, J., Olsen, J.V., and Mann, M. (2006). In-gel digestion for mass spectrometric characterization of proteins and proteomes. *Nat Protoc* 1, 2856-2860.
- Stanley, E.R., Berg, K.L., Einstein, D.B., Lee, P.S., Pixley, F.J., Wang, Y., and Yeung, Y.G. (1997). Biology and action of colony--stimulating factor-1. *Mol Reprod Dev* 46, 4-10.
- Stern, S., Debre, E., Stritt, C., Berger, J., Posern, G., and Knoll, B. (2009). A nuclear actin function regulates neuronal motility by serum response factor-dependent gene transcription. *J Neurosci* 29, 4512-4518.
- Takaoka, A., Yanai, H., Kondo, S., Duncan, G., Negishi, H., Mizutani, T., Kano, S., Honda, K., Ohba, Y., Mak, T.W., *et al.* (2005). Integral role of IRF-5 in the gene induction programme activated by Toll-like receptors. *Nature* 434, 243-249.
- Takeda, K., and Akira, S. (2004). TLR signaling pathways. *Semin Immunol* 16, 3-9.
- Takeda, K., and Akira, S. (2005). Toll-like receptors in innate immunity. *Int Immunol* 17, 1-14.

- Tanaka, T., Akira, S., Yoshida, K., Umemoto, M., Yoneda, Y., Shirafuji, N., Fujiwara, H., Suematsu, S., Yoshida, N., and Kishimoto, T. (1995). Targeted disruption of the NF-IL6 gene discloses its essential role in bacteria killing and tumor cytotoxicity by macrophages. *Cell* 80, 353-361.
- Teusch, N., Lombardo, E., Eddleston, J., and Knaus, U.G. (2004). The low molecular weight GTPase RhoA and atypical protein kinase Czeta are required for TLR2-mediated gene transcription. *J Immunol* 173, 507-514.
- Thomson, A.W., Turnquist, H.R., and Raimondi, G. (2009). Immunoregulatory functions of mTOR inhibition. *Nat Rev Immunol* 9, 324-337.
- Trost, M., English, L., Lemieux, S., Courcelles, M., Desjardins, M., and Thibault, P. (2009). The phagosomal proteome in Interferon-gamma-activated macrophages. *Immunity* 30, 143-154.
- Tushinski, R.J., Oliver, I.T., Guilbert, L.J., Tynan, P.W., Warner, J.R., and Stanley, E.R. (1982). Survival of mononuclear phagocytes depends on a lineage-specific growth factor that the differentiated cells selectively destroy. *Cell* 28, 71-81.
- Vallabhapurapu, S., and Karin, M. (2009). Regulation and function of NF-kappaB transcription factors in the immune system. *Annu Rev Immunol* 27, 693-733.
- van Erp, K., Dach, K., Koch, I., Heesemann, J., and Hoffmann, R. (2006). Role of strain differences on host resistance and the transcriptional response of macrophages to infection with *Yersinia enterocolitica*. *Physiol Genomics* 25, 75-84.
- Villen, J., Beausoleil, S.A., Gerber, S.A., and Gygi, S.P. (2007). Large-scale phosphorylation analysis of mouse liver. *Proc Natl Acad Sci U S A* 104, 1488-1493.
- Watts, C. (2008). Location, location, location: identifying the neighborhoods of LPS signaling. *Nat Immunol* 9, 343-345.
- Weichhart, T., Costantino, G., Poglitsch, M., Rosner, M., Zeyda, M., Stuhlmeier, K.M., Kolbe, T., Stulnig, T.M., Horl, W.H., Hengstschlager, M., *et al.* (2008). The TSC-mTOR signaling pathway regulates the innate inflammatory response. *Immunity* 29, 565-577.
- Wells, C.A., Ravasi, T., Faulkner, G.J., Carninci, P., Okazaki, Y., Hayashizaki, Y., Sweet, M., Wainwright, B.J., and Hume, D.A. (2003). Genetic control of the innate immune response. *BMC Immunol* 4, 5.
- West, A.P., Koblansky, A.A., and Ghosh, S. (2006). Recognition and signaling by toll-like receptors. *Annu Rev Cell Dev Biol* 22, 409-437.
- West, M.A., Wallin, R.P., Matthews, S.P., Svensson, H.G., Zaru, R., Ljunggren, H.G., Prescott, A.R., and Watts, C. (2004). Enhanced dendritic cell antigen capture via toll-like receptor-induced actin remodeling. *Science* 305, 1153-1157.
- Yaffe, M.B. (2002). Phosphotyrosine-binding domains in signal transduction. *Nat Rev Mol Cell Biol* 3, 177-186.

- Yaffe, M.B., and Elia, A.E. (2001). Phosphoserine/threonine-binding domains. *Curr Opin Cell Biol* 13, 131-138.
- Yaffe, M.B., and Smerdon, S.J. (2001). PhosphoSerine/threonine binding domains: you can't pSERious? *Structure* 9, R33-38.
- Yang, D.Q., and Kastan, M.B. (2000). Participation of ATM in insulin signalling through phosphorylation of eIF-4E-binding protein 1. *Nat Cell Biol* 2, 893-898.
- Yang, X.J., and Gregoire, S. (2006). A recurrent phospho-sumoyl switch in transcriptional repression and beyond. *Mol Cell* 23, 779-786.
- Yates, R.M., and Russell, D.G. (2005). Phagosome maturation proceeds independently of stimulation of toll-like receptors 2 and 4. *Immunity* 23, 409-417.
- Zanivan, S., Gnad, F., Wickstrom, S.A., Geiger, T., Macek, B., Cox, J., Fassler, R., and Mann, M. (2008). Solid tumor proteome and phosphoproteome analysis by high resolution mass spectrometry. *J Proteome Res* 7, 5314-5326.
- Zhang, D., Zhang, G., Hayden, M.S., Greenblatt, M.B., Bussey, C., Flavell, R.A., and Ghosh, S. (2004). A toll-like receptor that prevents infection by uropathogenic bacteria. *Science* 303, 1522-1526.
- Zhao, Q., Wang, X., Nelin, L.D., Yao, Y., Matta, R., Manson, M.E., Baliga, R.S., Meng, X., Smith, C.V., Bauer, J.A., *et al.* (2006). MAP kinase phosphatase 1 controls innate immune responses and suppresses endotoxic shock. *J Exp Med* 203, 131-140.
- Zhu, C., Rao, K., Xiong, H., Gagnidze, K., Li, F., Horvath, C., and Plevy, S. (2003). Activation of the murine interleukin-12 p40 promoter by functional interactions between NFAT and ICSBP. *J Biol Chem* 278, 39372-39382.

Appendix

The following supplementary tables are included as Excel spreadsheets on an enclosed CD.

- Tab. S1. Reproducibly identified macrophage phosphorylation sites.**
- Tab. S2. Phosphorylation sites on known TLR signalling molecules.**
- Tab. S3. LPS-regulated phosphoproteins associated with enriched GO terms.**
- Tab. S4 Microarray analysis of gene expression in nascent and total cellular RNA
– regulated and non-regulated genes.**
- Tab. S5. Phosphorylation sites on TFs with binding site enrichment in
LPS-regulated promoters.**

Acknowledgements

I would like to thank everybody who provided helping hands during my time as a PhD student:

First and foremost, I thank my supervisor Prof. Dr. Roland Lang for his outstanding support during the past years I spent in his lab. With his great ambition and confidence in me he has substantial proportion for the success of this work. Thank you, Roland, for your excellent cooperativeness, and also for letting me finish in Munich!

Another great thank you goes to Dr. Jesper Olsen at the Max-Planck-Institute for Biochemistry in Munich, without whom this project would not have been possible. He performed the mass spectrometric analyses and greatly assisted with expert advice during the whole course of this project!

I am also very grateful to Prof. Dr. Christian Bogdan, Prof. Dr. Dirk Busch, Prof. Dr. Dr. h.c. Hermann Wagner and Prof. Dr. Matthias Mann for giving me the opportunity to work in their institutes in Munich and Erlangen, where I enjoyed excellent scientific environments. Many thanks also to Prof. Wagner for his continuous interest in my project.

Furthermore, I would like to thank Prof. Dr. Johannes Buchner for supporting me as doctoral advisor, Prof. Dr. Bernhard Küster as the third examiner and Prof. Dr. Sevil Weinkauff for chairing the thesis committee.

I also thank our collaborators Dr. Lars Dölken at the Gene Center, Munich, and Dr. Cornelia Frech from Genomatix Software GmbH for advice on nascent RNA and promoter analyses, respectively.

For the fun we had in and outside the lab I want to thank all my colleagues, especially those of the Lang group. My PhD colleagues Kerstin Werninghaus, Magda Niedzielska and Dr. Michael Hammer, my office colleagues Andrea Hartl, Dr. Laura Layland and Dr. Nuria Rodriguez, and Dr. Cuiping Pan at the Max-Planck-Institute for Biochemistry, were always there for technical help, discussions and open to share all ups and downs. Dr. Jörg Mages greatly assisted with advice on programming with R, even after his departure! Another big thank you goes to Katja

Frühauf for the microarray data on nascent transcription, and many valuable scientific and private conversations, and to Magda Niedzielska for her brilliant assistance during my final spurt. For the friendly atmosphere, numerous evenings in the Biergarten and elsewhere, and for lots of support during work I would also like to thank all other members of the lab, including the technical assistants Angela Servatius, Harald Dietrich, Renate Siegelmann and Silvia Weidner, as well as all students who contributed temporarily.

The last but not least great thank you goes to my parents and to my husband Christian Weintz for their continuous support and their persistent confidence in me. Thank you for everything!